Seagrass and Epiphyte Hyperspectral Imaging for Efficient Integrated Measurement of Water Quality

GLO CMP Cycle 17 #13-040-000-6907

FINAL REPORT

PI: Mehrube “Ruby” Mehrubeoglu

Co-PIs: Kirk Cammarata, Paul Zimba, James Simons

May 2015

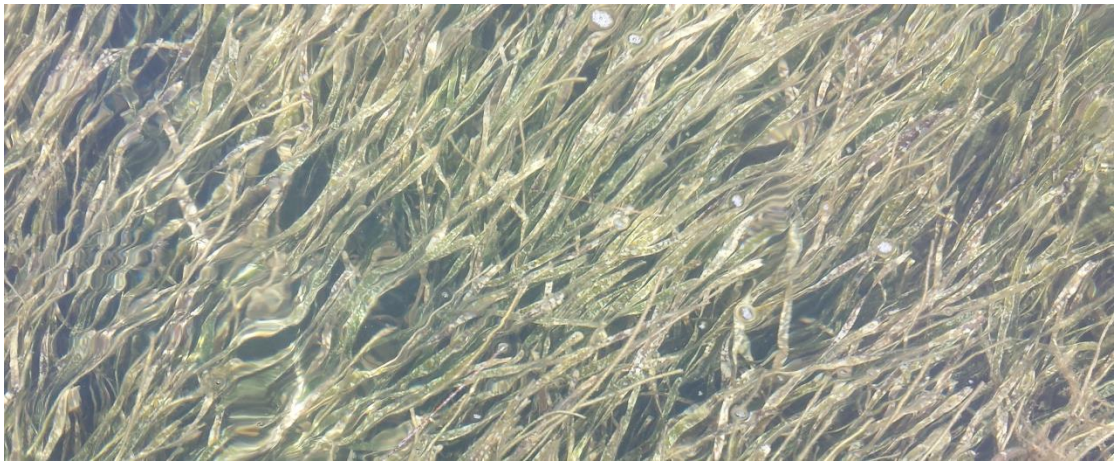

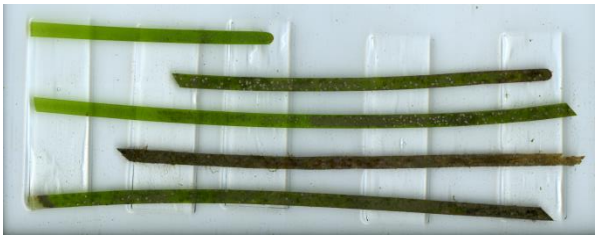

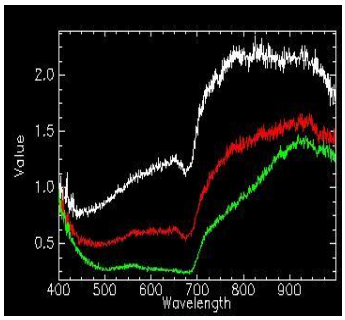

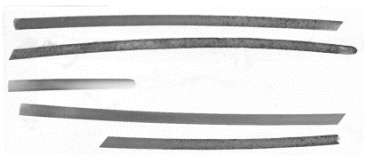

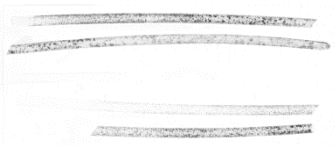

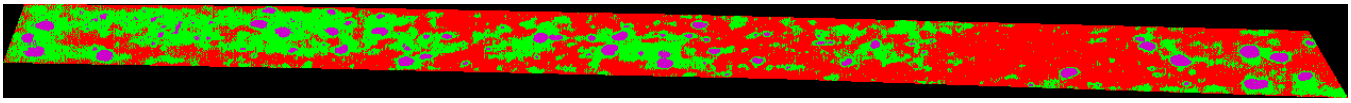

1. INTRODUCTION

Seagrasses and their algal epiphytes respond similarly to environmental factors such as light and nutrients, yet they also compete for these resources; however, eutrophication leads to epiphyte proliferation in ways detrimental to overall seagrass productivity and function (Ralph *et al.*, 2006) leading these systems to act as stationary time-integrated sentinels of water quality and ecosystem status. Seagrass monitoring (beyond areal coverage) relies heavily on morphometric- and biomass-based measures.

Image analysis-based methodology offers faster data acquisition, small sample requirements, and archival of images for relatively little effort and cost as they are minimally invasive. One of the significant challenges of application of imaging is optimization of imaging parameters, development and analysis of appropriate protocols, and correlation to existing measures. Fluorescence-based imaging technology was incorporated into a CMP-Cycle 14 Project (Radloff et al.). Direct correlation of fluorescence measures to algal epiphyte biomass ranged from $r2 > 0.9$ to poor because that particular imaging technique was sensitive to the types (species) of organisms predominating at different sites or seasons. In the work presented here, additional image analysis and algal pigment studies have been incorporated to determine the overall abundance, biomass, morphometrics and percent epiphyte coverage from seagrasses using three imaging technologies.

Three complementary imaging technologies (hyperspectral imaging, fluorescence imaging, visible scans) have been investigated and compared in this study to assess their effectiveness to determine epiphyte levels as an indicator of water quality. Three sites were selected for seagrass sample collection and water quality measurements. Hyperspectral and other vision-based technologies were evaluated against biomass and HPLC pigment analysis to show their feasibility for integrated measurement of water quality.

Analytical routines based on CPCe, MATLAB and ENVI have been used or created to extract information related to the above-mentioned parameters from the scanned seagrass images. Seagrass leaves collected in the field were scanned with the hyperspectral imaging system in the field to collect spatial information and spectral response of the blades and its colonies, then returned to the lab and scanned on high-quality color and fluorescence scanners. In the interest of time, hyperspectral scanning was accomplished after returning from field trips outdoors using the portable hyperspectral camera, and benchtop hyperspectral imaging system in the HOPI Lab. Images were analyzed using the three software tools for percent epiphyte cover, epiphyte assemblage structure to the lowest practical taxon, and spatial gradients in epiphyte cover on the segrass leaves. Imaging analyses results were compared by epiphyte pigment analyses and traditional measures, such as biomass. Diagnostic pigment biomarkers are a rapid means for assessing algal community composition. Each algal division

contains unique carotenoids that can identify algae to the divisional or lower phylogenetic level, providing unbiased estimation of algal composition relative to other methods. This method has been widely used in plant, algal studies.

The data have been compiled to be placed on local data servers. Findings so far have been presented at academic symposia and a conference, and incorporated into public outreach activities through a brochure and seagrass castings in resin. A set of imaging and analytical routines that can be adopted for seagrass analysis have been included in the appendices.

To summarize, this report compares three imaging technologies to detect epiphyte on seagrasses from three sites selected during the course of this project. The methods used from sampling to data analysis are presented in the next section. Methods discussed include field-based water quality measurements, hyperspectral imaging, visible scans, and other laboratory measurements, such as biomass and pigment analysis. Results and comparison of the methods are presented in Section 3. Outreach efforts are summarized in Section 4. Conclusions and findings are presented in Section 5. Future work is listed in Section 6. Appendices contain outreach brochure on seagrasses and water quality, poster and conference paper, portable camera settings for collecting images outdoors, ENVI-based image viewing normalization procedure, MATLAB programs for hyperspectral image analysis, and MATLAB code for fluorescent image spatial analysis developed for the project.

2. METHODOLOGY

Figure 1 summarizes the steps taken in this project from physicochemical measurements to data analysis based on collected seagrass samples. To summarize, 3 sites were identified for sampling for the project. Water quality measurements were taken during field trips, and seagrass and core samples collected. Three types of imaging were performed on seagrass samples to compare results and test imaging methods. The imaging methods used included hyperspectral imaging (in the field, after the field trip outdoors and in the lab), visible range imaging (visible scans of seagrass leaves using a scanner), and fluorescence imaging. The samples also underwent pigment analysis using HPLC, and biomass analyses using scraping method. All data were then analyzed and results compared.

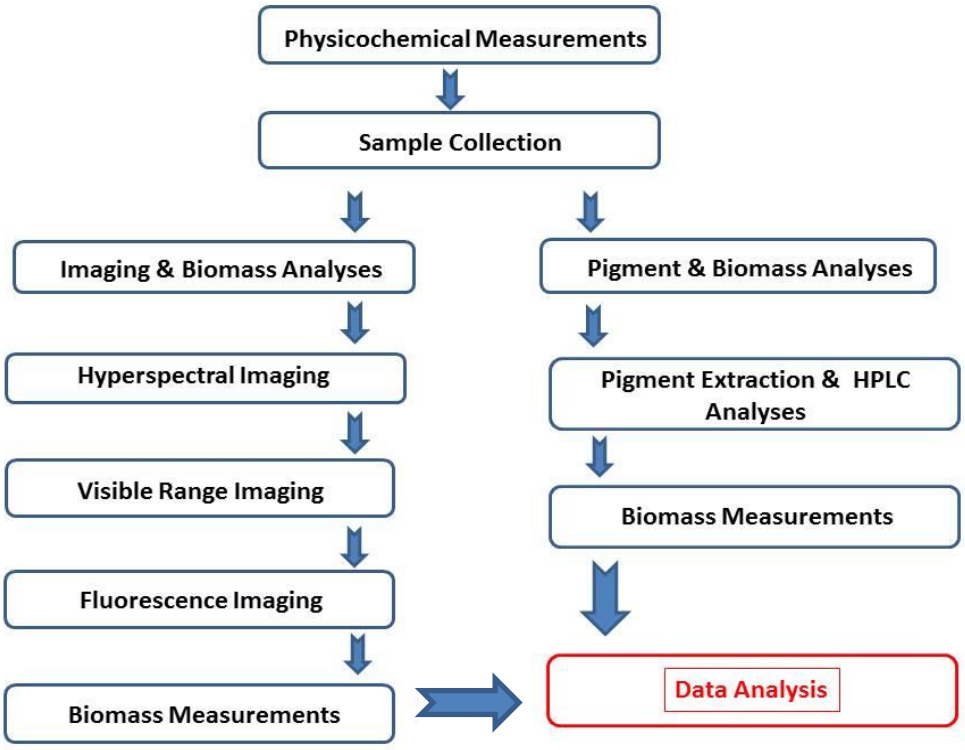

Figure 1. The methods and steps used from physicochemical measurements to data analysis.

The remainder of this section describes the methods for sample collection site selection, water quality measurements, seagrass and epiphyte imaging, and other laboratory measurements, including biomass and HPLC. The results are described and compared in Section 3 Results and Discussion.

2.1 Seagrass Sampling and Location Development

Seagrass sampling took place at 3 sites (7b (alternate), 21B and Steadman's Island as shown in the map in Figure 2) which were identified as the sites for this. Project site selection was based on preliminary samplings with guidance from some TPWD sites with preliminary data suggesting different epiphytes and conditions. Although the original goal was to select different sites near TCEQ water quality monitoring stations, there were too few available with the seagrass conditions targeted with this project. There is are TCEQ sampling station in the general vicinity of sampling sites 7b-alt (Station 7B) and 21B (Station 21B), but the stations were not close enough to the sampling locations to represent conditions specific to at either site. Steadman's Island did possess a monitoring station nearby with the same name. In summary, final sampling sites were determined after field research and information gathered from other local scientists who had observed viable *Thalassia* seagrass growth at these sites.

Safety and accessibility were among the selection criteria. (PLEASE NOTE THAT ALTHOUGH MAY HAVE BEEN LABELLED DIFFERENTLY IN THE REPORT, ALL DATA REPORTED ARE FROM 7b (alternate), 21B AND STEADMAN ISLAND AS SHOWN ON THE MAP BELOW. Further details can be found from the latitude and longitude recordings from field trips presented in Section 3.1.2 Water Quality Measurements)

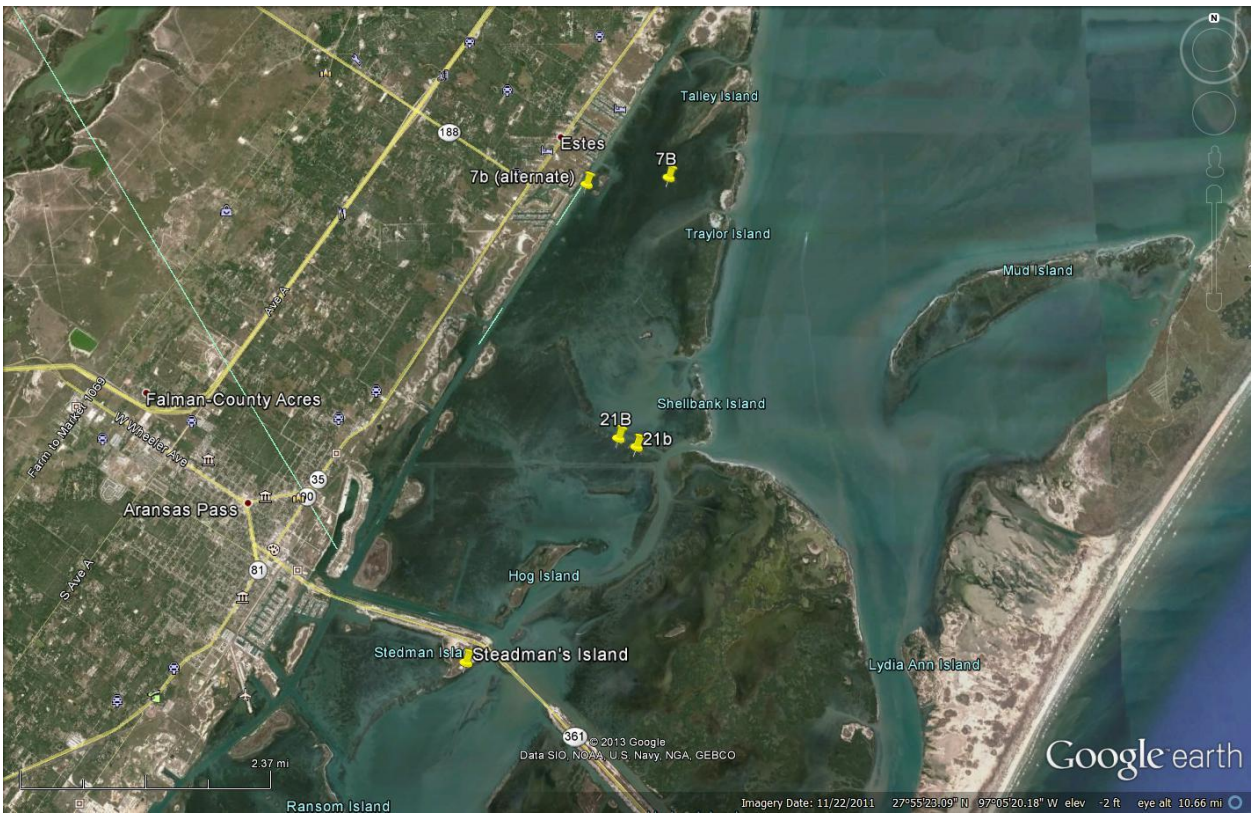

Figure 2. The three seagrass *Thalassia* sampling sites (7b (alternate), 21B and Steadman's Island). Other marked sites include investigated sites for potential sampling at the beginning of the project.

About ten leaves per measurement per site were targeted, resulting in the collection of 3-4 shoots per measurement. The measurements included biomass, fluorescence imaging, visual scans, hyperspectral imaging, and HPLC. The number of shoots collected depended on the number of leaves in the shoot, which varied between 2 and 4 depending on location and sampling season.

Seagrass shoots and leaves were inserted in Ziploc bags or opaque white plastic bottles upon extraction from sampling sites, and kept in a cooler with ice until returning from the field trip. Upon return from the field trip, they were either immediately imaged, or refrigerated until the following day for continued laboratory measurements or imaging.

2.2 Water Quality Measurements

The following water quality measurements were taken at each sampling event: water temperature, dissolved oxygen, percent saturation, salinity, conductivity, and PH. Turbidity was measured in the last two field trips. Barometric pressure was recorded on August 6, 2014, sampling event. Together with water quality measurements, water sample depth, date and time of data collection, latitude and longitude of sampling location as well as depth realm (surface and canopy) were recorded.

Water quality measurements and other data collected in the field during the project are summarized in Section 3.1.2 Water Quality. Initial trips were exploratory in nature to help solidify the procedures and SOP document.

Figure 3. Water quality measurements and recording in field. (Photo by M. Mehrubeoglu)

2.3 Seagrass and Epiphyte Imaging

Three types of seagrass and epiphyte imaging were performed. One was visible scans using high-resolution scanner that required the seagrasses to be flat and without water bubbles. The second type of images acquired were fluorescence scans with green and red fluorescence. Finally the third type of imaging performed was hyperspectral imaging. Hyperspectral scans were acquired in the field, in the lab, and outdoors after returning from the sampling field trips.

2.3.1 Hyperspectral Imaging

Hyperspectral images were collected from the seagrass leaf samples either in the field, right after returning from the field, or the next morning, but no later than within 24 hours of sample collection. The seagrass samples were kept in Ziploc bags or opaque white plastic bottles in a cooler during scans, or refrigerated If not immediately imaged. Samples were kept in the dark to minimize if not prevent bleaching of epiphytes or pigment degradation. Image acquisition time depends on the camera used, and strength of ambient light (irradiance), which affected the decisions on how many in-field images could be acquired. The benchtop hyperspectral imaging system (Headwall Photonics) in the lab uses a broadband light source, which generates heat and desiccates the leaves within minutes. The system must be ready to scan samples fast to avoid drying and curling of the seagrass leaves. The portable hyperspectral camera (Surface Optics, SOC 710) has a much faster processing time, but requires strong sunlight exposure for fast processing to keep the integration times low.

2.3.1.1 Hyperspectral Image Acquisition

The seagrass leaves were cut to fit the leaves within the camera view, and cut pieces of a single leaf imaged side by side (in portable hyperspectral camera) or individually (with benchtop hyperspectral camera). The final analysis combined results from cut portions to assess individual whole seagrass leaves or seagrass shoots (a single shoot contains multiple seagrass leaves). The seagrasses were laid flat on a matt surface (in our case, black felt material). The samples remained moist within the container they were stored in. Figure 4 shows the portable hyperspectral camera in use in the field, as well as individual seagrass leaves imaged. Seagrass leaves were laid as flat to the surface and as parallel to the edge of the container as possible to assist with image processing later. The cut seagrass leaves were held down with weights. A gray reference panel was imaged with the seagrass leaves for image normalization purposes.

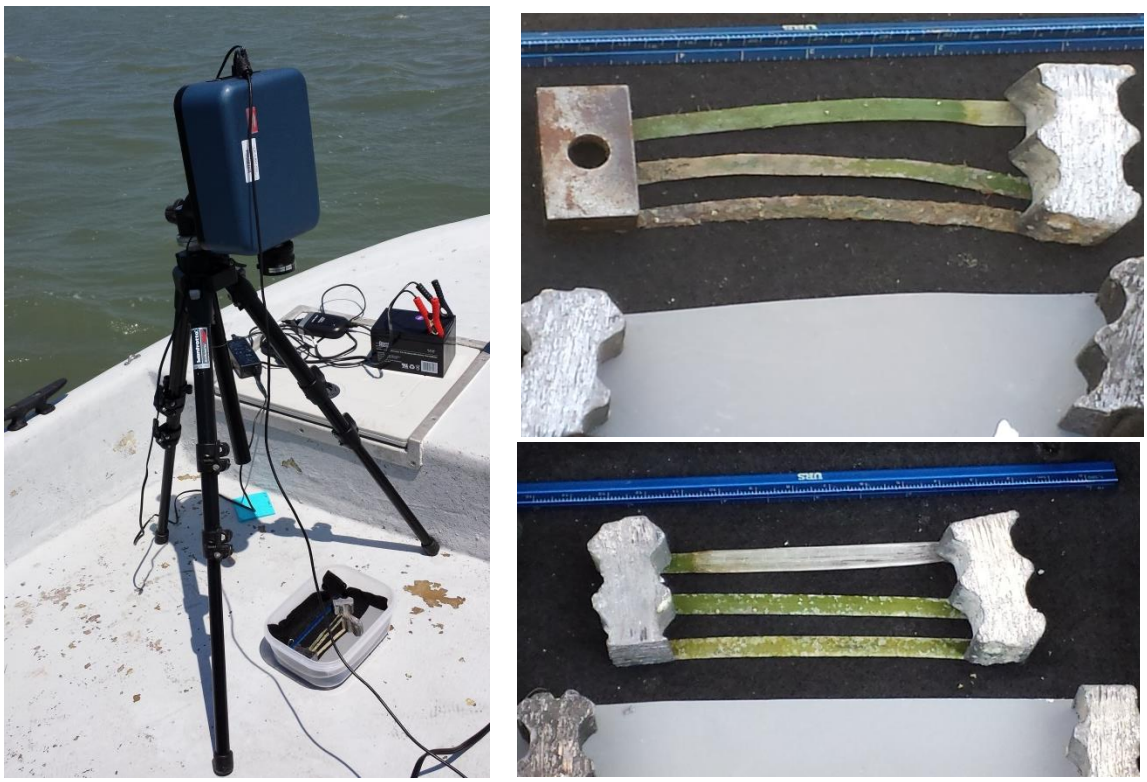

Figure 4. In-field hyperspectral imaging with the portable hyperspectral camera (left). Sampled seagrass leaf (right top, right bottom) cut to fit within the field of view of the camera. (Photos by M. Mehrubeoglu)

Hyperspectral images contain both spatial (picture-like) (see Figure 5) and spectral properties (Figure 6 - Figure 8). Both types of information can then be analyzed using image processing techniques to classify seagrass surface coverage.

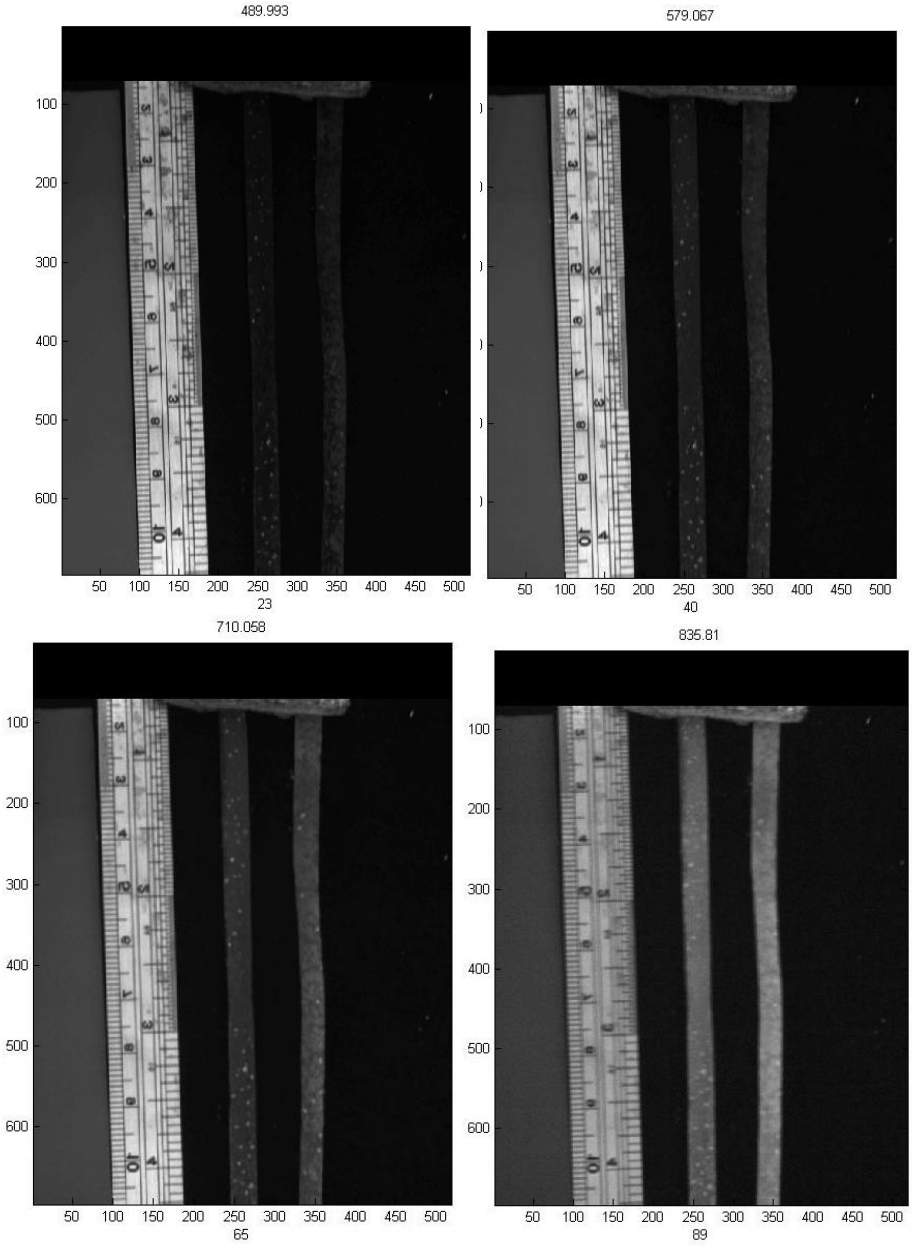

Figure 5. Hyperspectral image scans of *Thalassia* seagrass at four wave bands (X-axis label) and wavelengths (title of each image (in nm)). X- and Y-axes represents the number of pixels. The left of each image (to the left of the ruler) depicts the gray reference panel used for normalizing the images. These graphs show that different information can be extracted at different wave bands from hyperspectral images (from sampling event on October 24, 2013).

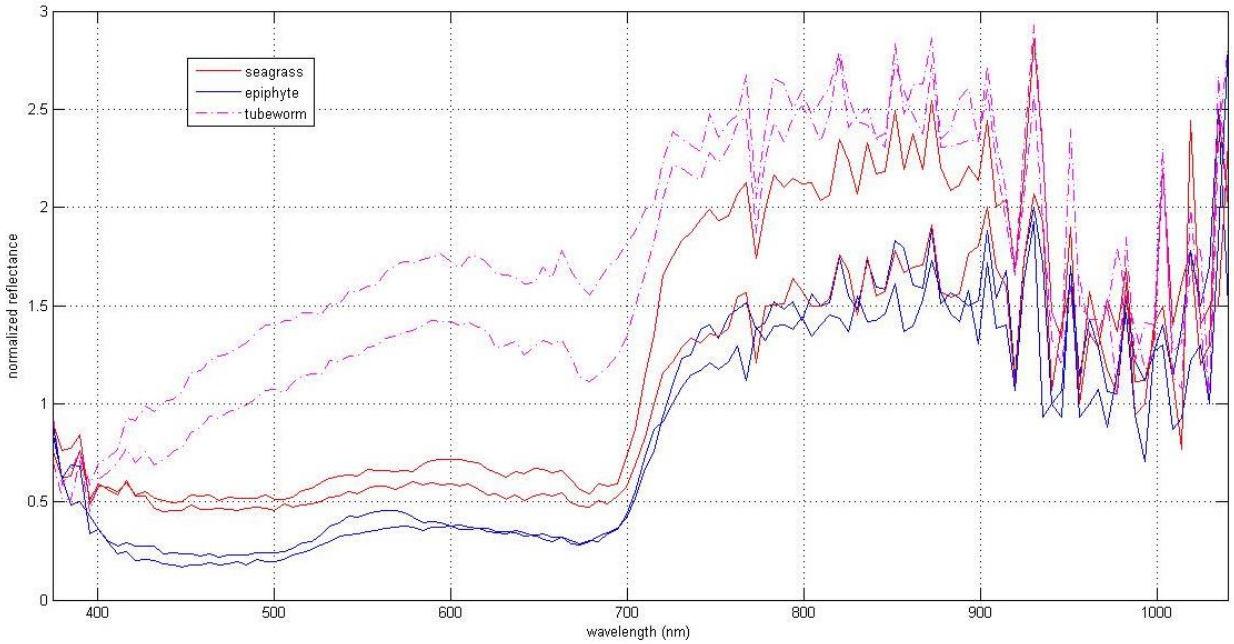

Figure 6. Normalized spectra representing seagrass leaf (unobstructed or exposed), epiphyte colony, and tubeworm obtained from hyperspectral images collected with the portable hyperspectral camera. (Data from 24 October 2013 sampling event).

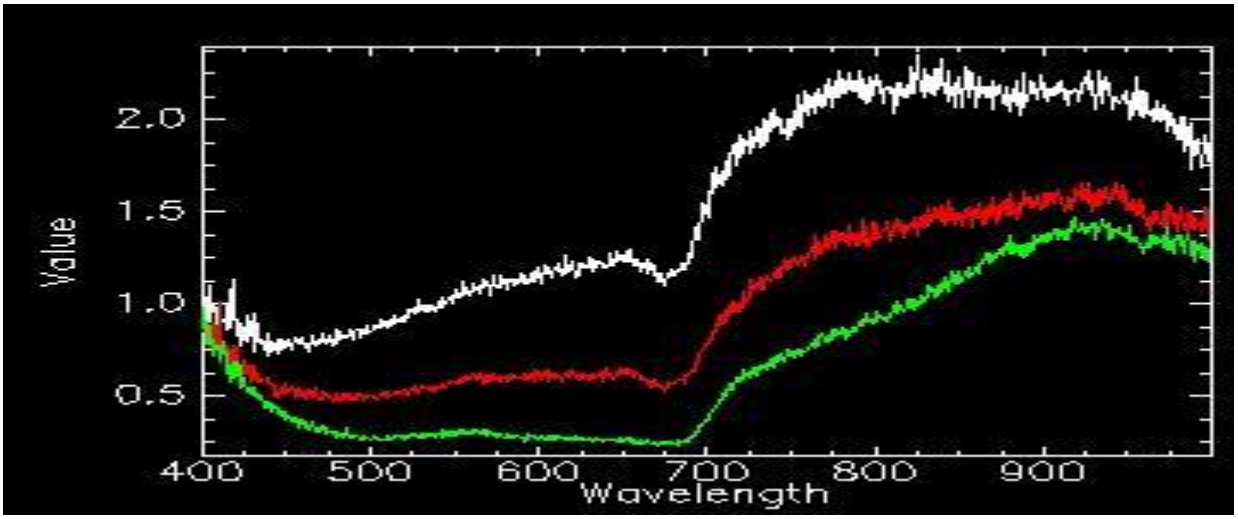

Figure 7. Normalized spectra representing seagrass leaf (bottom, green plot), sample epiphyte (middle, red plot), and tubeworm or carbonates (top, white plot) collected with the benchtop camera in the HOPI Lab. Seagrass leaf represents unobstructed or exposed, in this case, very dark green leaf pixels. Epiphyte colony was gray colored algal epiphytes. Tubeworms were white carbonates. The normalized spectra are obtained by dividing the spectral signatures by gray reference panel spectrum. (Data from 6 August 2014 sampling event). (Wavelength measured in nanometers (nm), horizontal axis. Vertical axis has no units).

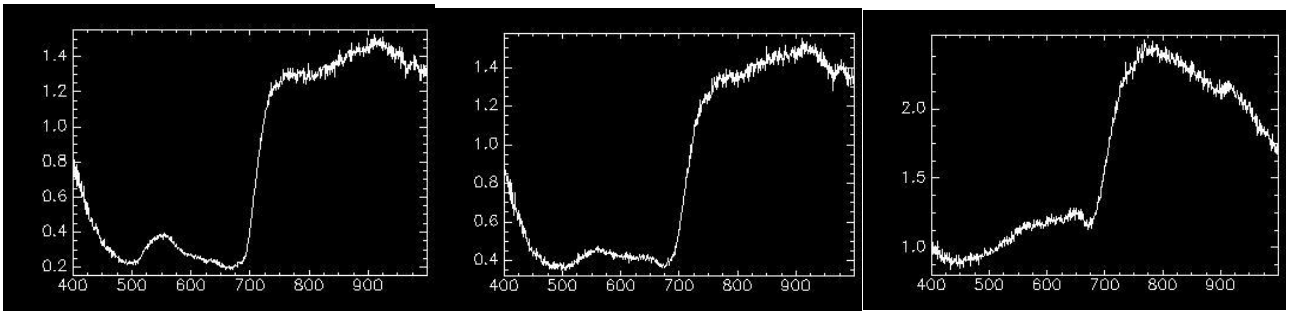

(a) **(b)** **(c)**

Figure 8. Normalized spectra of (a) (very dark) green leaf, (b) (gray-colored) algal epiphyte, and (c) tubeworm (*foraminiferan* or serpulid casing) or white carbonates shown in Figure 7 (The spectra have not been spatially smoothed).

The in-field image acquisition procedure is summarized in APPENDIX E.

2.3.1.2 Hyperspectral Image Analysis

The portable hyperspectral camera possessed 128 bands, whereas the lab-based benchtop camera can acquire images with 811 bands. The size of the images from the portable hyperspectral camera was 640x480x128 = 39,321,600 (over 39 million) pixels, whereas the size of the benchtop hyperspectral system varied between 1600x40x811 = 51,904,000 (over 51 million) to 1600x150x811 = 194,640,000 (over 194 million) pixels, constituting a challenge in image analysis due to the sheer size of the hyperspectral image files.

The hyperspectral images were analyzed using a variety of software tools, including the host software of the portable hyperspectral camera, ENVI, and MATLAB. The choice of software depended on the size of images, and algorithms developed. Hyperspectral images of seagrass leaves were normalized in ENVI software tool using the procedure described in detail in APPENDIX F.

2.3.2 Visible Scans

Visible scans refer to visible wavelength-range images obtained using a high-resolution color scanner.

2.3.2.1 Scanning Process

Visible scans were acquired by cutting the blades in a shoot into sections short enough to fit in the high-resolution scanner, similar to what was done for hyperspectral imaging. Visible scans were obtained for both sides of the seagrass leaves (front and back) with the Epson Perfection V750 Pro flatbed scanner. The individual blades were laid flat on the scanning platen, which is then flooded with ASW. In many cases, natural twisting of the leaves necessitated the application of weight (clear glass microscope slides) to keep the blade flat. Submersion was important as it minimized the air bubbles

trapped underneath the blade. Any air bubbles were removed by lightly tapping the leaf. Visible wavelength range scans were obtained using 24-bit color scanning at 1200 dpi and saved as .tiff files. Figure 9 shows a visible scan image acquired in the lab.

Figure 9. Visible wavelength range image (visible scan) of a shoot with 3 leaves

2.3.2.2 Visible Image Analysis

Visible scans were analyzed using Coral Point Count with Excel Extensions software tool (CPCe V3.6) developed by Kohler and Gill (Kohler 2006). With this tool, a user-defined number of pixels are randomly selected by the CPCe software. The number of points selected for each seagrass leaf image depended on the orientation of the leaf in the image (straight or at an angle, the latter of which results in many more background pixels), or the number of pieces cut from the leaf (in effect, the length of the entire leaf). 100 points on each leaf was targeted to establish statistical significance of results. After the number of points were randomly overlay on the image, an expert then labels each of the randomly selected pixels.

Although originally developed for coral surface analysis, the meaning of class labels was modified to meet the needs of the project: The expert was asked to classify each of the marked pixels to belong to one of the four classes: green bare seagrass leaf, epiphyte, 'senescent leaf', or 'not interested'. Background was labeled as a subcategory of 'not interested' class. Epiphytes were also labeled in subcategories as green algal epiphyte, gray algal epiphyte, unidentified epiphyte, and tubeworm corresponding to carbonate casings (see APPENDIX D for the legend used for the CPCe software).

Once the random data points in the image were labeled, the user can then create a statistical profile of the composition of the surface of the seagrass blade from visible scans (pictures) without having to analyze every single pixel. Statistical of interest in this project were percent epiphytes, percent green bare seagrass leaf, and percent tubeworms (possibly identified as *foraminiferan* or

serpulid casing (Fikes 2012)). Epiphyte to green seagrass leaf ratio was also calculated to compare with hyperspectral imaging results.

2.3.3 Fluorescence Scans

2.3.3.1 Fluorescence Image Analysis with ImageQuant

Fluorescence assays were performed on the epiphytes scraped off of the leaves from 3 whole shoots combined. The scraped matter included tubeworms, though fluorescence does not capture tubeworms signatures. In this analysis of fluorescence data, which is separate from spatial analysis of fluorescence images, pixel numbers are not considered, but rather fluorescence intensity is investigated. Fluorescence intensity is normalized "per whole shoot". These results are thus comparable to the biomass measures, as well as hyperspectral image analysis data when expressed on a whole-shoot basis. The difference between red fluorescence (red F) and green fluorescence (green F) intensities are based on the types of epiphytic algae being measured from the seagrass samples. Red F captures ALL the epiphytes, whereas green F captures only a subset of algal types. The results are used for comparative analysis other imaging techniques as well as biomass calculations. The results are presented in plate assay summaries.

2.3.3.2 Fluorescence Spatial Image Analysis with MATLAB

Image processing techniques were used in code written in MATLAB software tool for this purpose. First the fluorescence images were converted to binary (black and white only) images using thresholding. Then pixels above the threshold were counted, and recorded. Green F represents epiphyte coverage. Red F captures all epiphytic and seagrass blade information. Red F images were therefor used to represent the seagrass blade area. Pixel counts from binary green F images were divided by those from red F images and multiplied by 100 to find the % epiphyte coverage using the following formula:

$$\% \text{ Epiphyte Coverage} = P_{epi} / P_{leaf} * 100,$$

Where P_{epi} represents the total number of pixels from thresholded binary red F images, and P_{leaf} represents the total number of pixels from thresholded binary green F images. The results and images are presented in Section 3.2.5.

2.4 Other Laboratory Measurements

2.4.1 Biomass for Fluorescence Imaging

For biomass analysis, after the seagrasses were scanned, leaves of each imaged shoot are transferred to a flat-bottomed plastic tray with a small volume (approximately 10 mL) of distilled water and scraped with glass microscope slides to remove epiphytes as completely as possible without excessive removal of the seagrass leaf cells. Removed epiphytes are quantitatively collected and transferred with DI water rinses into 50 mL graduated centrifuge tubes. Volume is adjusted to a standard final

volume (typically 25 mL) and recorded. Representative aliquots (0.5 mL; volume recorded) of the removed epiphytes are transferred to 1.7 mL microcentrifuge tubes and stored dark at 4° C for subsequent fluorescence plate assay measurements. The remainder of the removed epiphytes are quantitatively transferred into pre-labeled, pre-weighed 7 cm diameter aluminum dishes and dried to constant weight at 60° C for determinations of epiphyte dry weight. Dry weights of whole-shoot samples are corrected for the removed aliquots. Seagrass leaves from which epiphytes were removed are transferred into pre-labeled, pre-weighed paper bags or plastic beakers and dried to constant weight at 60° C for determinations of seagrass dry weight.

2.4.2 HPLC-Related Measurements

2.4.2.1 Sampling for HPLC

In the early sampling trips, HPLC was performed on whole leaf samples that were brought back from the field. In the latest sampling trips, leaf hole punches from 10 leaves were obtained in the field from top (oldest), middle, and bottom (youngest) parts of each blade with about 3 mm diameter, and stored in small opaque test tubes to minimize light interaction, and stored in a cooler with ice (see Figure 10 and Figure 11). Once returned to the lab, the punched leaf discs were immediately placed in the freezer at -80^{o} overnight or until analyses to break the cell wall to make the extraction of pigments easier. The leaf disks were then individually ground using mortar and pestle with 2 ml of 100% acetone, and extracted in the dark at 4^{o}C for 4 hours. Extracts were filtered. Phytoplankton community composition was assessed by pigment analysis using high performance chromatography (HPLC) methodology described by Zimba (Zimba *et al.* 1999). Pigments (carotenoids and chlorophylls) were quantified using a HP1100 equipped with DAD and fluorescence detectors (Agilent Technologies, Palo Alto, CA). Identification of specific divisions of algae is possible using taxon-specific pigment biomarkers. A pigment library was used to identify samples; unknown samples were quantified by linear regression of known commercial standards.

Figure 10. Leaf punches from a single shoot (3 seagrass leaves) taken during the sampling event in the field on the boat. Three hole punches were made on each seagrass leaf, one from the top, one from the middle, and one from the bottom. (Photo by M. Mehrubeoglu)

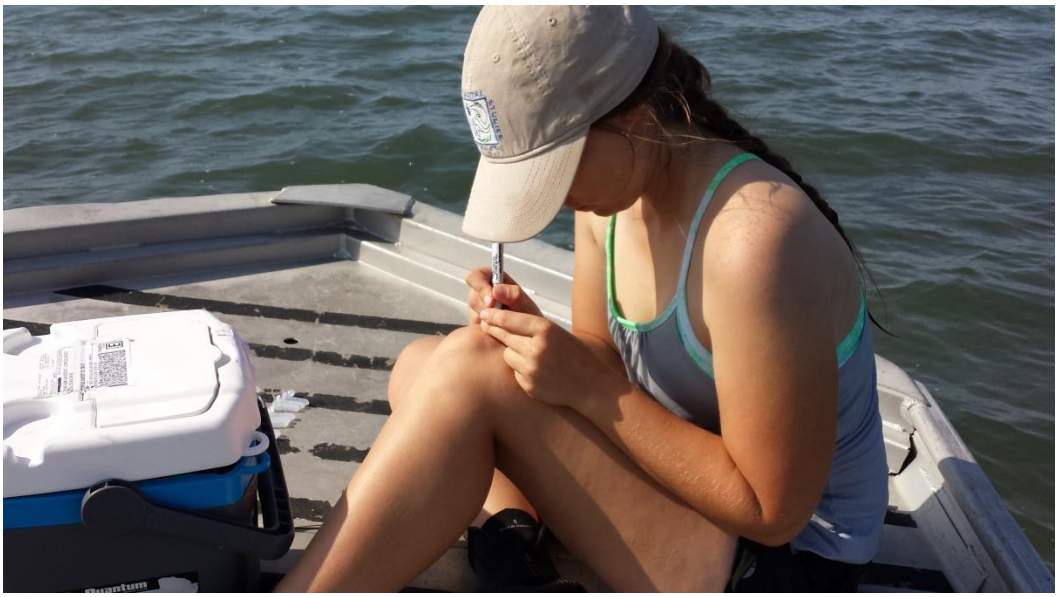

Figure 11. Labeling and storing seagrass leaf punches in the field. (Photo by M. Mehrubeoglu)

2.4.2.2 Epiphyte Removal Efficiency from Seagrasses

As part of this CMP grant, the traditional method of epiphyte removal (scraping) versus a chemical treatment method (MES buffer with shaking) was evaluated. As part of this study, an alternative epiphyte removal procedure that was effective in epiphyte removal, and did not damage the seagrass leaves was developed by the HPLC lab. A physiological buffer (pH 6) was used to dissolve carbonates, while minimizing dissolution of plant material. The efficacy relative to the scrape method was then evaluated.

Shoots of the seagrasses *Thalassia testudinum* and *Halodule wrightii* were collected from three south Texas estuaries separate from the sampling events described in the rest of this report as an independent assessment of methodology. Samples from Laguna Madre included three northern locations along the western shoreline, with additional samples collected from Bahia Bay and Redfish Bay between Rockport and Port Aransas. Individual short shoots were individually bagged and stored in the dark until processing in the laboratory. Laboratory lighting was minimized (red lights) to prevent pigment damage during all processing steps.

2.4.2.2.1 Scraping Method

Individual seagrass blades were placed on Plexiglas sheets (250x250 cm) and a glass slides was used to scrape both top and bottom surfaces (Dauby and Poulicek 1995). Epiphyte material was added to a microcentrifuge tube and immediately frozen (-80C). Microcentrifugre tubes were extracted using 100% acetone for carotenoid, xanthophylls, and chlorophylls as previously described (Zimba et al. 1999). Seagrass blades were dried (60C) and weights were recorded. Seagrass blades were extracted in 100% acetone then

pigments quantified as previously described (Zimba et al. 1999). (We note that for data of this research scraping method was used.)

2.4.2.2.2 MES Buffer

Blades were placed in 50 mL polypropylene test tubes and 10 mls MES Buffer was added to each tube (0.1 M, pH 6.1). Tubes were shaken at 1 revolution/second for 60 seconds. Blades were removed from the centrifuge tube after agitation, and subsamples of dislodged material were concentrated on glass fiber filters (GF/C, 1.2 micrometer pore size). Filters were frozen at -80C until analyses.

2.4.2.2.3 Pigment Analyses

Pigment analyses were made of epiphyte and seagrass blades using HPLC-DAD methods (Zimba et al. 1999). Area counts for each pigment were confirmed by authentic standards used to generate standard curves for each pigment. Data was normalized to blade weight. Results are reported in Section 3.2.11.1 Epiphyte Removal Efficiency from Seagrasses.

3. RESULTS AND DISCUSSION: DATA AND IMAGE ANALY-SES

3.1 Physicochemical Assessments of Sampling Sites

3.1.1 Light Attenuation

Sampling sites were too shallow to utilize the secchi disk method to assess light penetration to the seagrass canopy. However, LiCor PAR (Photosynthetically Active Radiation) sensors were used to assess light attenuation with depth and to calculate K_d, the light attenuation coefficient (higher values corresponding to greater turbidity and less light penetration). K_d is computed from the slope of the data in Figure 13 and Figure 14. Measurements performed on two occasions approximately 1 year apart showed consistent relative rankings of light attenuation comparing the 3 sites (see Table 1 and Figure 12).

Table 1. Percent surface irradiance (% SI) and light attenuation coefficient (K_d) collected in field in summer in 2013 and 2014 at three different locations (X: 7B-Alt, Y: 21B, Z: Steadman's Island)

	8/25/2013		8/09/2014	
SITE	**% SI**	**K_d (m^{-1})**	**% SI**	**K_d (m^{-1})**
X	55.9	1.53	64.9	0.74
Y	40.9	2.12	70.2	1.76
Z	20.3	1.74	59	0.88

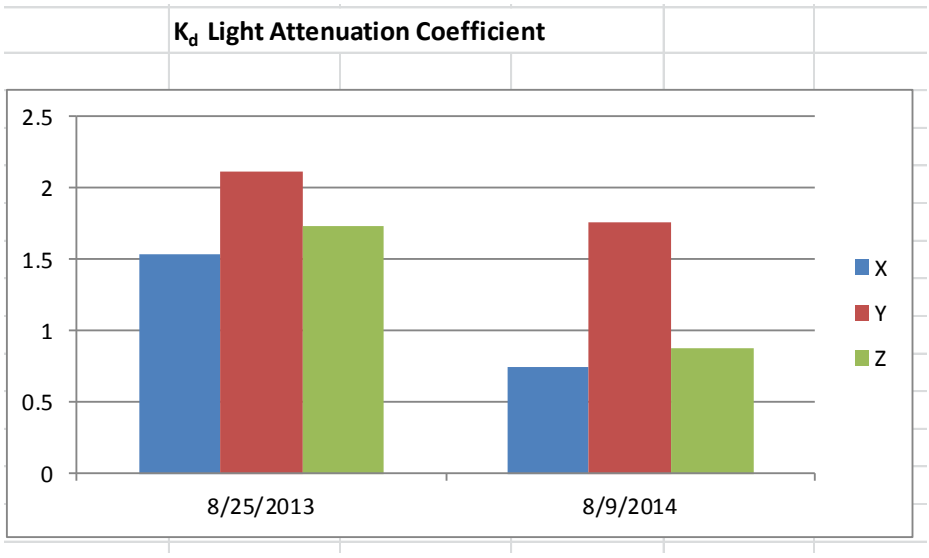

Figure 12. Light attenuation coefficient calculated at three sites from two sampling trips about a year apart (2013 and 2014). (X: 7B-Alt, Y: 21B, Z: Steadman's Island). Light attenuation coefficient is found as the slope of light vs. depth plots in Figure 13and Figure 14.

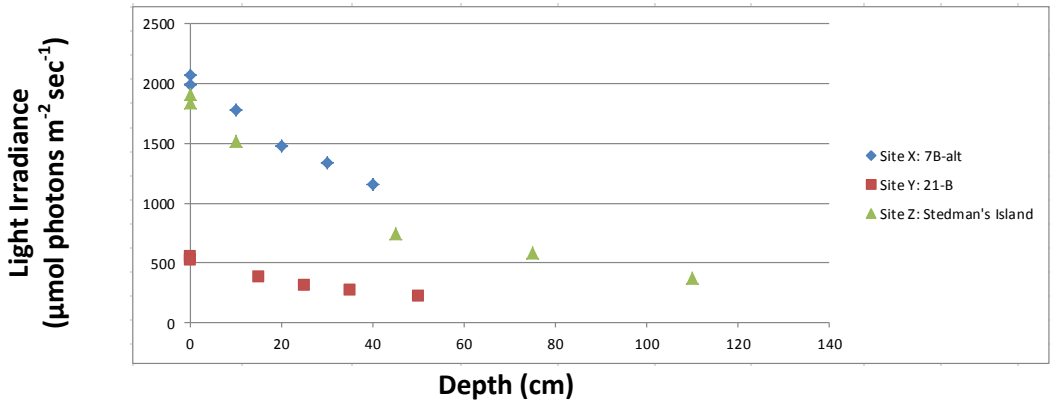

Figure 13. Light attenuation plots from 25 August 2013 sampling event.

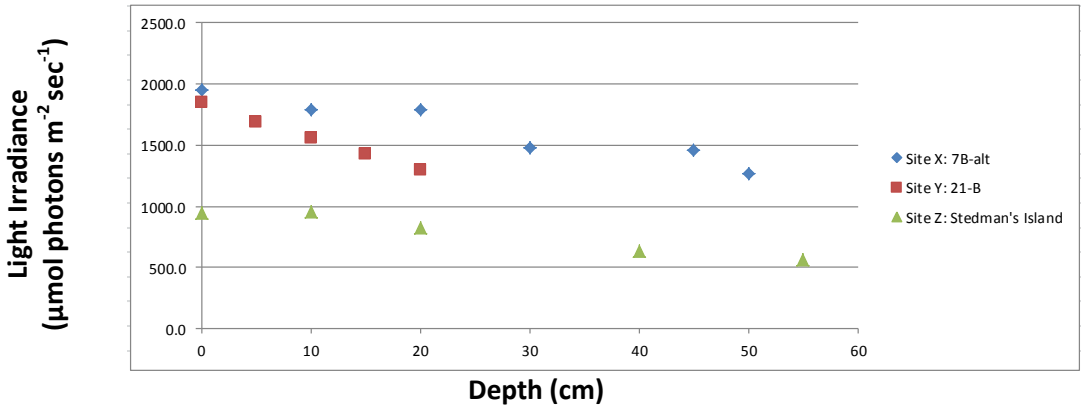

Figure 14. Light attenuation plots from 9 August 2014 sampling event.

Site 21B (Y) exhibited the greatest light attenuation coefficients, followed by Stedman's Island (Z) and 7B-Alt (X). This may be a reflection of greater degrees of open fetch, muddy bottom and less vegetative coverage at Site 21B. The latter assertion is supported by the consistently lower shoot density observed in cores from Site 21B (Figure 15, 4 sampling events). However, % Surface Irradiance at seagrass canopy height was in all cases sufficiently high (above 20% SI) to support healthy seagrass (Table 1). But this Site 21B clearly stood out as different.

Mean # Shoots/Core

Name	7/25/2013	8/24/2013	8/6/2014	8/9/2014
X	25.67	21.67	12.00	15.67
Y	11.00	8.00	3.67	13.67
Z	16.00	12.00	12.00	15.00

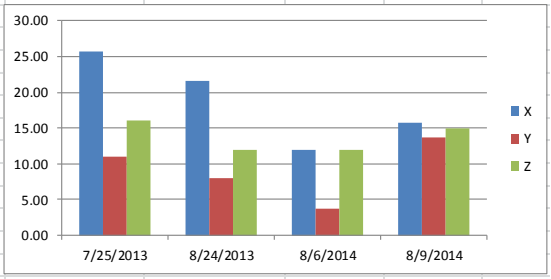

Below Ground Biomass/Core

Name	7/25/2013	8/24/2013	8/6/2014	8/9/2014
X	5.61	7.27	19.27	6.74
Y	1.70	1.27	0.92	5.77
Z	4.80	3.40	8.98	9.59

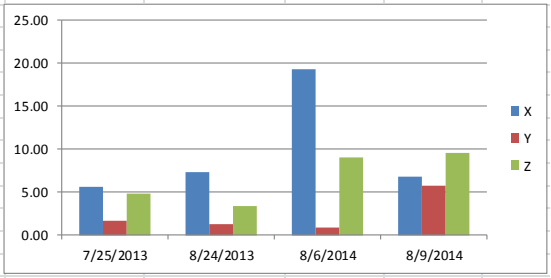

Above Ground Biomass/Core

Name	7/25/2013	8/24/2013	8/6/2014	8/9/2014
X	4.74	4.98	5.25	4.51
Y	1.91	1.59	1.70	4.63
Z	2.80	2.60	4.28	6.65

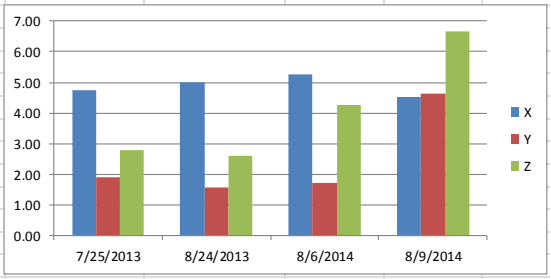

Root/Shoot Ratio

Name	7/25/2013	8/24/2013	8/6/2014	8/9/2014
X	1.23	1.46	3.74	1.50
Y	0.88	0.76	0.67	1.31
Z	1.77	1.20	2.15	1.55

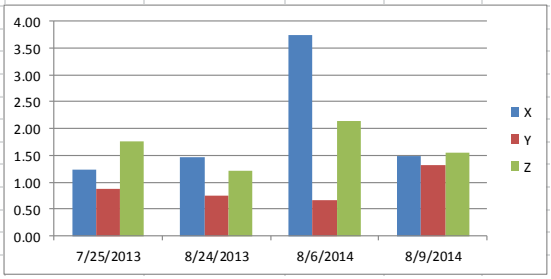

Figure 15. Core analysis from 4 sampling events (7/15/2013, 8/24/2013, 8/6/2014, 8/9/2014)

3.1.2 Water Quality

Water quality measurements and other field information from sites are summarized in Table 2 and 3.

Table 2. Field data collected for the project on water quality during 2013 (nd: no data)

FIELD DATA														
Date Collected (2013)	Time (hhmm)	Station # and Name	Station Depth (m)	Latitude (N)	Longitude (W)	Water Sample Depth (m)	Depth Realm	Water Temp. (°C)	Dissolved Oxygen	Percent Saturation	Salinity	Conductivity	pH	Turbidity
05/13/13	0944	7B	0.78	27.95485	97.09572	0.05	surface	22.93	5.62	77.8	22.54	35229	8.1	nd
05/13/13	0944	7B	0.78	27.95485	97.09572	0.774	canopy	22.92	4.58	78.9	23.63	38282	8.1	nd
05/13/13	1115	21B	0.50	27.91629	97.08855	nd	nd	nd	nd	nd	nd	nd	nd	nd
05/13/13	1150	SI	0.50	27.88610	97.11481	nd	nd	nd	nd	nd	nd	nd	nd	nd
07/25/13	0950	7B	nd	27 57 18.7	97 05 46.9	0.152	surface	28.82	5.69	91.3	38.67	58121	7.9	nd
07/25/13	0950	7B	nd	27 57 18.7	97 05 46.9	0.305	canopy	28.83	5.68	91.4	38.69	58157	7.9	nd
07/25/13	1130	21B	0.508	27 54 58.1	97 05 17.0	0.152	surface	30.43	11.22	184.9	38.62	58137	8	nd
07/25/13	1130	21B	0.508	27 54 58.1	97 05 17.0	0.254	canopy	30.42	11.34	186.9	38.67	58195	8	nd
07/25/13	1225	SI	0.406	27 53 09.8	97 06 53.7	0.152	surface	31.55	19.08	322	39.65	59556	8.4	nd
07/25/13	1225	SI	0.406	27 53 09.8	97 06 53.7	0.305	canopy	31.58	18.57	314.5	39.66	59564	8.4	nd
08/14/13	1020	SI	nd	27 53 10.6	97 06 52.8	0.2	surface	29.70	8.89	147.2	41.3	62277	8.2	nd
08/14/13	1020	SI	nd	27 53 10.6	97 06 52.8	0.6	canopy	29.72	9.33	156.1	41.83	62324	8.3	nd
08/24/13	1056	SI	0.97	27 53 10.9	97 06 50.6	0.49	surface	30.25	7.41	121.5	38.41	57821	8.1	nd
08/24/13	1056	SI	0.97	27 53 10.9	97 06 50.6	0.70	canopy	30.28	6.92	113.7	38.48	57923	8.2	nd
08/24/13	1259	21B	0.70	27 54 949	97 05 303	0.06	surface	30.29	5.95	98.4	39.09	58725	8.1	nd
08/24/13	1259	21B	0.70	27 54 949	97 05 303	0.25	canopy	30.28	5.92	97.3	38.94	58523	8.1	nd
08/24/13	1430	7B	0.80	27 57 307	97 05 750	0.05	surface	30.57	7.75	127.5	38.23	57600	8.3	nd
08/24/13	1430	7B	0.80	27 57 307	97 05 750	0.28	canopy	30.62	7.86	129.2	38.43	57835	8.3	nd
08/25/13	1100	SI	0.97	27 53 10.9	97 06 50.6	nd	nd	nd	nd	nd	35.00	nd	nd	nd
08/25/13	1300	21B	0.70	27 54.949	97 05.303	nd	nd	nd	nd	nd	34.00	nd	nd	nd
08/25/13	1430	7B	0.80	27 57.306	97 05.749	nd	nd	nd	nd	nd	33.00	nd	nd	nd
10/20/13	0827	7B	0.39	27 57 18.0	97 05 43.5	0.04	surface	21.13	5.72	78.5	34.20	51904	7.8	nd
10/20/13	0827	7B	0.39	27 57 18.0	97 05 43.5	0.12	canopy	21.14	5.63	77.3	34.20	51906	7.9	nd
10/20/13	0923	SI	0.338	27 53 06.2	97 07 00.0	Nd	surface	20.03	6.35	83.4	31.16	47756	8	nd
10/20/13	0923	SI	0.338	27 53 06.2	97 07 00.0	0.147	canopy	19.38	6.08	79.8	31.92	48771	8.1	nd
10/24/13	1458	7B	0.748	27 57 17.9	97 05 43.4	0.36	surface	25.77	14.03	213.1	36.15	54625	8.3	nd
10/24/13	1458	7B	0.748	27 57 17.9	97 05 43.4	0.479	canopy	25.78	14.93	225.7	36.15	54638	8.3	nd
10/24/13	1347	21B	0.687	27 54 58.6	97 05 18.4	0.363	surface	23.71	11.09	160.6	35.37	53528	8.2	> SI
10/24/13	1347	21B	0.687	27 54 58.6	97 05 18.4	0.571	canopy	23.71	11.28	163.6	35.36	53516	8.2	nd
10/24/13	1232	SI	0.63	27 53 06.9	97 07 00.2	0.36	surface	23.92	13.55	198.4	34.70	52714	8.3	< 21B
10/24/13	1232	SI	0.63	27 53 06.9	97 07 00.2	0.59	canopy	23.95	14.08	204	34.76	52711	8.3	nd

Table 3. Field data collected for the project on water quality during 2014
(sur: surface, can: canopy, SI: Steadman's Island; nd: no data)

FIELD DATA															
Date Collected (2014)	Time (hhmm)	Station # and Name	Station Depth (m)	Latitude (N)	Longitude (W)	Water Sample Depth (m)	Depth Realm	Water Temp. (°C)	Dissolved Oxygen	Percent Saturation	Salinity	Conductivity	pH	Turbidity	Barometric Pressure
08/06/14	1050	7B	0.50	nd	nd	0.00	sur	31.56	7.36	126.0	42.55	63392	8.6	0.0	765.2
08/06/14	1050	7B	0.50	nd	nd	0.50	can	31.59	7.44	127.4	42.55	63370	8.6	4.5	765.2
08/06/14		21B	0.60	nd	nd	0.54	sur	31.48	7.54	125.4	40.22	60306	8.2	7.1	766
08/06/14		21B	0.60	nd	nd	0.60	can	31.41	7.48	126.0	40.27	60354	8.2	9.3	766
08/06/14	1400	SI	0.70	nd	nd	0.50	sur	32.06	9.26	158.1	40.59	60810	8.2	5.0	766.1
08/06/14	1400	SI	0.70	nd	nd	0.70	can	32.03	9.44	160.9	40.6	60825	8.2	6.1	766
08/09/14	0915	SI	0.75	27.88576	97.11519	0.00	sur	29.91	5.66	93.8	41.09	61358	8.3	-0.3	nd
08/09/14	0915	SI	0.75	27.88576	97.11519	0.09	can	29.84	5.67	94.0	41.10	61393	8.2	0.1	nd
08/09/14	1057	21B	0.36	27.915815	97.08389	0.122	sur	30.12	5.62	92.8	40.42	60483	8.2	9.4	nd
08/09/14	1057	21B	0.36	27.915815	97.08389	nd	can	nd	nd	nd	nd	nd	nd	nd	nd
08/09/14	1230	7B	0.66	27.955	97.09648	0.122	sur	31.11	8.14	138.7	41.94	62542	8.3	-2.8	nd
08/09/14	1230	7B	0.66	27.955	97.09648	0.006	can	31.11	8.65	146.6	41.96	62557	8.3	-2.3	nd

3.2 Biological Assessments of Sampling Sites

3.2.1 Biomass Parameters from Core Samples

Site 21B consistently stands out with lowest mean number of shoots per core, lowest mean below-ground biomass, lowest mean above-ground biomass, and lowest mean ratio of below-ground to above-ground biomass (Figure 15, 4 sampling events). In contrast, Site 7B-Alt generally exhibited the highest values for these parameters. These data support field observations that the *Thalassia testudinum* seagrass beds were most robust at Site 7B-Alt and least so at Site 21B.

3.2.2 Biomass Assessments of Epiphytes and Seagrass Leaf Weights for 3 Whole Shoots

Epiphytes were removed by scraping and biomass determined. Site 7B-Alt consistently had the lowest mean epiphyte biomass to mean leaf biomass ratio (Figure 16). Site 21B had the highest mean epiphyte biomass (on a 3-shoot basis) for 3 of the 4 samplings, while Stedman's generally ranked low for leaf biomass (on a 3-shoot basis) and Site 21B ranked variably in this category.

The ratio may be most-telling as this would indicate epiphyte accumulation relative to the seagrass leaf material present. (Note that tubeworms are included in the epiphyte biomass assessment).

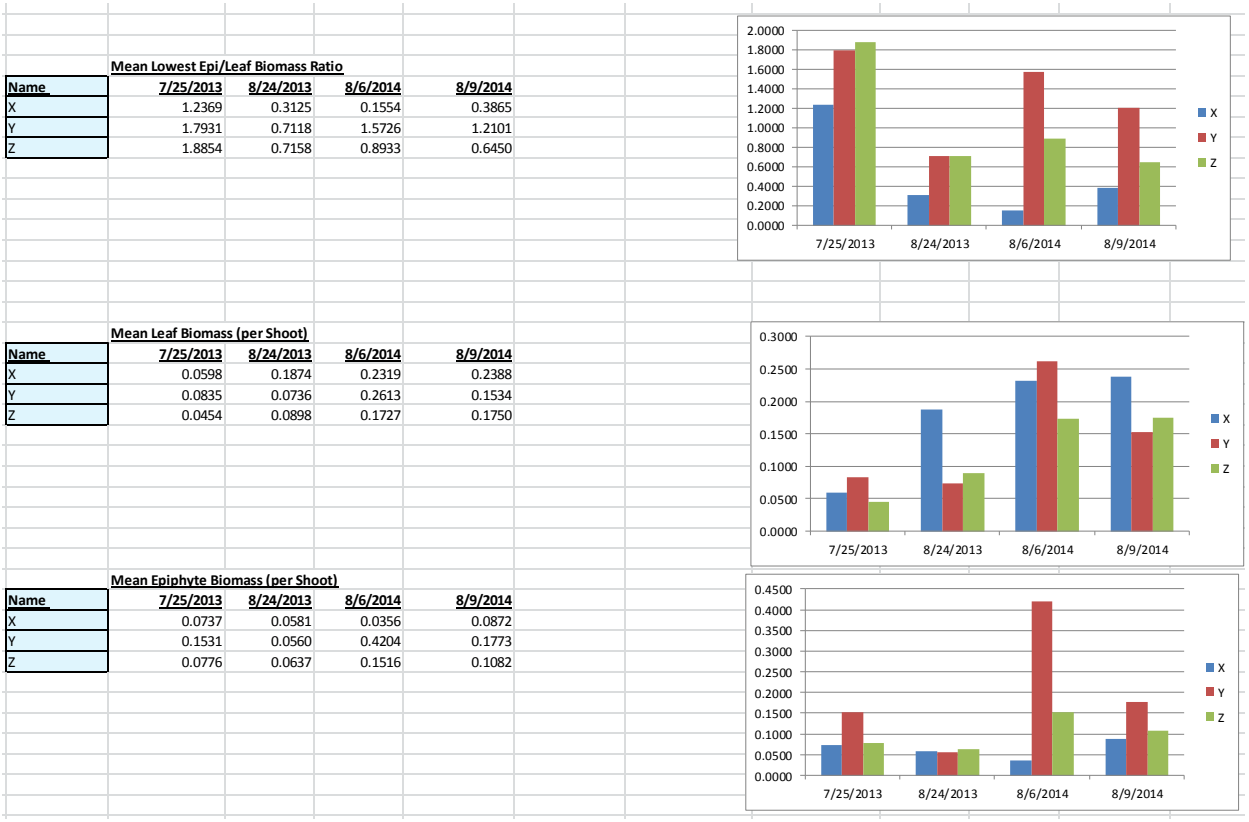

Mean Lowest Epi/Leaf Biomass Ratio

Name	7/25/2013	8/24/2013	8/6/2014	8/9/2014
X	1.2369	0.3125	0.1554	0.3865
Y	1.7931	0.7118	1.5726	1.2101
Z	1.8854	0.7158	0.8933	0.6450

Mean Leaf Biomass (per Shoot)

Name	7/25/2013	8/24/2013	8/6/2014	8/9/2014
X	0.0598	0.1874	0.2319	0.2388
Y	0.0835	0.0736	0.2613	0.1534
Z	0.0454	0.0898	0.1727	0.1750

Mean Epiphyte Biomass (per Shoot)

Name	7/25/2013	8/24/2013	8/6/2014	8/9/2014
X	0.0737	0.0581	0.0356	0.0872
Y	0.1531	0.0560	0.4204	0.1773
Z	0.0776	0.0637	0.1516	0.1082

Figure 16. Mean leaf and mean epiphyte biomass computations from 4 sampling events (7/25/2013, 8/24/2013, 8/6/2014, 8/9/2014)

3.2.3 Leaf Counts Per Shoot from 3 Whole Shoots

Leaf counts per shoot were quantified from visible and fluorescence scanning data (Figure 17). Mean values for 3 whole shoots showed that Site 7B-Alt generally had higher leaf counts (4 out of 6 sampling events) and are consistent with more robust seagrass growth at this site. (No sample data is available from Steadman's Island from May 2013)

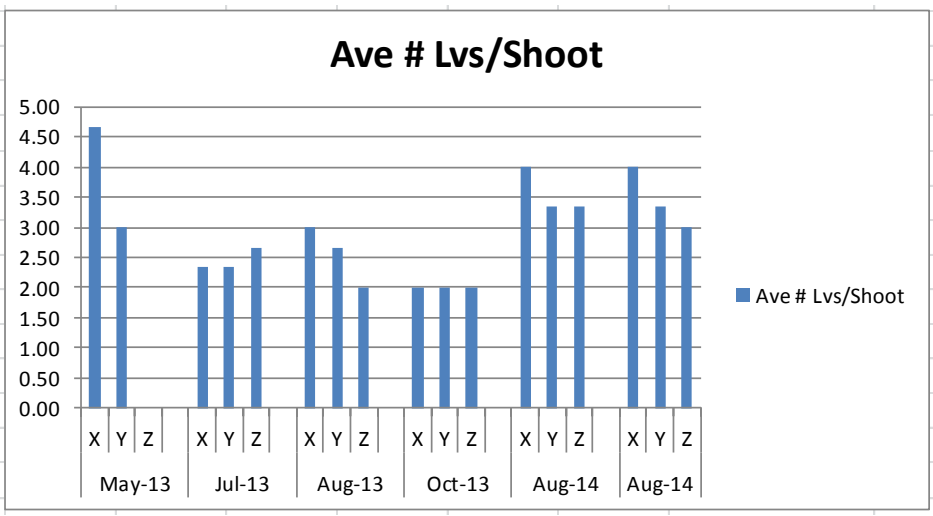

Figure 17 Average number of seagrass leaves per shoot from 6 independent sampling events (X: 7B-Alt, Y: 21B, Z: Steadman's Island)

3.2.4 Leaf Area Estimates From Fluorescence Scanning and Comparison to Leaf Biomass (with IMAGEQUANT)

Fluorescence scanning proxies for leaf area were obtained from the *Red Number of Pixels* parameter (Red Fluorescence) (Figure 18) and compared to epiphyte-free leaf biomass obtained for the exact same 3 shoots used in scans of each sample (Figure 19). Site 7B-Alt consistently had the highest number of red F (fluorescence) pixels (per shoot) and Stedman's Island generally had the lowest.

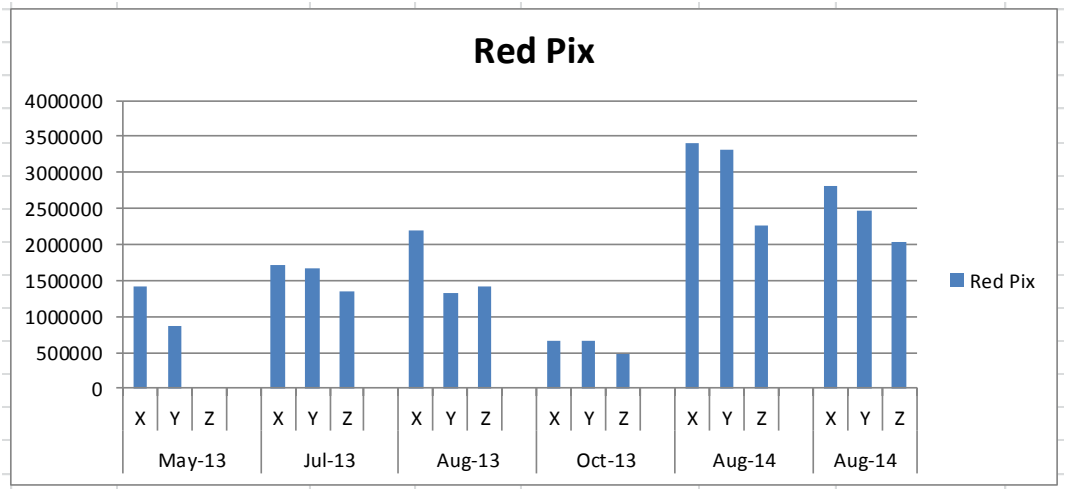

Figure 18. Leaf area in pixels (vertical axis) across 3 locations and 6 sampling events (X: 7B-Alt, Y: 21B, Z: Steadman's Island; sampling from 13 May 2013, 25 July 2013, 24 August 2013, 24 October 2013, 6 August 2014, 9 August 2014).

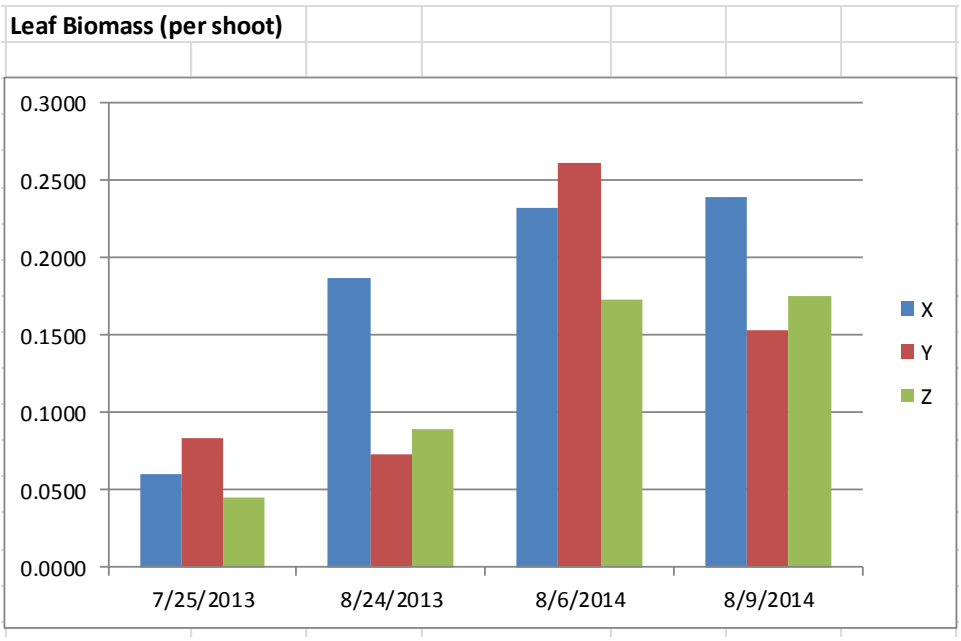

Figure 19. Average leaf biomass per shoot per location per sampling date (X: 7B-Alt, Y: 21B, Z: Steadman's Island; sampling from 25 July 2013, 24 August 2013, 6 August 2014, 9 August 2014).

In comparisons of 7B-Alt vs. Steadman's Island, Site 7B-Alt consistently exhibited higher numbers of red pixels and leaf biomass (as well as a greater number of leaves per shoot, leaf biomass per shoot and leaf biomass per core as seen above). The relative levels of fluorescence scan-based red pixel number and the corresponding biomass per shoot data in Figure 18 and Figure 19 were correlated for each sampling event for 7B-Alt and Steadman's Island.

Inconsistencies arose in the relative rankings of the red pixel and leaf biomass data for samples from Site 21B compared to the same from the other two sites. However, it is known that the red pixel number over-estimates leaf area when there are abundant filamentous algal epiphytes or when heavy epiphyte accumulations are knocked loose and separate from the leaf on the fluorescence scanning platen. In each case, epiphyte material lying outside the boundaries of the leaf area proper, fluoresces and falsely contributes to interpreted leaf area. Thus, this inconsistency in leaf area-leaf biomass for Site 21B is actually consistent with the high epiphyte accumulations at this site deduced from Figure 20. Even with this observation of site comparisons, it is important to note that the seasonal trends for 21B correlate perfectly over the 4 sampling events between red fluorescence pixel counts, and biomass calculations (Figure 18 and Figure 19).

3.2.5 Epiphyte Accumulations Estimated From Fluorescence Scanning of Leaf Samples and Comparison to Epiphyte Biomass For the Exact Same Scanned Leaves (per 3 shoots)

Total green fluorescence (Figure 20) was expected to correlate with epiphyte biomass as an indicator of epiphyte abundance. Site 7B-Alt generally had the lowest average epiphyte green fluorescence over average of 3 shoots (except for Aug 2013 samples which had abnormally high values for unaccounted reasons in Figure 20). This finding compares favorably with low epiphyte biomass seen at 7B-Alt (Figure 21); however, 21B generally had the highest epiphyte biomass (except for August 2013 data, Figure 21) whereas total green fluorescence did not always make this distinction. The most likely explanation may be that there are differences in the algal epiphyte communities, which would alter the relationship between relative green fluorescence levels and relative biomass levels. Not all algal types have equivalent fluorescence, *or biomass*, but fluorescence is more sensitive to changes in algal epiphyte community.

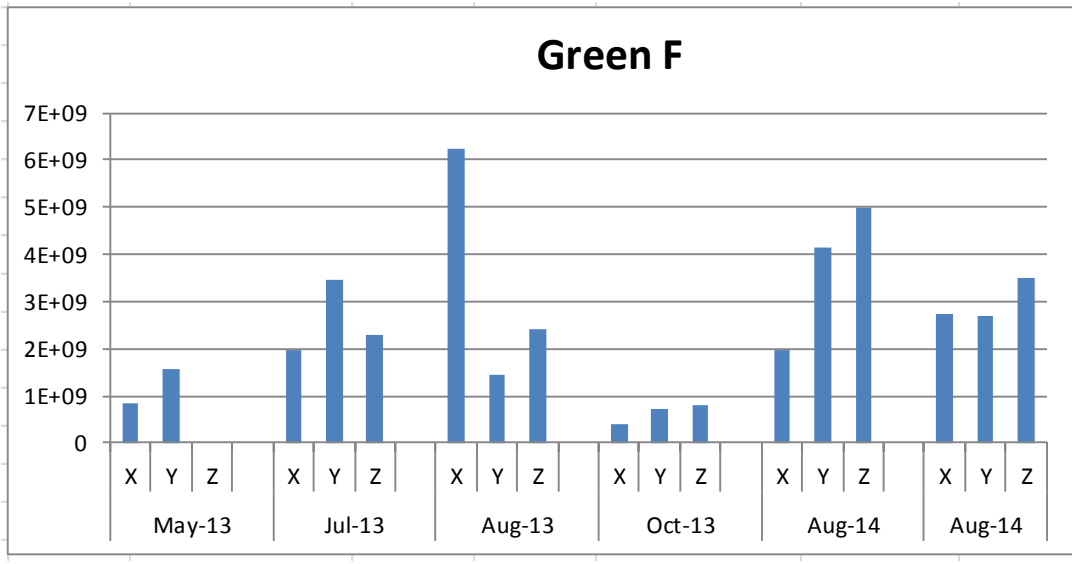

Figure 20. Green Fluorescence (Green F) based epiphyte surface area computations from pixel count (vertical axis: green fluorescence (epiphyte) pixel count of leaf area). (No fluorescence scans were recorded for leaves sampled from Steadman's Island on 13 May 2013)

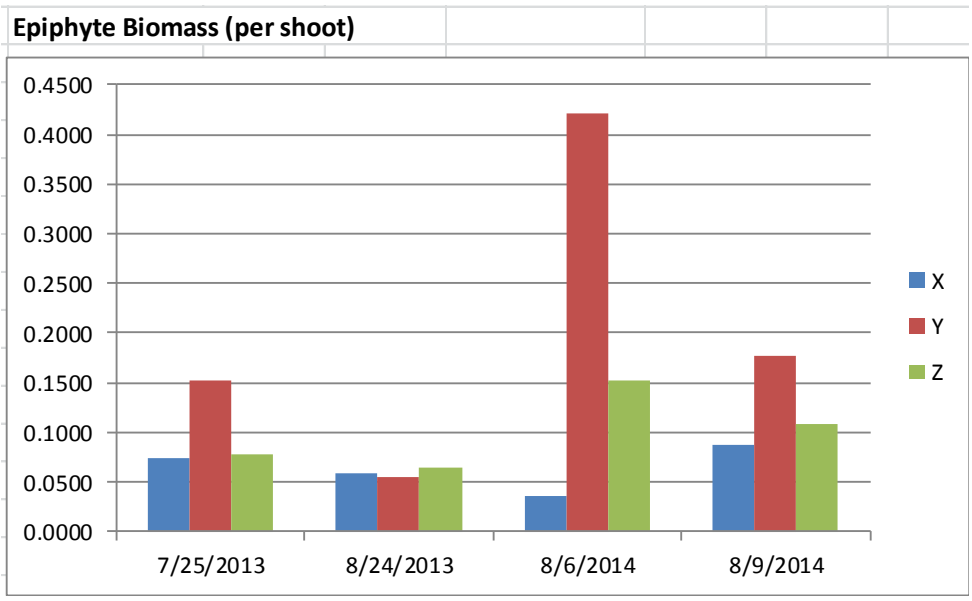

Figure 21. Epiphyte biomass measurements (average over a shoot) at 3 locations over 4 sampling events (X: 7B-Alt, Y: 21B, Z: Steadman's Island).

3.2.6 Spatial Analysis of Epiphyte Coverage Detected by Fluorescence Scanning

Figure 22 shows the fluorescence scan images of green (left) and red (right) fluorescence scans. Green was used to identify pixels representing epiphytes. Red was used to determine the total area of seagrass leaves in pixels.

Figure 22. Fluorescence scan of green (left) and red (right) from a single shoot with three seagrass leaves. Samples were collected from Site 21B.

A measure of epiphyte accumulation which may be important for seagrass ecophysiology is the relative amount of the leaf surface area that has been colonized and covered by epiphytes (percent coverage). This spatial information can be obtained by counting pixels that are classified as epiphyte (green fluorescence pixels) relative to the total number of seagrass leaf image pixels (approximated by red fluorescence pixels). The latter (red fluorescence pixels) captures both leaf and its surface coverage. As an example of this type of image analysis, the leaves of a whole shoot from each site was analyzed by classifying image pixels using thresholding technique and then counting the pixels (see Figure 23 and Figure 24) above or below the threshold, depending on how the algorithm is set up (See APPENDIX H for the MATLAB program to compute percent coverage of epiphytes using spatial analysis of fluorescence images). Site 7B-Alt had the lowest % leaf coverage by epiphytes (41%) compared to approximately 47% for 21B and 45% for Stedman's Island (Figure 25). The site differences in the rankings of % coverage are similar to rankings by the other measures of epiphyte accumulation. However, and perhaps surprisingly, the relative differences in coverage between sites seemed small compared to relative differences observed for other epiphyte accumulation metrics. Comparison of the largest 3 leaves of the shoots from each site yielded % coverage ranges (oldest to youngest leaf, respectively) of 66-87%, 46-62% and 10-30%. The discrepancy of % coverage between each side of the same leaf was between 1% and 4% (Figure 25) for the

difference between average % coverage on top and average % coverage at the bottom of a single shoot of blades).

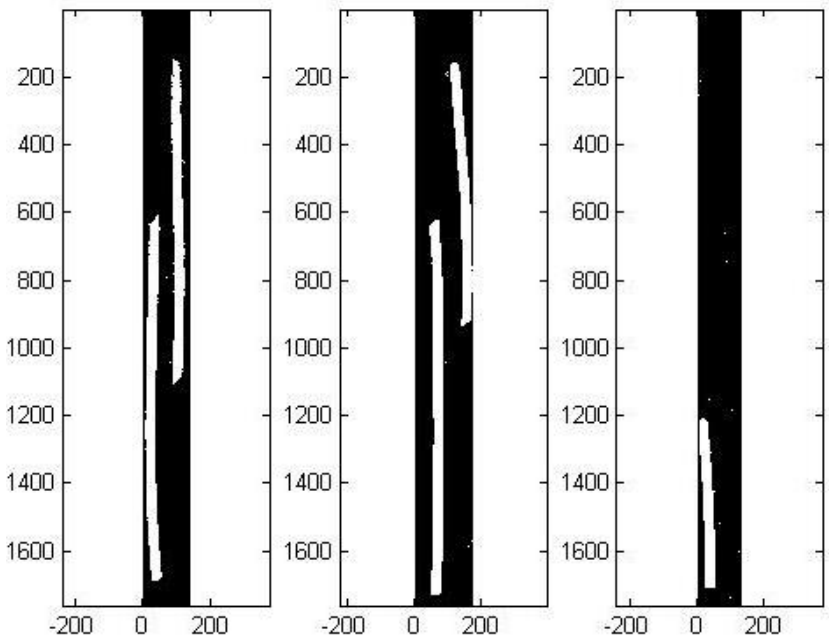

Figure 23. Total area of the seagrass leaf (white pixels) from spatial analysis of seagrass fluorescence scans and image processing techniques. Each sub-image represents a single seagrass leaf.

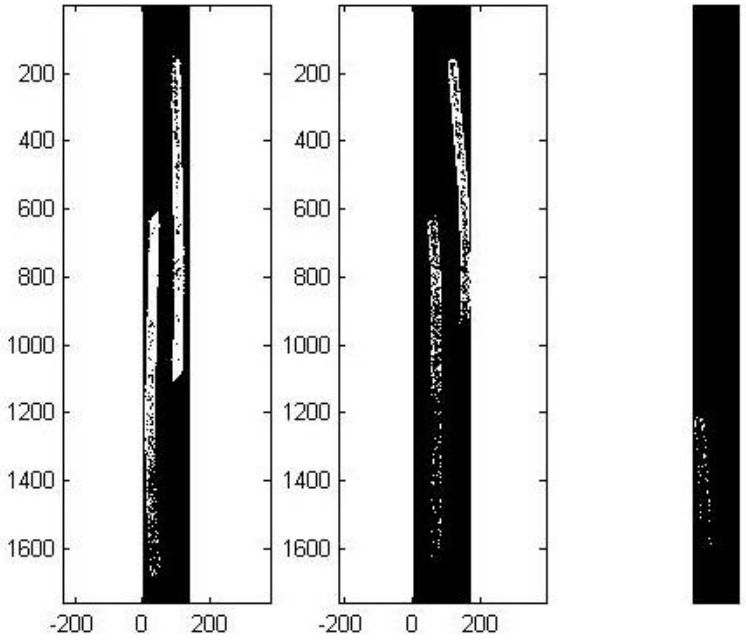

Figure 24. Total epiphyte coverage on seagrass leaf using spatial analysis of seagrass fluorescence scans and image processing techniques, for the same seagrass leaf and green fluorescence scan in Figure 22 (left).

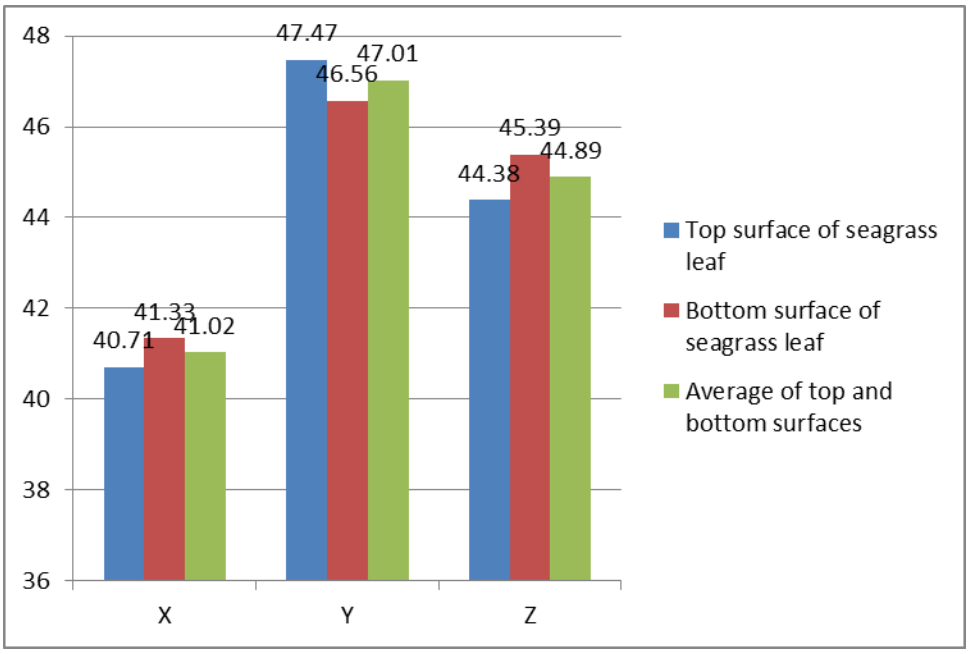

Figure 25. Average % coverage of epiphytes on seagrass leaves over a single shoot of leaves (% coverage is computed as the ratio of total pixels identified as epiphytes (Figure 24) divided by total pixels for the seagrass leaf area (Figure 23). Average values from spatial images of fluorescence scans over one shoot with 3 (Z) to 4 (X, Y) seagrass leaves are plotted. (Sampling from 8/9/14).

3.2.7 Normalized Epiphyte Accumulations From Fluorescence Scanning Compared to Biomass

Total epiphyte abundance will be a function, at least in part, of the seagrass leaf area that is available for settlement. However, what is likely more important as an indicator of epiphyte shading of a seagrass leaf, is the *relative* accumulation of epiphytes per unit of seagrass (leaf area, as can be estimated by biomass or number of pixels with red fluorescence). Thus, epiphyte measures should be compared on a *normalized* basis.

Green fluorescence *relative to red pixels* is expected to correlate with epiphyte biomass *relative to leaf biomass*, as *relative* indicator of epiphyte abundance. This allows fluorescence-based estimates to be compared with purely biomass-based estimates.

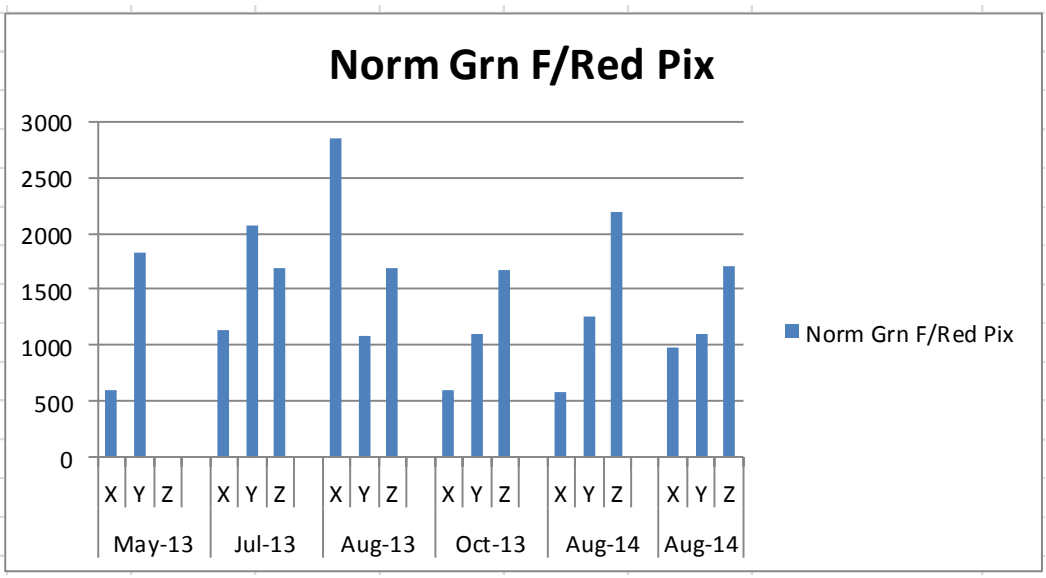

Figure 26. Normalized green fluorescence to red fluorescence pixel ratios over 6 sampling events and 3 locations. This ratio is expected to correlate with epiphyte biomass to seagrass leaf biomass ratio. (No fluorescence scans were recorded for leaves sampled from Steadman's Island on 13 May 2013)

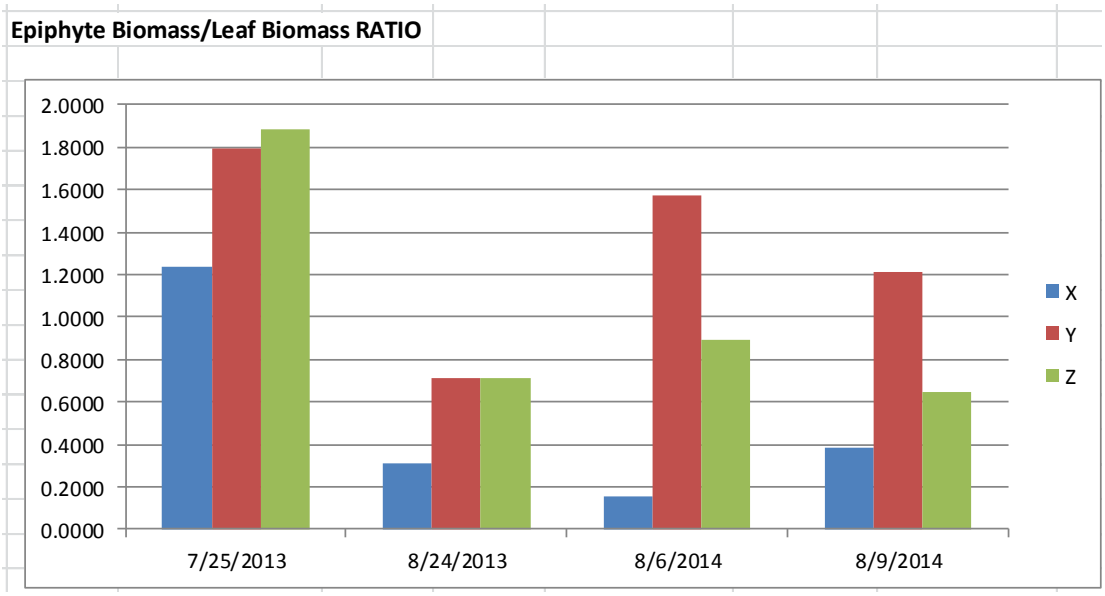

Figure 27. Epiphyte biomass to leaf biomass ratios for 3 sites over 4 sampling events. (X: 7B-Alt, Y: 21B, Z: Steadman's Island)

Site 7B-Alt (X) had the lowest normalized green epiphyte fluorescence ratios (relative to the number of red pixels as leaf area indicator), except for Aug 2013 samples which had abnormally high values (Figure 26) due to unknown reasons. The low epiphyte loading at 7B-Alt, identified

through normalized red-to-green fluorescence scans compared favorably with low epiphyte biomass to leaf biomass ratios seen at 7B-Alt from epiphyte-to-leaf biomass ratio plots in Figure 27; epiphyte biomass to leaf biomass ratios were consistently the lowest at 7B-Alt for all sampling events. 21B generally had the highest normalized epiphyte biomass during the 2014 sampling events, whereas Stedman's generally had the highest normalized epiphyte fluorescence during the same sampling events. When only Steadman's Island and 21B results are compared for the 4 sampling events, it is observed that 21B had higher normalized epiphyte biomass than Steadman's Island for the three sampling events, whereas Steadman's Island had the higher normalized epiphyte fluorescence for the same sampling events. The results were reversed for the two sites for the July 2013 sampling event, with higher normalized epiphyte biomass at Steadman's Island than at 21B, and higher normalized epiphyte fluorescence at 21B than Steadman's Island (Figure 26 and Figure 27).

The likely explanation for the differences may be that there are differences in the algal epiphyte communities at each site, which would alter the relationship between relative green fluorescence levels and relative biomass levels (Not all algal types have equivalent fluorescence or biomass). It should also be noted that the epiphyte biomass measures can also be biased to higher values if sediment particles are trapped in the epiphyte biofilms, a phenomenon that is commonly observed.

The hypothesis that certain inconsistencies in relative comparisons of Site 21B and Stedman's Island are due to algal epiphyte community composition differences, as well as the possible contributions of the above-mentioned bias in leaf area estimates used to normalize the epiphyte fluorescence data, can be tested by examining both red and green fluorescence *intensities* obtained for epiphytes removed from the seagrass leaves. This is accomplished by fluorescence Plate Assays of the epiphytes used for biomass measurements. The algal epiphyte pigment analysis also provides insight into any differences in the community composition and is discussed in Section 3.2.11 HPLC Pigment Analysis Results.

3.2.8 Plate Assay-Based Fluorescence Indicator of Algal Epiphyte Community Composition

Removal of epiphytes and analysis of their fluorescence properties, free of fluorescence interference from the seagrass leaf, permits assessment of the red-excited fluorescence of the epiphytes in addition to the green-excited fluorescence presented above. This detects more efficiently different classes of epiphytes than those detected by green-excited fluorescence, which primarily targets phycoerythrin-containing algae. In contrast, the red excited (632 nm) fluorescence most efficiently detects the chlorophylls which are present in all algal epiphytes, but especially high in abundance in green algae. Thus, differences in algal communities will have different relative intensities of green- and red-excited fluorescence, as expressed in the ratio of red-excited F (fluorescence) to green-excited F (fluorescence) resulting in the red-to-green fluorescence (R/G) ratio. Communities dominated by red algae have high levels of green

fluorescence intensity *relative to red fluorescence intensity* (not pixel number), whereas communities dominated by other algal types will show more red fluorescence intensity relative to green fluorescence intensity. The ratio of Red F to Green F is thus a *relative* indicator of epiphyte community composition.

Fluorescence quantitative data summaries are presented in Figure 28 through Figure 31.

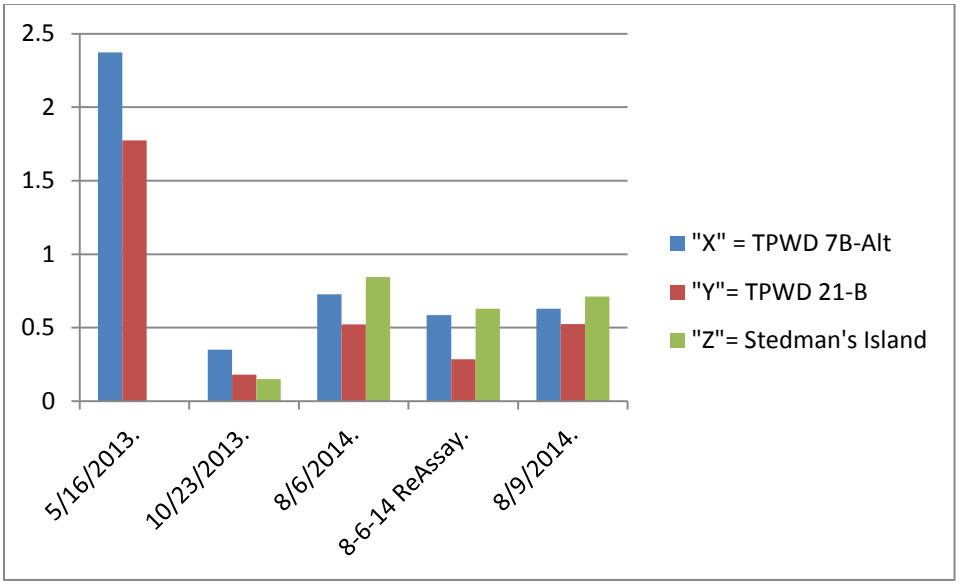

Figure 28. Red fluorescence to green fluorescence ratio (R/G ratio) across 6 sampling events at 3 sampling sites. (No fluorescence scans were recorded for leaves sampled from Steadman's Island on 13 May 2013) (Dates in the chart indicate data analysis dates.)

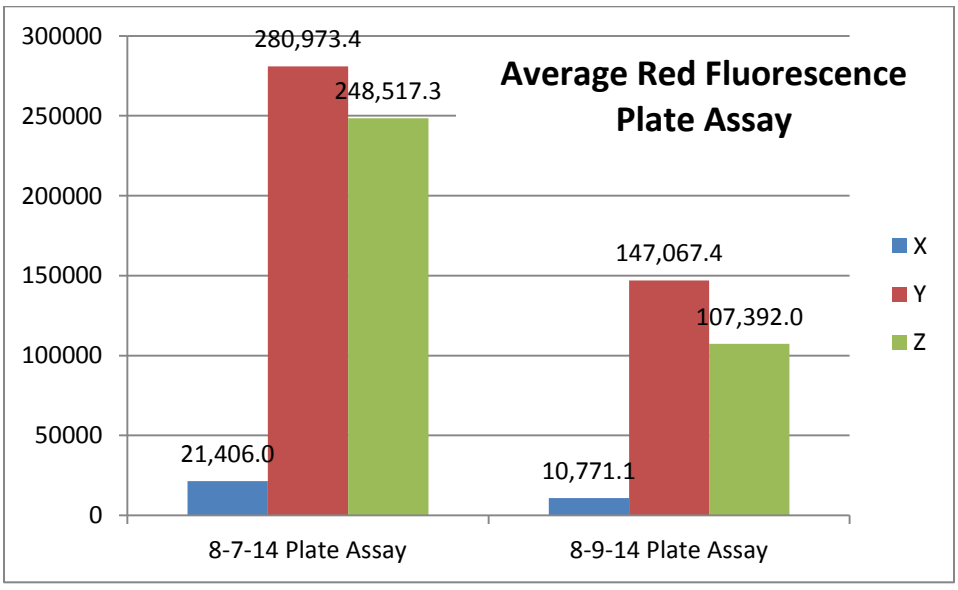

Figure 29. Red F (red fluorescence) data for two plate assays. Vertical axis represents average red pixels per site.

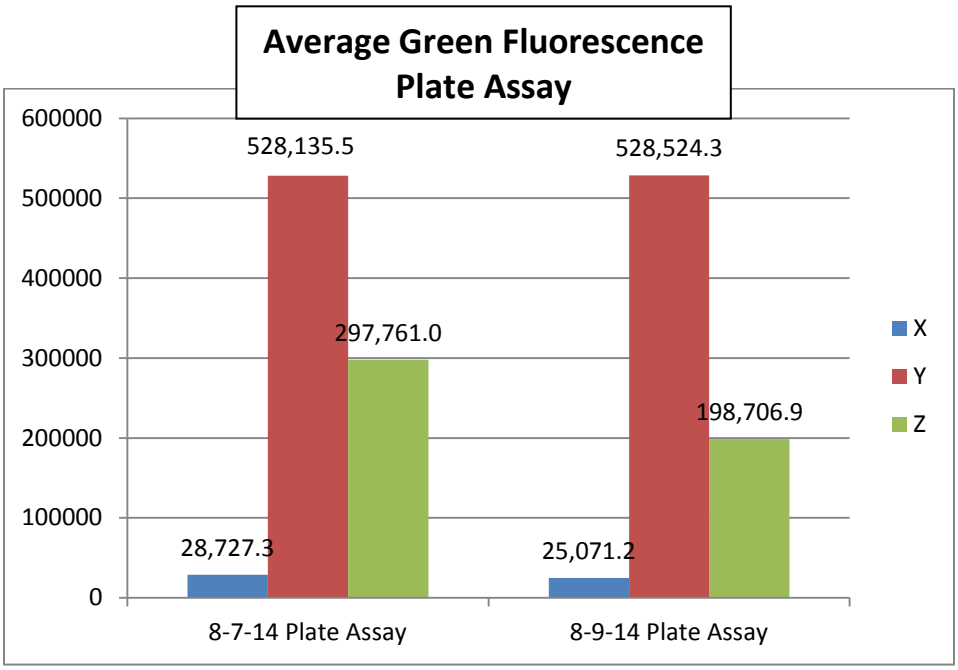

Figure 30. Green F (green fluorescence) data for the same two plate assays as in Figure 29. Vertical axis represents average green pixels per site.

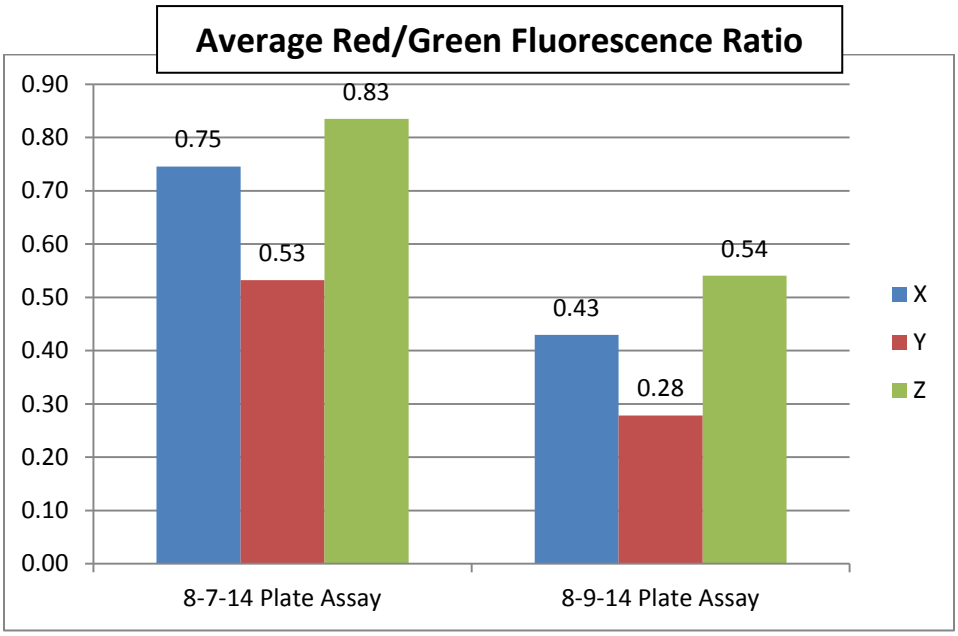

Figure 31. Red/Green fluorescence ratio (R/G ratio) for the plate assays in Figure 29 and Figure 30.

Site 21B consistently had the lowest Red F/Green F Ratio for removed epiphytes from the 2014 plate assays, indicating a different algal epiphyte community composition compared to the

other sites (Figure 28 and Figure 31). The ratios at 21B were approximately 30-50% lower. The difference could be explained by greater levels of red algae (and their green F (fluorescence) scans), and/or by lower levels of other algal types (e.g., diatoms, greens, browns). Consideration of the red-and green- fluorescence levels separately (Figure 29 and Figure 30) indicates that both of these levels are relatively high at 21B compared to 7B-Alt, a finding consistent with higher epiphyte accumulations at 21B. Interestingly, Stedman's Island also exhibited high, but intermediate levels of red- and green fluorescence, but the R/G ratio was high similar to 7B-Alt. These findings also correlate with greater light attenuation at 21B, which would alter light quality in addition to light quantity, plus lower leaf biomass, fewer numbers of leaves per 3 shoots, and higher epiphyte biomass per 3 shoots. Higher turbidity and greater light attenuation would be expected to enhance algal epiphyte components adapted to greater depths by utilization of phycoerythrin accessory pigments exhibiting green-excited fluorescence.

Additional confirmation of our interpretation of the results comes from consideration of pigment analysis results discussed in Section 3.2.11.2 HPLC Pigment Analysis Results.

3.2.9 Hyperspectral Imaging & Analysis

Two types of hyperspectral images were collected. One set of images were collected with a benchtop system (Headwall Photonics Hyperspec™ VNIR P-Series, S/N 64-195) in the lab with a broadband light source, and the other with a portable camera (Surface Optics) in the field (on the boat right after samples were extracted), or on campus in ambient light after returning from field trips, to save time in the field.

The preliminary results from the portable hyperspectral camera were reported in the conference paper presented in Santorini, Greece, during 14-17 October 2014 (Mehrubeoglu *et al.* 2014, see APPENDIX C for full conference paper). Here, we present the results from the benchtop system which combined ENVI software tools and MATLAB algorithms to analyze seagrasses from the 9 August 2014 sampling event.

Figure 32 shows a digital photograph of the top (oldest) portion of a seagrass leaf cut to fit the hyperspectral camera view. This leaf was imaged with the benchtop hyperspectral imaging system. RGB rendering of the hyperspectral image using ENVI software is shown in Figure 33. Note that the seagrass leaf was held down using weights on each side; hence, a small portion of the seagrass is not included in the mapping that follows. Weights were necessary to keep the seagrasses flat, and minimize their curling as they dehydrated under the broadband light source in the lab. Figure 34 shows the cropped and background removed image of the seagrass leaf in Figure 33 in RGB color mode, broadened to emphasize the appearance of epiphytes and tubeworms, which then underwent Gaussian blurring (low-pass filtering).

Cropping of the seagrass blade was achieved through the **region of interest** tool in RGB color mode. Blurring allows improved visualization of epiphyte coverage on the seagrass blade by changing the color bins and their gray-level content, since only a distribution of 255 different colors are used in an 8-bit representation of the image. The result is categorization of the signals or pixels into epiphytes, tubeworms, green seagrass blade (uncovered) or background.

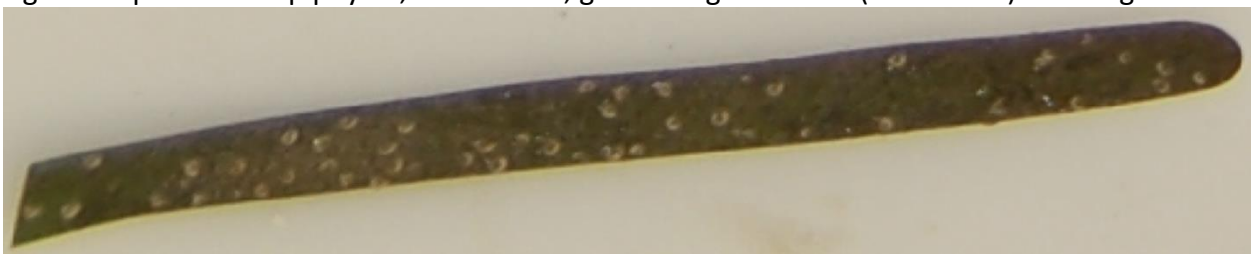

Figure 32. Digital photograph of a cut seagrass leaf (top, representing oldest portion) taken with AF-S DX Nikon digital camera. (Photo by Dustin Smith)

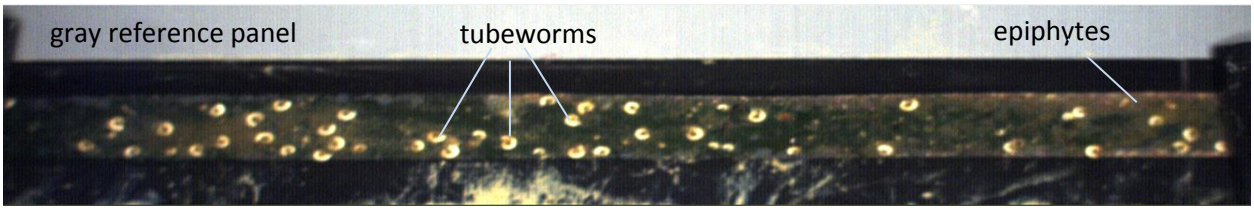

Figure 33. RGB (red, green, blue) rendering of the hyperspectral image of seagrass pictured in Figure 32, using ENVI 4.8 software tool. Top portion of the image represents the gray reference panel used for normalizing the image. (R: 640 nm, G: 550 nm, B: 460 nm, automatically chosen by ENVI)

Figure 34. Same seagrass image as in Figure 33, cropped, background removed, and Gaussian blurred (low-pass filtered).

Figure 35 shows the final map of the seagrass sample pictured in Figure 32 with four-level segmentation. Percent epiphyte coverage is computed as the ratio of green pixels to all pixels representing seagrass, multiplied by 100; Percent tubeworm coverage is computed as the ratio of purple pixels to all pixels representing seagrass, multiplied by 100. Similarly, % area of exposed seagrass leaf is computed as the ratio of red pixels to all pixels representing seagrass, multiplied by 100. Black pixels representing the image background is excluded from analysis.

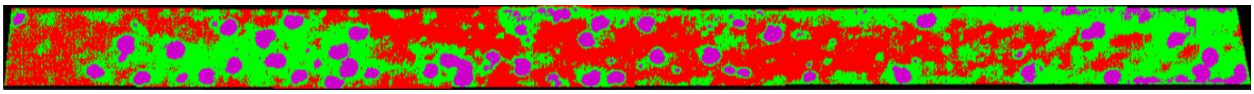

0		Background
0.1 - 0.35	Red	Seagrass
0.35 - 0.60	Green	Epiphytes
0.60 - 9	Purple	Tubeworms

Figure 35. Final mapping of a seagrass leaf portion demonstrating leaf surface coverage. Red pixels represent exposed seagrass leaf with no coverage. Green pixels represent epiphytes, whereas purple pixels belong to tubeworms. Image background is shown with black pixels.

Figure 36 shows the average percent surface coverage over 3 (7B, Steadman's Island) or 4 (21B) seagrass shoots per site at the three sites, targeting about 10 seagrass leaves per site using ENVI software tools and MATLAB. Each seagrass leaf was cut into multiple sections to fit within the camera view. Figure 36 shows that epiphyte coverage was highest at 21B followed by Steadman's Island, then 7B, with 43%, 33% and 24% coverage, respectively. Conversely, exposed leaf area with no coverage per shoot (including all leaves, young and old), had the highest percentage at 7B, followed by Steadman's Island, then 21B, with 69%, 63% and 50% green leaf area, respectively. In addition to epiphytes and leaf area, area covered by tubeworms was also analyzed. On the average, for this set of data, most tubeworms were observed at 7B followed by 21B then Steadman's Island with over 7%, less than 7% and 5% surface coverage, respectively.

Figure 37 summarizes the epiphyte to exposed seagrass ratio per site over multiple shoots (3 at 7B, 4 at 21B and 3 at Steadman's Island). The same figure also shows the combined epiphyte and tubeworm to exposed seagrass leaf ratio, since the combined epiphyte and tubeworms are more representative of the fluorescence an biomass measurements (during scraping all is included in the epiphyte measurements). The average ratio over all shoots per site shows the highest ratio for Steadman's Island followed by 7B, then 21B. Finally, Figure 38 shows the average leaf length per site that can then be compared to the hyperspectral imaging results. The average leaf length is inversely related with average epiphyte coverage plotted in Figure 36, which may suggest that seagrasses with less epiphyte coverage may flourish more than those with more epiphyte coverage and thus different water quality at the three sites. For the samples used with the portable hyperspectral camera, the average seagrass leaf length followed different trends as shown in Figure 39, although for this seagrass sample set, the shortest was those from 21B, but the longest was from Steadman's Island. Average seagrass leaf length trends also varied for the samples used for HPLC and biomass analysis (see Figure 55).

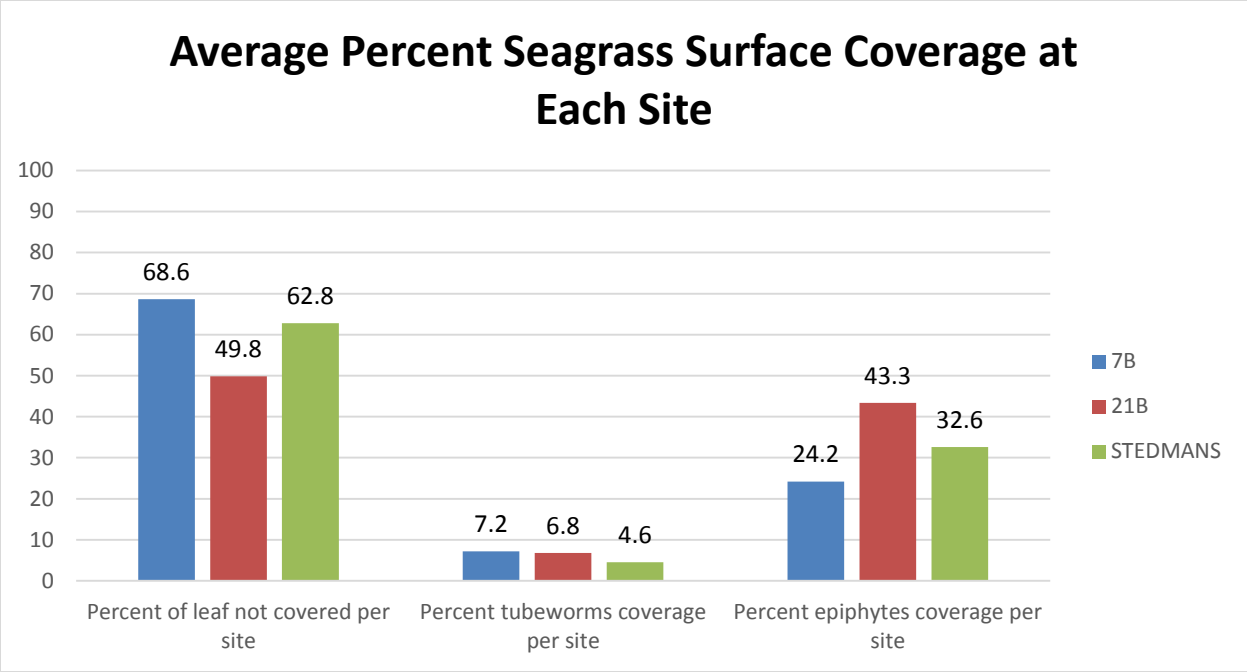

Figure 36. Average percent coverage of seagrass leaves from lab-based hyperspectral image analysis at 3 sampling locations (7B, 21B and Steadman's Island). Average is computed over 3 shoots of seagrass leaves per site.

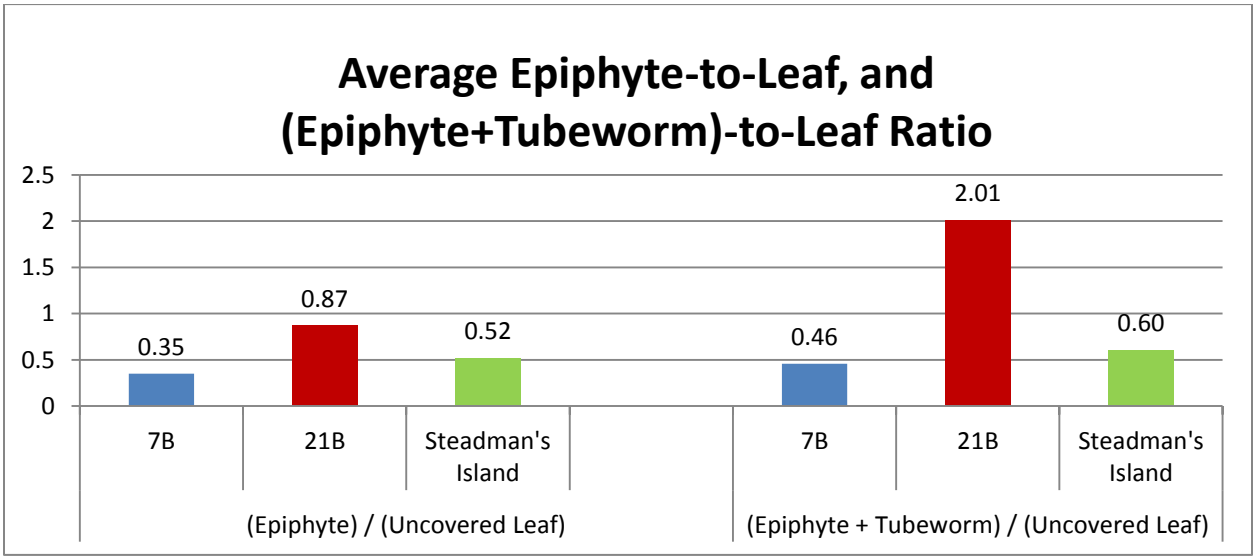

Figure 37. Average epiphyte to seagrass leaf (without coverage) ratio per site (LEFT), and average (epiphyte + tubeworms)-to-exposed seagrass leaf ratio per site (RIGHT) from lab-based hyperspectral image analysis (tubeworms represent white carbonates).

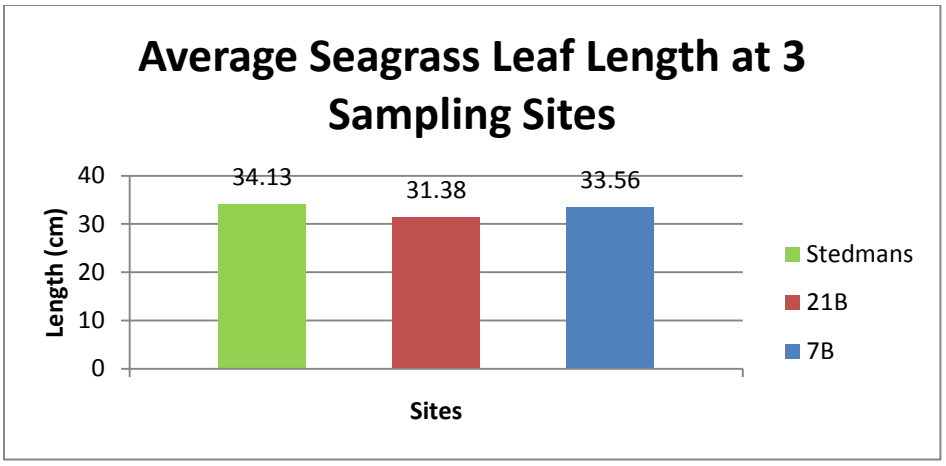

Figure 38. Average seagrass leaf length at three sampling sites (7B, 21B, Steadman's Island) for the samples used for lab-based hyperspectral imaging (9 August 2014).

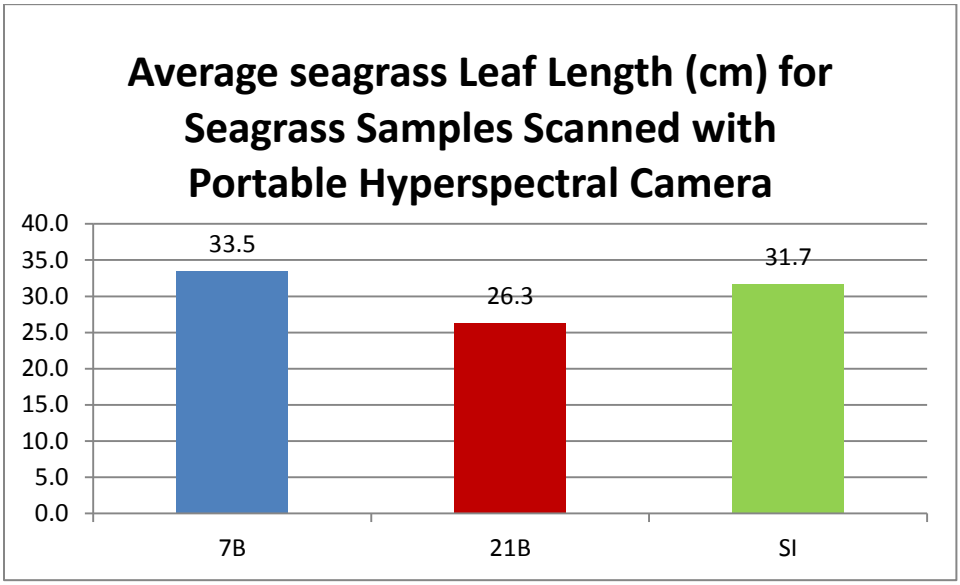

Figure 39. Average seagrass leaf length at three sampling sites (7B, 21B, Steadman's Island) for the samples used with the portable hyperspectral camera (Sampling date: 6 August 2014). (Number of shoots – 7B: 3, 21B: 4, Steadman's Island: 3; Number of blades per shoot – 7B: 3, 4, 4, 21B: 2, 2, 3, 3, SI: 3, 3, 3)

3.2.10 Visible Imaging and Analysis

Visible imaging involved taking scans of seagrass leaves with a high-resolution scanner described in the methods section (Section 2.3.2) have been analyzed using CPCe 3.6 software

tool as a means to establish a statistical profile of the surface coverage of seagrass leaves. An expert has identified randomly selected pixels and labeled them, after which percent coverage is computed. Results are for samples collected on 9 August 2014. Figure 40 shows percent epiphyte coverage computed from seagrass visible scans obtained from samples at the August 9, 2014, sampling event. The data is percent average values over a single shoot with multiple leaves. Tubeworms and senescent leaf pixels are excluded from the epiphyte count. The CPCe analysis demonstrates highest percent average epiphyte coverage in 21B, followed by Steadman's Island, and 7B. 7 B seagrass samples showed the highest variation of epiphyte coverage between front and back of the leaves. One reason for the higher variance in epiphyte coverage in site 7B could be attributed to the possible shoot with young leaves. It has been observed that sometimes young leaves will stick together on one surface as they grow, not allowing anything to attach to that surface, leading to biased populations each side of such leaves.

Although the percentages are much higher, the trends in the three sites of % epiphyte coverage correlate directly with hyperspectral imaging results.

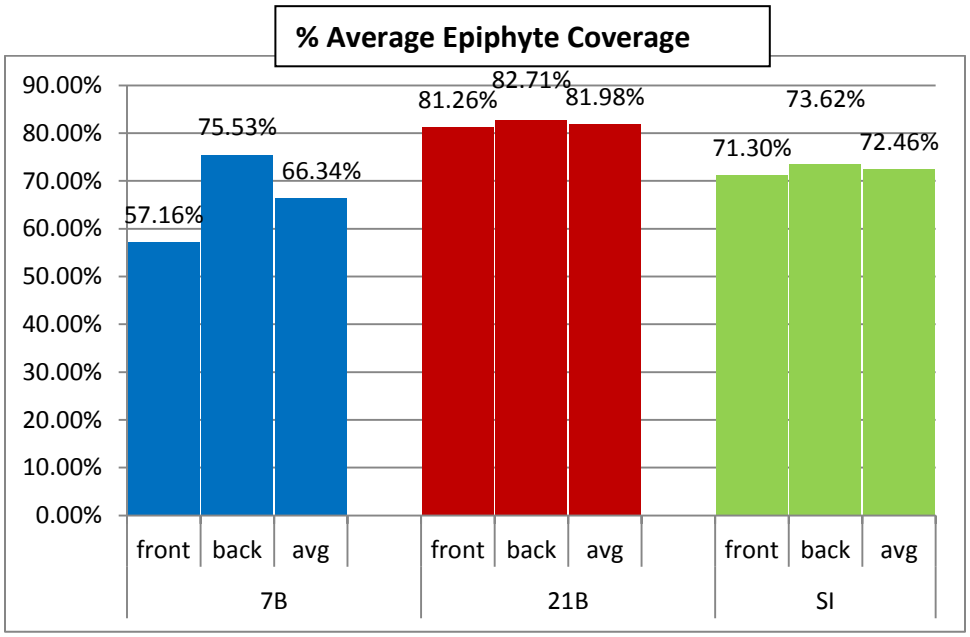

Figure 40. Percent average epiphyte coverage over a single shoot with a total of 3 (21B, SI) or 4 (7B) leaves from each site (SI: Steadman's Island, avg: average). (Seagrass sampling date: 9 August 2014).

In Figure 41, % epiphyte coverage computations were repeated, this time including senescent leaf pixels in the total epiphyte leaf count, as was done in hyperspectral image analysis. The same trends

(highest coverage in 21B, followed by Steadman's Island and 7B) are observed for % average epiphyte coverage with senescent leaf pixels included in epiphytes. Tubeworms were not included in the count. Again, 7B showed the highest variance in the % average epiphyte coverage between the front and back of the leaves.

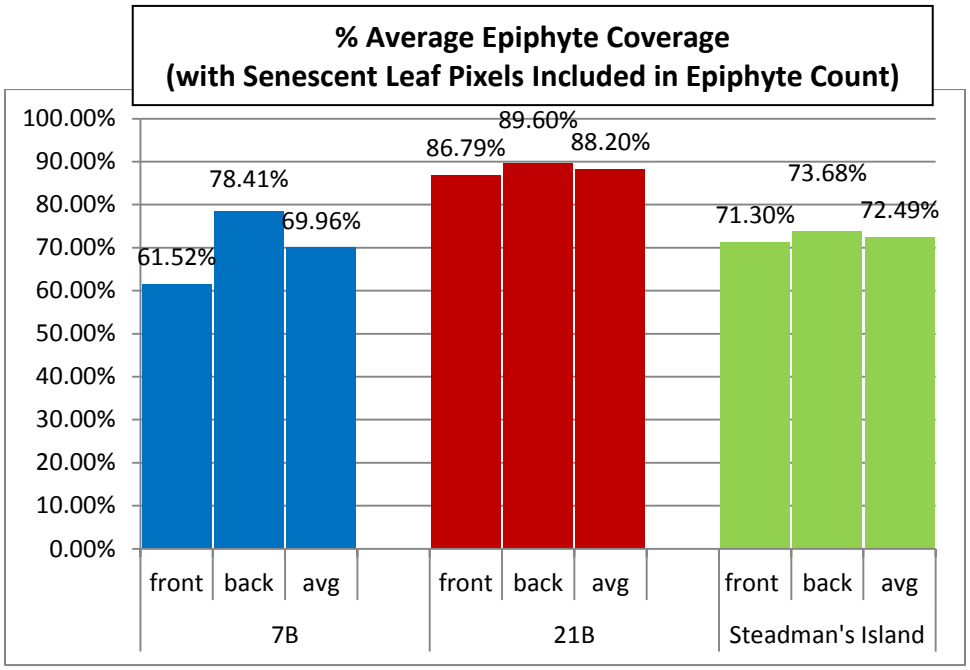

Figure 41. Percent average epiphyte coverage (including senescent leaf pixels as epiphytes) over a single shoot with a total of 3 (21B, SI) or 4 (7B) leaves from each site (SI: Steadman's Island, avg: average), for the same data as in Figure 40.

Figure 42 summarizes the average epiphyte to exposed (uncovered) seagrass leaf ratio, which follows the same trends as % epiphyte coverage. The ratios from visible scan analysis suggest all sites had more epiphytes than uncovered seagrass based on the random statistical pixel labeling. Figure 43 shows similar trends as before, but with even higher average epiphyte to exposed seagrass ratios, when the senescent leaf pixels are included in the epiphyte pixel count. In Figure 44, % average tubeworm coverage is depicted. The highest % average tubeworm coverage was found at 7B, followed by Steadman's Island, then 7B. These trends follow epiphyte coverage at the three sites extracted from visible scans. All seagrass leaves were scanned both front and back.

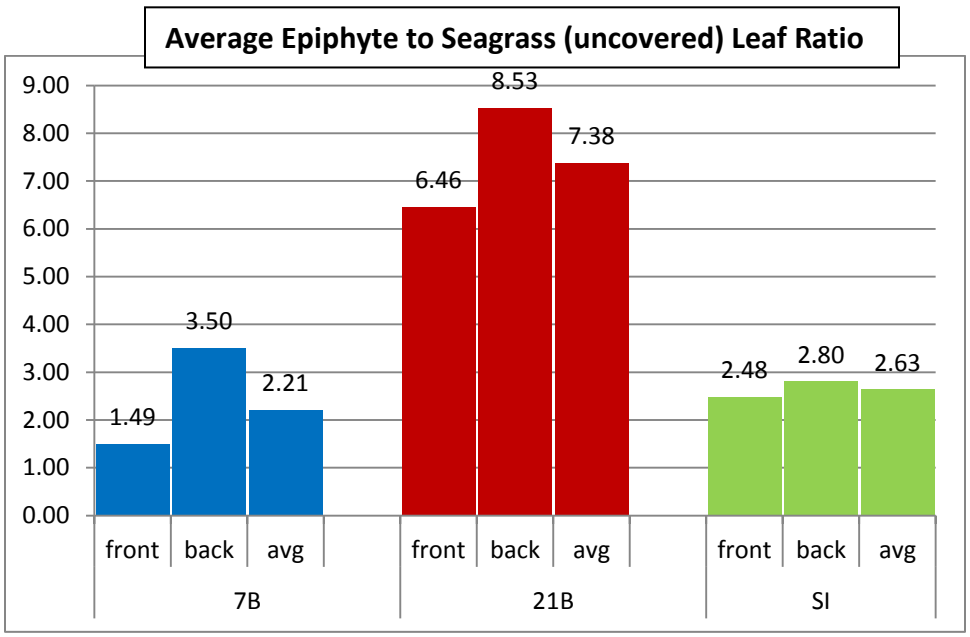

Figure 42. Average epiphyte to uncovered seagrass leaf ratio. Averaging performed over a single shoot with a total of 3 (21B, SI) or 4 (7B) leaves from each site (SI: Steadman's Island, avg: average) (Seagrass sampling date: 9 August 2014).

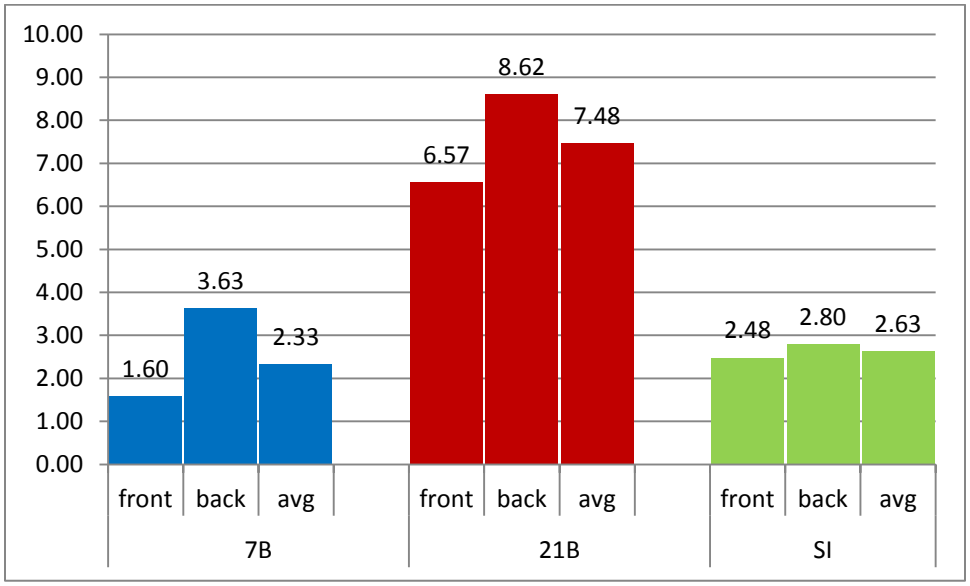

Figure 43. Average epiphyte to exposed (uncovered) seagrass leaf ratio, with senescent leaf pixels included with the epiphytes. Averaging performed over a single shoot with a total of 3 (21B, SI) or 4 (7B) leaves from each site (SI: Steadman's Island, avg: average) (Seagrass collection on 9 August 2014).

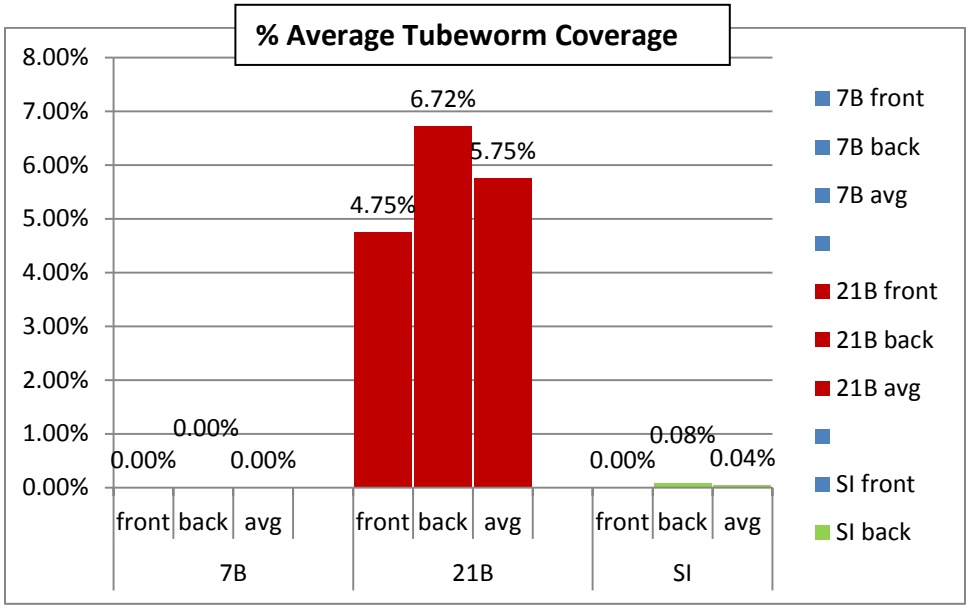

Figure 44. Percent average tubeworm (possibly foraminiferan or serpulid casing (Fikes 2012)) coverage over a single shoot with a total of 3 (21B, SI) or 4 (7B) leaves from each site (SI: Steadman's Island, avg: average). (Seagrass sampling date: 8 August 2014)

3.2.11 HPLC Pigment Analysis

3.2.11.1 Epiphyte Removal Efficiency from Seagrasses

Based on the study of seagrasses from locations from Laguna Madre from separate sampling events described in this report, the dominant epiphyte division on all seagrass was the division Bacillariophyceae (diatoms) with lesser contribution by prokaryotic phototrophs (cyanobacteria). Diatoms contributed over 80% of the epiphytic biomass.

To best remove epiphytes, a time series of MES buffer exposure/shaking was performed (Figure 45). A nonlinear breakpoint at 58 seconds was identified as the point when removal began to flatten out, so comparative samples for the scrape/MES assessment used a 60 s interval.

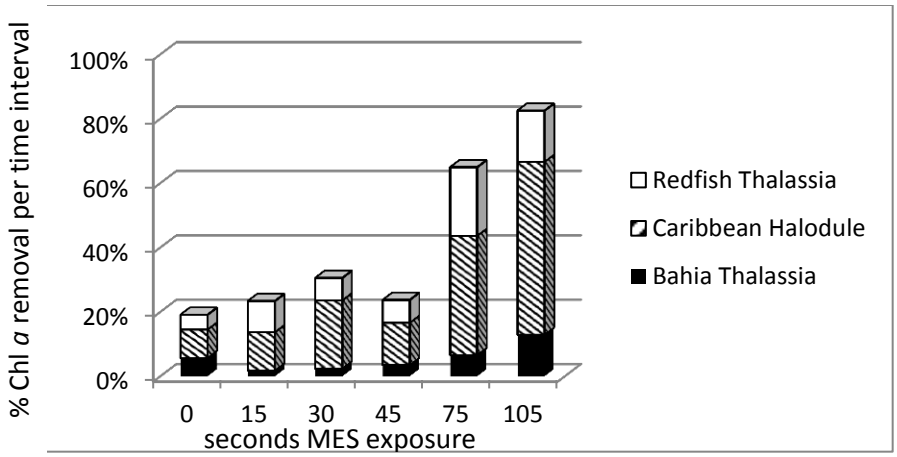

Figure 45. Removal efficiency of different MES exposure periods. A breakpoint is clear between 45-75 seconds. Sample size: Redfish Bay: n=5, Caribbean (Flour Bluff) n= 14, Bahia Bay, n=4.

Seagrass shoot epiphytes were removed using scraping, followed by MES treatment, and the reverse procedure of MES buffer exposure followed by scraping were compared (Figure 46). Nearly 70% of epiphyte biomass was removed by scraping, whereas over 80% was removed from MES treatment, resulting in higher recovery of algal pigments from MES treatment. Greater damage to the seagrass surface resulted from scraping.

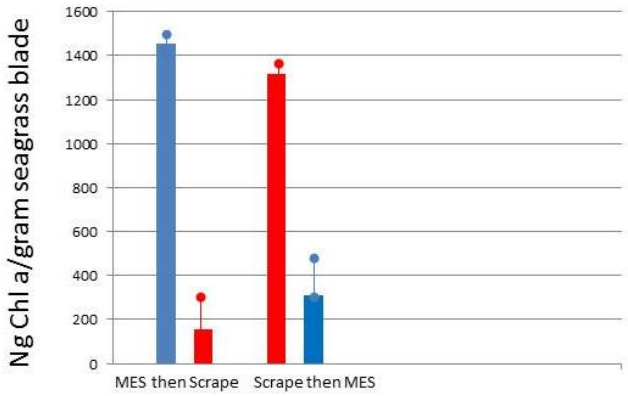

Figure 46. Epiphyte chlorophyll a concentration following MES/scrape or Scrape/MES treatments of *Halodule* (n=17) and *Thalassia* (n=9) blades. Note the higher removal using MES buffer.

Damage to shoots was assessed by measuring Chlorophyll *b* content of the epiphyte material as seagrass epidermis contains Chlorophyll *b*. Nearly three-fold higher Chl *b* was found in scrape samples relative to MES buffer samples (Figure 47).

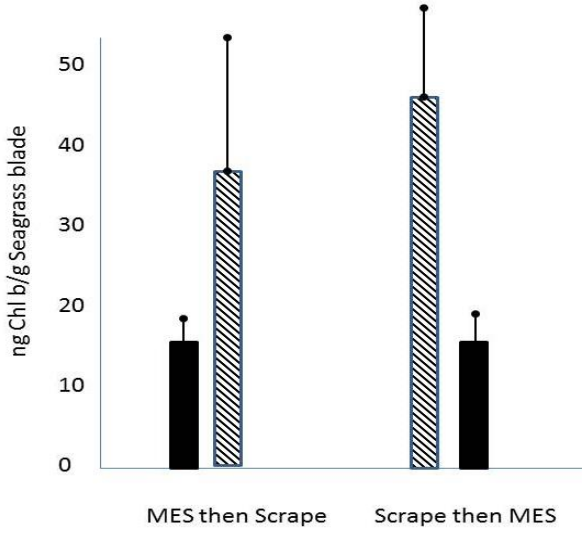

Figure 47. Chlorophyll *b* concentration in epiphyte slurry following epiphyte removal from *Halodule (n=7)* and *Thalassia* (n=5) blades.

Accurate estimation of epiphyte biomass is critical to evaluate seagrass health. Several tiered approaches of evaluating seagrass health have been developed following the pioneering work of Hilary Neckles (reviewed in Neckles et al. 2012). The tiered approach where differing levels of effort are used for evaluating seagrasses is widely used in many states including Texas (EPA 1994)-their guidelines suggest adequate characterization of epiphyte loading.

It is clear from this research that a better evaluation of epiphyte loading is critical to assess seagrass health. For example C:N ratios of seagrass are used to estimate health, however damage to the blades would strongly influence this ratio when damaging actively photosynthetic tissue.

The use of a physiological buffer to remove carbonates is also useful for assessing epiphyte biomass. Carbonates accretion from photosynthesis and from pH changes would increase the apparent weight of epiphytes, making accurate comparisons between regions difficult.

We note that scraping method was used in this research to extract pigments for HPLC. The findings of the above study show MES treatment to be preferred over scraping method.

3.2.11.2 HPLC Pigment Analysis Results

This section describes pigment analysis results from samples collected from 7B, 21B and Steadman's Island.

For the data sampled on August 9, 2015, fucoxanthin was the dominant carotenoid pigment and is diagnostic for diatoms (Bacillariophyta). Lutein and Chl *b* result from scraping damage to seagrass epidermis, and can also be associated with green algae. The pigment values were relatively low from 8-6-14 leaf discs. The HPLC pigment data have been normalized using seagrass leaf length only, since no seagrass leaf width measurements were taken.

Using Chl *a* as an overall epiphyte plus leaf abundance indicator (with its own degree of bias), pigment analysis results show low levels of epiphytes per shoot at site 7B, and increasing levels at Steadman's Island, little Chl *b* at any site (suggesting low levels of green algae and little leaf scraping damage), and relatively high levels of fucoxanthin (diatoms) at 21B and Stedman's Island. Note that the ratio of fucoxanthin/Chl *a* is nearly 2-fold difference between 21B (lower) and Stedman's Island. For the 8-9-14 data, which measured higher levels, ratio is approximately 0.5 for 21B and approximately 0.9 for Steadman's Island (ratios computed from Figure 48). The ratio for 7B-Alt is approximately 0.2, supporting different community compositions. This leads to the interpretation that based on the HPLC pigment analysis, more diatoms are observed at Steadman's Island vs. 21B. Note that HPLC analyses do not detect red algal component and could therefore explain the discrepancies compared to the biomass and imaging methods.

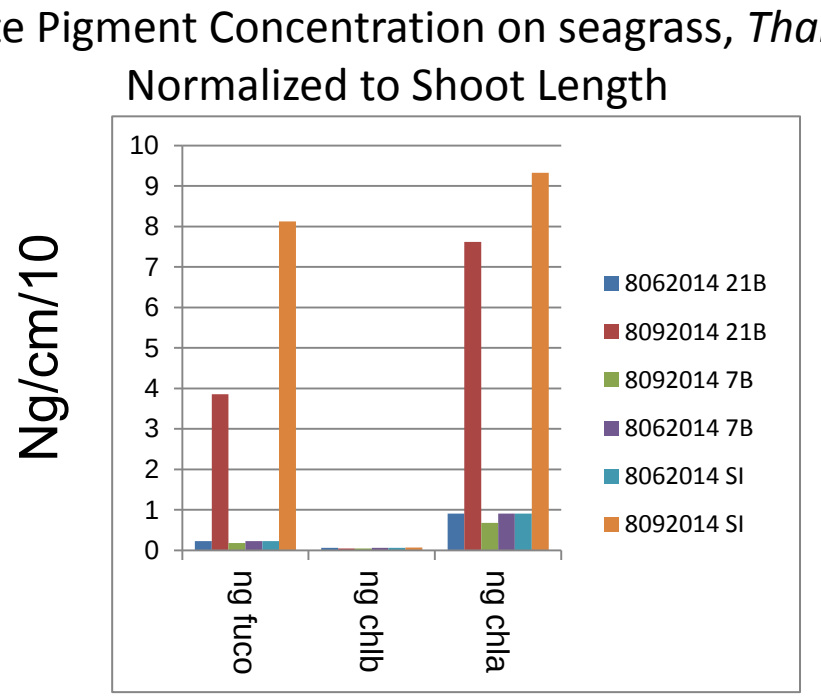

Figure 48. HPLC pigment analysis from 2 sampling events in August 2014 (8/6/14 and 8/9/14) at 3 sites (7B, 21B, SI (Steadman's Island). Chlorophyll *a* (chl *a*), Chlorophyll *b* (chl *b*), and fucoxanthin (fuco) are reported. (Pigment concentrations are reported in nanograms per centimeter (ng/cm). Vertical axis values must be multiplied by 10.)

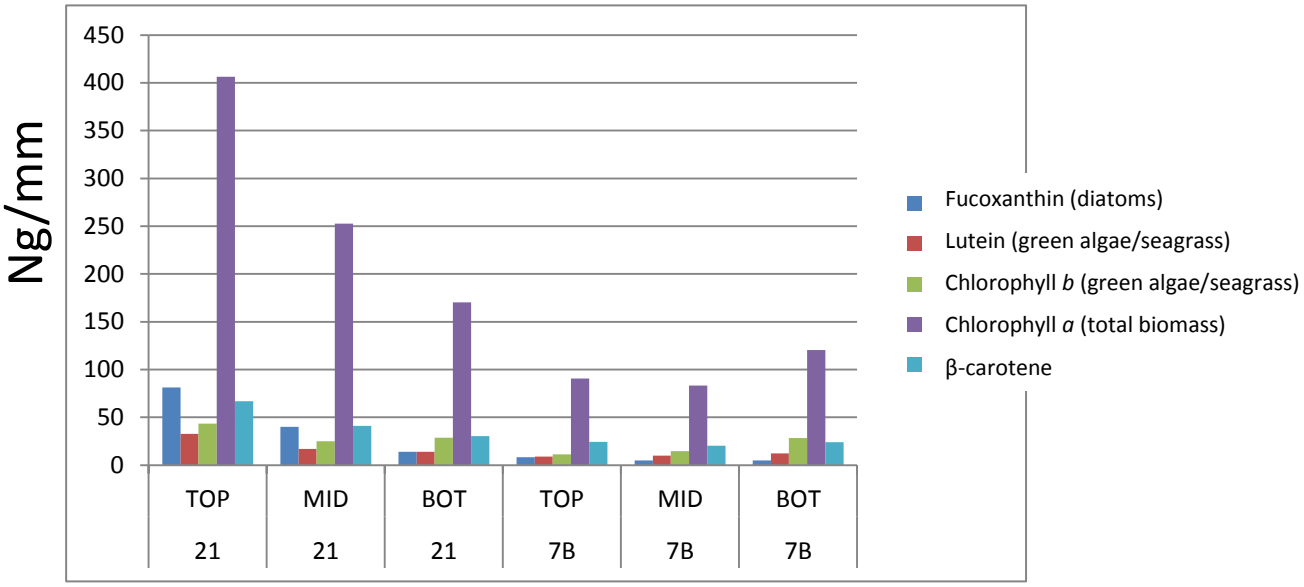

Figure 49. HPLC pigment analysis results (Data from 6 August 2014 sampling) for sites 21B and 7B.

From Figure 49, Chlorophyll *a* is identified as the most abundant pigment, followed by β-carotene in 4 of 6 sample punches (middle and bottom punches from 21B, and top and middle punches from 7B), fucoxanthin in 2 of 6 sample punches (top and mid punches from 21B), and Chlorophyll *b* in 1 of 6 sample leaf punches (bottom punch from 7B). Fucoxanthin was abundant in top and middle leaf punches from 21B (second highest, following Chl *b*), but not so abundant from samples from 7B. As would be expected, Chl *b* was relatively high in bottom punches, which represents younger portion of the leaf and sometimes with less coverage (Pigment concentrations (vertical axis) are reported in nanograms per millimeter (ng/mm)).

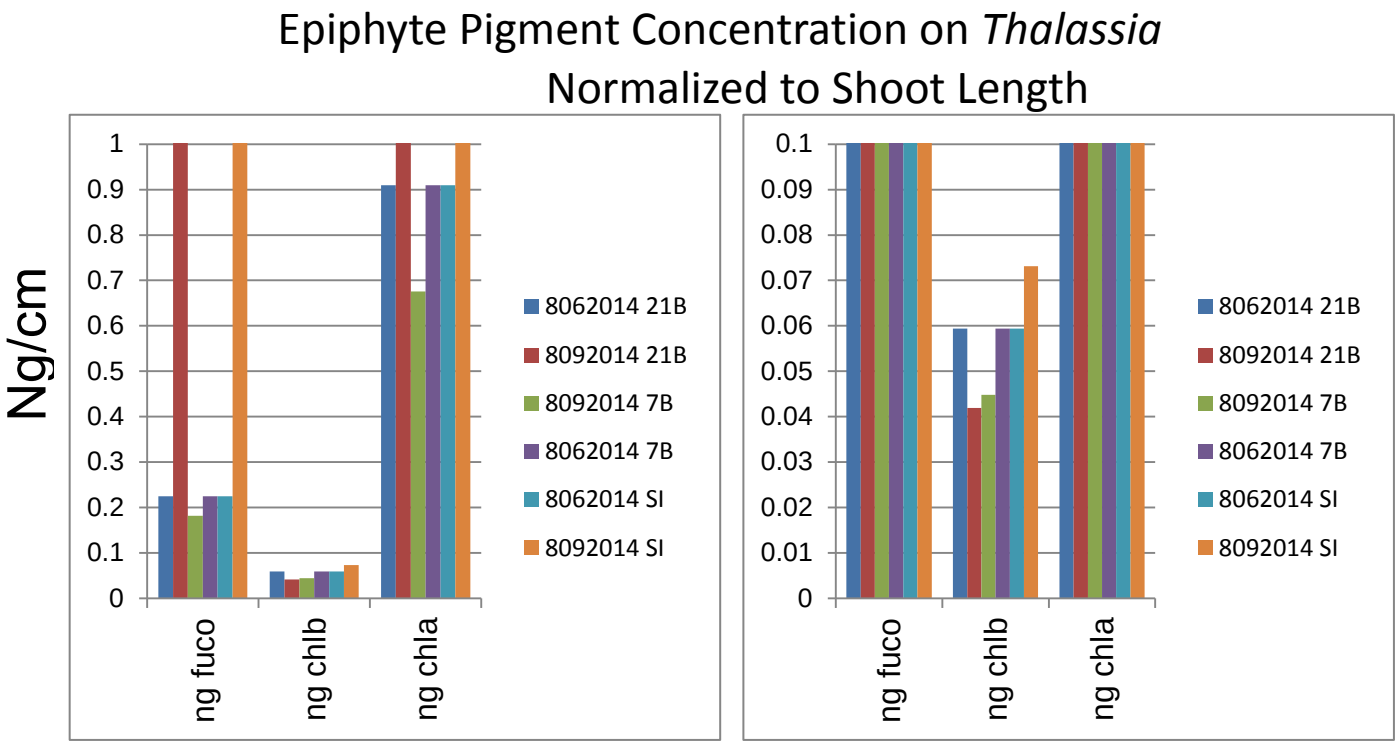

Figure 50. HPLC pigment analysis results: Epiphyte pigment concentration-to-shoot length ratio, for the seagrass leaf punches taken in the field on 6 August 2014 and 9 August 2014. Plots on the right are the expanded view of the plots on the left.

When normalized to shoot length, fucoxanthin (fuco) appears to be the dominant pigment after Chlorophyll *a*, and is followed by Chlorophyll *b*, found in green algae and from the seagrass itself (Figure 50). The chart on the right is the expanded view of the chart on the left, and shows the Chl *a*, Chl *b* and fucoxanthin levels at the 3 sampling sites for the leaf punches taken on 6 August 2015 and 9 August 2015 in the field.

Figure 51 to Figure 54 show HPLC pigment characterization for punched leaf discs from seagrass samples collected on 6th and 9th of August, 2014, including both epiphytes and seagrass leaves. Fucoxanthin levels are much higher on both dates at 21B and Steadman's Island compared to 7B. The highest pigments in 7B are Chlorophyll *a* and Chlorophyll *b* suggesting lowest epiphyte loading at this site. This finding matches the findings from the three vision systems.

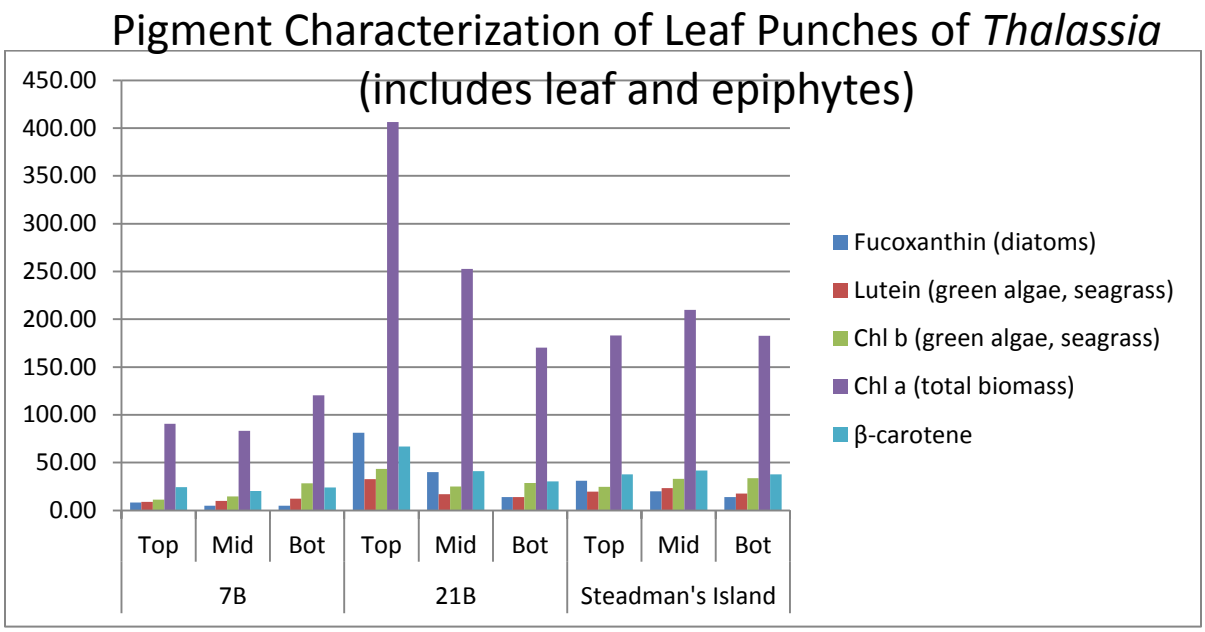

Figure 51. Pigment characterization of punched leaf discs including leaf and epiphytes (Data from 6 August 2014 sampling).

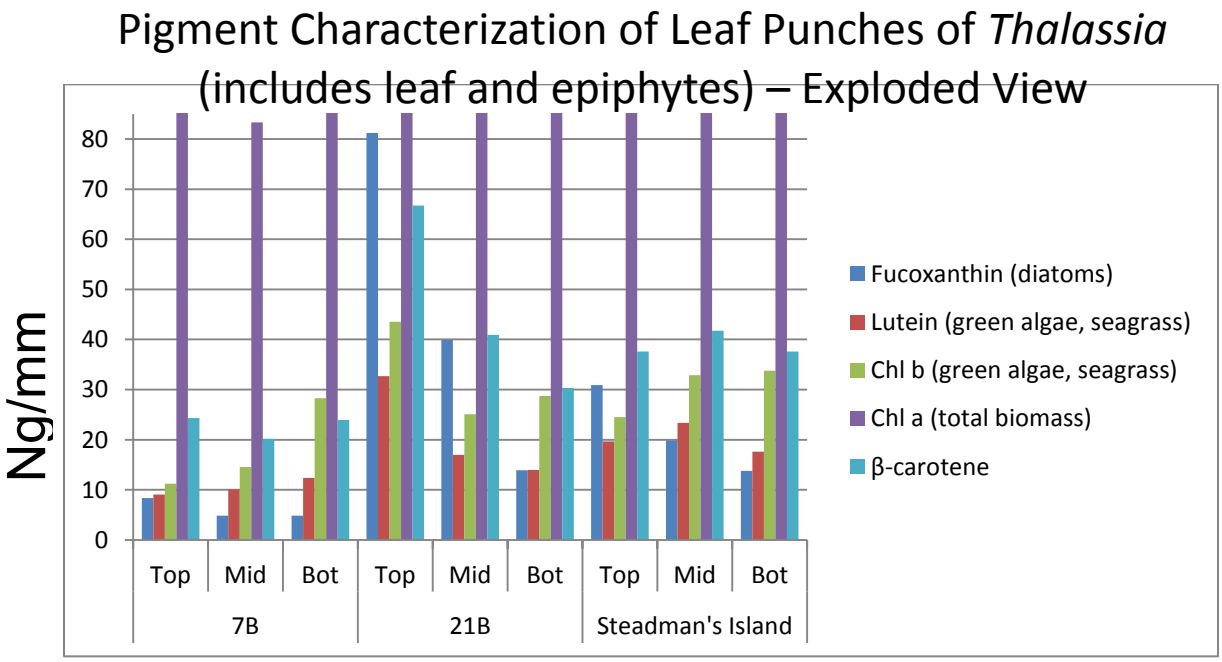

Figure 52. Exploded view of Figure 51. (Pigment characterization of punched leaf discs including leaf and epiphytes from 6 August 2014 sampling).

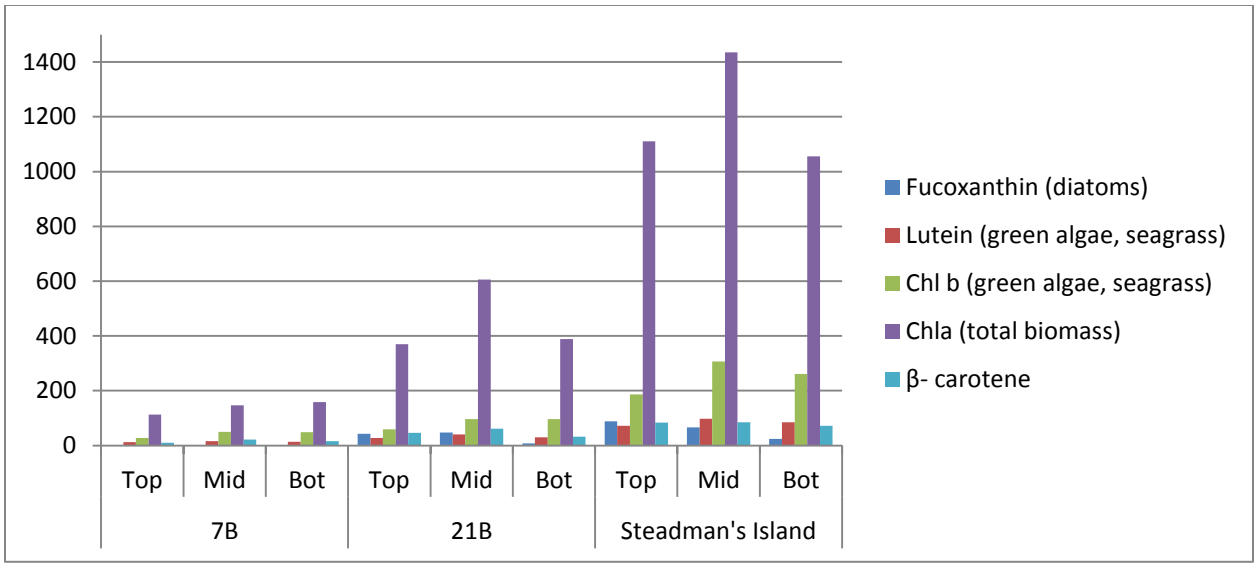

Figure 53. Pigment characterization of punched leaf discs including leaf and epiphytes (Data from 9 August 2014 sampling)

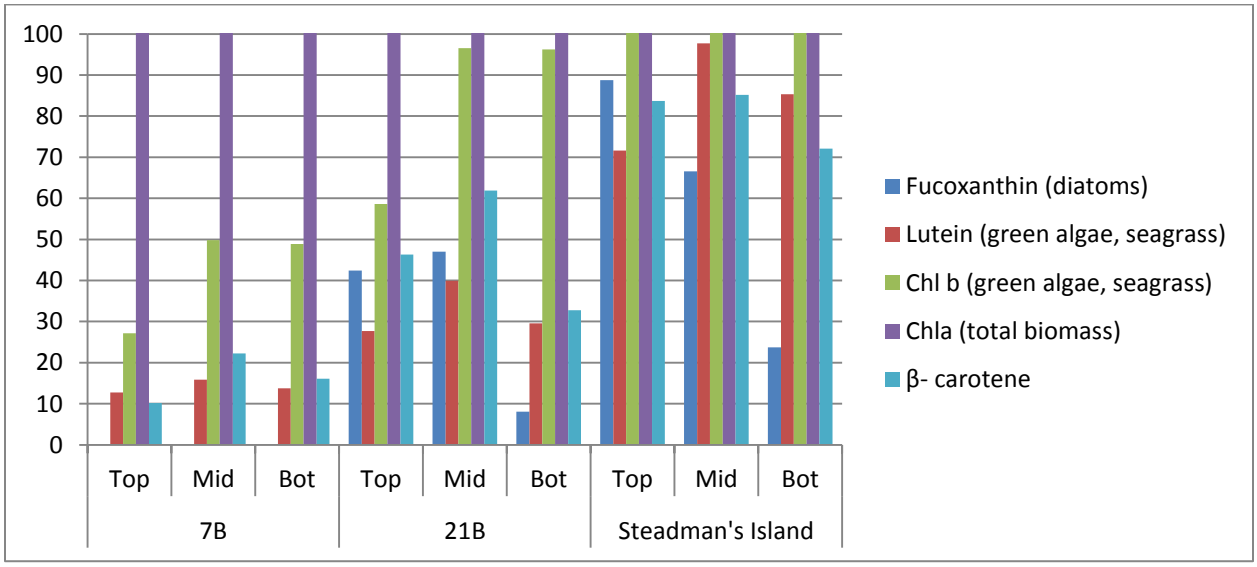

Figure 54. Pigment characterization of punched leaf discs including leaf and epiphytes; expanded view of Figure 53 (Data from 9 August 2014 sampling)

The results of the HPLC pigment analysis shows variations in algal communities among the three sites, suggesting different water quality environments at the three sites. Based on HPLC data alone, Steadman's Island and Site 21 locations are most impacted by epiphyte loading relative to site 7B, based on detected fucoxanthin levels. Fucoxanthin was abundant in 21B followed by Steadman's Island seagrass samples from 6 and 9 August, 2014, sampling dates.

Fucoxanthin is a major contributor to epiphyte biomass due to diatoms. These findings correlate directly with hyperspectral, epiphyte and visible trends. (HPLC does not detect red algae; Chl c_2 was not detected as a pigment.)

Figure 55 shows the average seagrass leaf length in cm per site over 4 shoots per site. The leaf length trends were different for the HPLC measured seagrass leaves (longest at 21B, shortest at 7B) compared to the seagrass samples used in hyperspectral imaging.

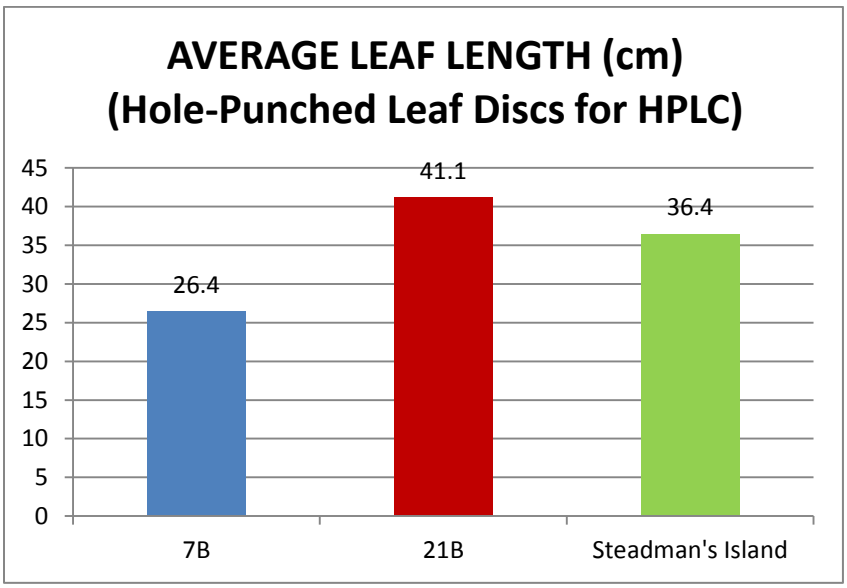

Figure 55. Average leaf length in centimeters per site for the hole-punched leaves used in HPLC analysis. Average is computed over 4 shoots per site. Each site had 2 shoots with two blades and two shoots with 3 blades. (Sampling Date: 9 August 2014)

3.3 Comparisons of Results from Biomass, Fluorescence Scanning and Pigment Analyses

Biomass, fluorescence, and pigment results are in agreement in that Site 7B-Alt seagrasses exhibit the lowest relative levels of epiphytes as well as lowest % leaf coverage. Higher epiphyte levels (and % coverage) are found at sites 21B and Steadman's Island, but the different methodologies differ as to relative rankings of these sites, most likely due to differences in the epiphyte community compositions and inherent biases found in each method. Combined application of the different methods has thus yielded insight into how the sites differ in their algal epiphyte communities. For instance, 21B has lower diatom abundance vs. Steadman's Island (Pigment analysis from 9 August 2014 data), and probably greater relative red algal contributions exhibiting green-excited fluorescence. These epiphyte community

composition differences are consistent with observed site differences in water clarity (greatest at 7B-Alt and lowest at 21B).

3.4 Comparisons of Results from Image Analysis of Hyperspectral and Visible Scans

Comparison of hyperspectral image analysis results and CPCe results from visible scans show that percent average epiphyte coverage results are correlated for each site, with highest coverage found in 21B, followed by Steadman's Island, then 7B. Similar trends are also observed for epiphyte to uncovered or exposed green leaf surface area ratios for the same sites, with highest values obtained for 21B, followed by Steadman's Island, then 7B; however, the quantified results appear to be significantly higher from visible scans' CPCe results than from hyperspectral image analysis. Overall, the same epiphyte trends are captured with the two methods.

3.5 Comparisons of Results from Hyperspectral Image Analysis, Fluorescence Image Analysis and Biomass Data

Comparing the average % epiphyte coverage computed from hyperspectral image analysis in Figure 36 to green fluorescence plate assays of Figure 30 for the same sampling date (9 August 2014), a direct correlation between epiphyte abundance at the three sites from hyperspectral images and epiphytes detected via green plate essay is observed. Similarly, the same trends are observed when hyperspectral epiphyte to exposed seagrass leaf ratio plots for the same data depicted in Figure 37 is compared to the epiphyte-to-seagrass leaf biomass ratio plots of Figure 27, with highest ratios observed for 21B, followed by Steadman's Island, then 7B. From the hyperspectral images, combined epiphyte and carbonate (tubeworm) to leaf ratio is computed as 0.46, 2.01, and 0.60 for 7B, 21B and Steadman's Island, respectively. Epiphyte to leaf biomass ratio was found to be about 0.39, 1.20, and 0.62 for 7B, 21B and Steadman's Island, respectively. Note that for this set of data, at 21B, the biomass ratio showed a higher epiphyte presence than the leaf itself, with a ratio over 1. At other two sites, epiphyte biomass was lower than leaf biomass. A separate comparison between hyperspectral-based % epiphyte coverage and fluorescence image analysis results also show that similar trends are captured with imaging both methods, with highest epiphyte coverage in 21B, followed by Steadman's Island, then 7B. Hyperspectral image analysis revealed percent average epiphyte coverage at 43%, 33%, and 24% for 21B, Steadman's Island, and 7B, respectively, whereas spatial analysis of fluorescence image scans using image processing techniques showed 47%, 45% and 41% epiphyte coverage for the same sites (see Figure 36 through Figure 38 for hyperspectral imaging results, and Figure 22 through Figure 25 for fluorescence spatial analysis results). Note that hyperspectral imaging results are reported using pure pixel analysis. Mixed pixel analysis attributing multiple classes or pigments to a given pixel has not been performed.

4. OUTREACH ACTIVITIES

4.1 Seagrass and Water Quality Awareness Brochure

An outreach brochure has been designed (see APPENDIX A) to increase awareness on seagrasses, their relation to water quality, and their contribution to benthic environments. The brochure is intended for children and adults in the community, and summarizes how to protect seagrasses.

4.2 Seagrass Castings in Resin

Seagrass samples with different epiphyte coverage have been cast in clear resin using test tubes. (Figure 55Figure 56). These seagrass-filled resins will be used for show-and-tell to describe seagrasses and the communities which live on them during outreach activities to K-12.

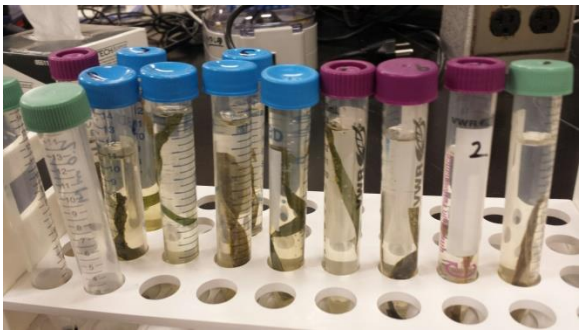

Figure 56. Seagrass samples in acrylic for show-and-tell and outreach activities

4.3 Conference Presentations and Papers

The following presentations and publications were created and presented as part of the outreach efforts (See Appendices for sample presentations and papers):

1) Whitney Robinson, Kirk Cammarata, Ruby Mehrubeoglu, S. Elizabeth Shanks, and Paul Zimba, "Comparison of Imaging Technologies and Biomass Measures of Algal Epiphytes on Seagrass to Develop New Water Quality Monitoring Tools," Texas A&M University System 11th Annual Pathways Student Research Symposium, Kingsville, TX, 8 November 2013.
2) Susan Elizabeth Shanks, Mehrube Mehrubeoglu, and Paul V. Zimba, "Identification of Microalgae in Sediments Using HPLC and Hyperspectral Imaging," Texas A&M University System 11th Annual Pathways Student Research Symposium, Kingsville, TX, 8 November 2013.

3) M. Y. Teng, M. Mehrubeoglu, S. King, K. Cammarata, and J. Simons, "Investigation of Epifauna Coverage on Seagrass Blades Using Spatial and Spectral Analysis of Hyperspectral Images," *5th Workshop on Hyperspectral Image and Signal Processing: Evolution in Remote Sensing (WHISPERS '13), Gainsville, Florida, June 25-28, 2013.* (presentation and conference paper)

4) M. Mehrubeoglu, L. McLauchlan, C. Trombley, S. E. Shanks, K. Cammarata, J. Simons, and P. V. Zimba, "Empirical Mode Decomposition of Hyperspectral Images for Segmentation of Seagrass Coverage," *2014 IEEE International Conference on Imaging Systems and Techniques, Santorini, Greece, October 14-17, 2014.* (conference paper and presentation)

5) Dustin K. Smith, Dr. Mehrube Mehrubeoglu, Dr. Kirk Cammarata, and Elizabeth Shanks, "Investigation of Seagrasses under Hyperspectral Imaging System", 3rd Annual Science Innovation Poster Session, Texas A&M University-Corpus Christi, 28 April 2015 (hosted by The Corpus Christi Chemistry Club) (poster presentation)

6) Dustin K. Smith, Dr. Mehrube Mehrubeoglu, Dr. Kirk Cammarata, and Elizabeth Shanks "Investigation of Seagrasses under Hyperspectral Imaging System," Honors Student Symposium, Texas A&M University-Corpus Christi, 2 May 2015. (oral presentation)

4.4 Visit to Elementary School

During National Engineers Week (E-Week) in 2015, Ruby Mehrubeoglu visited Windsor Park Elementary School, and gave a presentation to the entire 5th graders. The main topic was about various engineering fields. Technologies pertinent to this research in the context of engineering were also covered.

4.5 Efforts to put data on Science DMZ

Through an NSF project, TAMUCC has developed a Science DMZ which is an infrastructure that allows large data servers to be placed in a special network that can be accessed internally and externally without jeopardizing the University's network security. The Science DMZ will allow research groups and their big data to be kept on networks that can be shared through high speed nodes. When this project is completed, the data from the CMP project will be moved to these servers, which will make the data available to external community through authorized access.

5. CONCLUSIONS AND FINDINGS

All methods are capable of distinguishing site differences. Overall results demonstrate that generally, 21B had the highest epiphyte coverage followed by Steadman's Island, then 7B. We also note that the higher epiphyte accumulation at site 21B also correlated with the lower exposed seagrass leaf at that site for the hyperspectral and visible images. The results demonstrate that we are able to use imaging methods, including hyperspectral imaging,

successfully to duplicate trends identified with biomass and pigment analyses, which are expensive and time consuming.

The trends observed with the imaging technologies correlated with general water quality at the three sites. Nutrient data from nearby monitoring stations must be compared to confirm these conclusions.

Although statistical significance must be investigated, the general trends in the data support the following scientific findings from this research based on the three imaging technologies and physicochemical measurements:

1. All three imaging techniques revealed higher epiphyte coverage at site 21B, and lowest at 7B (for 9 August 2014 data). HPLC pigment measurements also supported the finding that 7B possessed the lowest epiphyte loading.
2. The findings from fluorescence intensity measurements, biomass for fluorescence samples, and fluorescence spatial analysis using MATLAB were correlated and identified that generally 21B had the most epiphytes followed by Steadman's Island then 7B.
3. HPLC revealed different epiphyte communities based on fucoxanthin levels found at 21B and 7B. Fluorescence imaging captures different types of algae that HPLC does not; for example, HPLC does not measure red algae.
4. The presence of high epiphyte loads near Steadman's and 21B are consistent with lowered water quality as compared to site 7b. This pattern is well established in historic TCEQ nutrient data sets.
5. The findings of the above study show MES treatment results in less damage to the epidermis than the traditional scraping method, and could be preferred over the scraping method.

About Image, Biomass and HPLC Analysis

Each method has its own biases: Hyperspectral imaging, similar to any other imaging technique in the visible spectrum, mainly detects surface coverage as light penetration and diffuse reflectance from the seagrass leaf is expected to be much higher from the superficial content at the measured wavelengths than the depths of the opaque leaf with epiphytes. Although some of the pixels are mixed pixels (possess information about more than one class (epiphyte, leaf, carbonates, etc.), for the purposes of this study, each pixel was assumed to be a pure pixel. Classification of pixels for % coverage quantification was done based on this assumption. Although the biomass of green leaf and epiphytes might vary significantly, imaging techniques may not catch all the information beneath the coverage of the seagrass leaf.

In fluorescence imaging, green F (fluorescence) will capture mainly red algal epiphytes but miss certain others. Red F will capture almost all biomass but not tubeworms (carbonates). HPLC does not capture red algae, and may be biased when scraping method is used, if the epidermis of the seagrass leaf is damaged. If so, more Chl *b* appears in epiphyte pigment measurements, further biasing results. Biomass measurements have similar issues with pigment analysis when the traditional scraping method is used to separate epiphytes from the seagrass leaf blade.

In addition, in biomass measurements, it is difficult to separate epiphytes from epifauna, and all of these are lumped together with epiphytes; in the biomass results reported, the scraped material will include tubeworms (carbonates) and other epifauna that is not considered epiphytes, whereas in hyperspectral and visible imaging these can be distinguished and identified separately.

All these biases must be considered when comparing and interpreting results from different methods.

About Hyperspectral Imaging

Hyperspectral Imaging presented itself as a promising technology for fast and efficient data collection from seagrass samples to compute percent epiphyte coverage and to correlate the results to water quality. Hyperspectral imaging can be used for water quality management as an integrated tool in water quality measurements from seagrasses. The images could be acquired within minutes once the hyperspectral system is set up, and samples are placed and held flat in the sampling station. The hyperspectral systems came with some challenges. When imaging using the benchtop hyperspectral imaging system, the heat generated from the broadband light source scorched the seagrasses and required that the seagrasses be removed from the imaging station as soon as the image acquisition was complete. When using the portable hyperspectral camera on the boat, if the sea conditions were rough, the motion of the boat resulted in glitches in the images, and required image retakes. Additionally, if there were fast-moving clouds during image acquisition, this caused dark and bright regions in the image. The solution for this was either to retake the image, or to normalize the image, though the former was preferred due to potentially non-linear response of the camera at different light levels.

Once the instrumentation is prepared, and samples properly placed for imaging, hyperspectral image acquisition is relatively fast and efficient, with the acquisition of many images possible from the same sample as minimally destructive method so long as the samples are kept moist; however, analysis of images are more challenging, first, due the sheer size of each hyperspectral image data - over 90MB for portable hyperspectral camera images for one shoot and over 250 MB for benchtop hyperspectral imaging system for one leaf segment. Image

analysis is a topic of continued research due to the variation among seagrass images and their surface coverage. Utilizing super computers and parallelized programs will allow faster analysis of hyperspectral images, as well as a higher number of images being processed, and is being investigated as future work.

Analysis of hyperspectral images in a fully automated fashion presents further challenges due to the variations in shape, size and orientation of seagrasses in the images, as well as random variations in the acquired data. Therefore, it is not yet possible to have a fully automated image analysis software tool which will take in hyperspectral images and output percent coverage in a leaf. User input is necessary in all the programs developed to identify region of interest to be used and analyzed in each image. We have used ENVI and MATLAB to process and view hyperspectral data cubes. The main algorithms developed in MATLAB, or the procedures used in ENVI are described in the appendices, together with hyperspectral imaging system settings for the portable hyperspectral camera (see APPENDIX D and APPENDIX G).

Overall, hyperspectral images contain a wealth of information that can further be explored to extract information about epiphytes, which can then be used as indicators of water quality.

6. FUTURE WORK

We have collected many images; however, the analysis of the entire batches requires high processing times. One of the future goals is to parallelize image analysis algorithms, and transfer data processing to a high-performance computer such as a supercomputer for faster data analysis output. In addition, one of the future goals includes refining image analysis algorithms for batch processing. Future work also includes increasing identified class sizes to investigate and separately identify multiple epiphyte types using hyperspectral imaging by fusion of spectral and spatial information with expert identification.

REFERENCES

1. Dauby, P. and M. Poulicek. 1995. Methods for removing epiphytes from seagrasses: SEM observations on treated leaves. Aquatic Botany 52:217-228.
2. Dunton, K.H, Kopecky, A.L., and Maidment, D. 2005. Regional Environmental Monitoring and Assessment Program, R-EMAP Region 6 – Monitoring Design Criteria and Biological Indicators for Seagrass Conservation in Texas, Final Report (1 April 2015). (EPA Project, Contract #829513010).
3. Fikes, Ryan, Deputy Director of Mexico Studies, “Example Epiphyte Taxa,” *personal communication* (2012).
4. Frankovich, T.A. and J.W. Fourqurean 1997. Seagrass epiphyte loads along a nutrient availability gradient, Florida Bay, USA. Mar. Ecol. Prog. Ser. 159:37-50.

5. Golzarian, M.R., R.A. Frick, K. Rajendran, B. Berger, S. Roy, M. Tester, D.S. Lun, "Accurate inference of shoot biomass from high-throughput images of cereal plants," *Plant Methods*, 2011, 7:2 (pp 1-11). (http://www.plantmethods.com/content/7/1/2 PLANT METHODS)
6. Kohler, K.E., and S.M. Gill, "Coral Point Count with Excel extensions (CPCe): A Visual Basic program for the determination of coral and substrate coverage using random point count methodology," Computers & Geosciences 32:9, pp. 1259–1269 (2006). DOI: 10.1016/j.cageo.2005.11.009
7. M. Mehrubeoglu, L. McLauchlan, C. Trombley, S. E. Shanks, K. Cammarata, J. Simons, and P. V. Zimba, "Empirical Mode Decomposition of Hyperspectral Images for Segmentation of Seagrass Coverage," *2014 IEEE International Conference on Imaging Systems and Techniques, Santorini, Greece, October 14-17, 2014.*
8. Morgan M.D. and C.L. Kitting. 1984. Productivity and utilization of the seagrass *Halodule wrightii* and its attached epiphytes. Limnol Oceanogr 29:1099-1176.
9. Neckles, H.A., Kopp, B.S., Peterson, B.J., and P.S. Pooler. 2012. Integrating scales of seagrass monitoring to meet conservation needs. Est. Coasts 35:23-46.
10. Nieunwenhuize, J., P.A. Erftmeijer, Y.E.M. Maas, M. Verwaal, and P.H. Nienhuis. Pretreatment artefacts associated with the removal of calcareous epiphytes from seagrass leaves. Aquatic Botany 48: 355-361.
11. Radloff, P. L., *Quality Assurance Project Plan, Statewide Seagrass Monitoring Protocol Development, Phase II,* Texas Wildlife Department, June 19, 2012.
12. Roberson, W., K. Cammarata, M. Mehrubeoglu, S.E. Shanks, and P. Zimba, "Comparison of Imaging Technologies and Biomass Measures of Algal Epiphytes on Seagrass to Develop New Water Quality Monitoring Tools," Texas A&M University System 11th Annual Pathways Student Research Symposium, Kingsville, TX, 8 November 2013. (poster presentation)
13. Ralph, P. J., Tomasko, D., Kenneth, M., Seddon, S., Macinnis-Ng C. M. O., "Human Impacts on Seagrasses: Eutrophication, Sedimentation, and Contamination," in *Seagrasses: Biology, Ecology and Conservation*, Chapter 24, pp. 567-593 (2006).
14. Shamir, L., JD. Delaney, Nikita Orlov, D. Mark Eckley, Ilya G. Goldberg, "Pattern Recognition Software and Techniques for Biological Image Analysis," *PLoS Computational Biology,* Nov. 2010, 6:11 (pp. 1-10). (www.ploscompbiol.com)
15. Zimba, P.V. & Hopson, M.S. 1997. Quantification of epiphyte removal efficiency from five submersed plant species. Aquatic Botany 58:173-179.
16. Zimba, P.V., Dionigi, C.P., & Millie, D.F. 1999. Evaluating the relationship between photopigment synthesis and 2-methylisoborneol accumulation in cyanobacteria. *J. Phycol.*35:1422-1429.

APPENDIX A

Trifold Outreach Brochure – Seagrass and Water Quality

(Outside Cover)

Trifold Outreach Brochure – Seagrass and Water Quality

(Inside Cover)

Challenges to Seagrasses

Light Limitation: Seagrass plants require light for photosynthetic energy production and growth. Decreased water clarity results from algal blooms, sediment disturbance and epiphyte overgrowth.

Physical Disturbances: Propeller scarring and new dredging of sensitive areas can uproot seagrasses. Hardening shorelines with bulkheads can increase wave energy and erosion of seagrass beds.

Excessive Runoff: Runoff from rainstorms carries nutrients, pesticides, and particulate matter with adsorbed pollutants.

Overfishing ("Top-Down Effects"): Seagrasses only thrive as part of healthy ecosystems that include top predators such as large Gulf of Mexico fishes. Loss of top predators causes smaller fish to increase in abundance, and these small fish then eat the "grazer" organisms (snails, amphipods, small crustaceans) that feed on algal epiphytes. This leads to proliferation of algal epiphytes, reducing the sunlight reaching seagrases.

In Field Hypesspectral Imaging System

What are "Epiphytes" and What do they do?

"Epiphytes" are organisms (algae, bacteria) that attach to the leaves of seagrasses and create a micro-ecosystem on the seagrass leaf. Small animals such as amphipods, snails and worms live among and eat the epiphytes. The photosynthetic algae absorb some of the sunlight and nutrients that would otherwise reach the seagrass leaf. Excessive accumulation of epiphytes may cause loss of the seagrass leaf.

Nutrients (fertilizer) in the water stimulate growth of epiphytes, but "grazers" keep them in-check in the same way that cattle graze pastures. If the grazers are removed, from overfishing or pesticides, the pasture overgrows.

Tropic Cascade Effects of Predator Loss

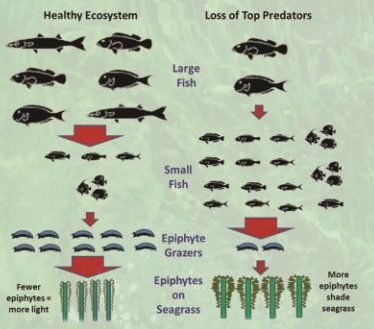

How do Scientists Study Epiphytes and their Effects on Seagrasses ?

The abundance and distribution of seagrasses are often monitored by aerial photography, but this does not tell us **why** seagrasses are in decline.

Scientists need to quantify and characterize the epiphytes on seagrasses in different environmental conditions such as high nutrient levels and/or low numbers of grazers.

Traditional Method: Scrape epiphytes off the seagrass and weigh them (Biomass).

New Technologies: A variety of **imaging technologies** can be used to characterize the quantity and spatial patterns of accumulation of algal epiphytes on seagrasses. These provide a more detailed knowledge of the water quality conditions. Hyperspectral and fluorescence images reveal pictures of epiphytes that are not visible to the human eye, whereas imaging with a simple flatbed scanner provides a fast, convenient method that is still rich in information about the epiphytes. Computer programs can be developed to automatically extract from the images quantitative information such as percent coverage and spatial gradients. Researchers are also using chemical analyses of algal pigments and new DNA sequencing technologies with bioinformatics to yield insights into water quality conditions.

APPENDIX B

TAMUCC 11th Annual Pathways Student Research Symposium, Kingsville, TX, 8 November 2013.

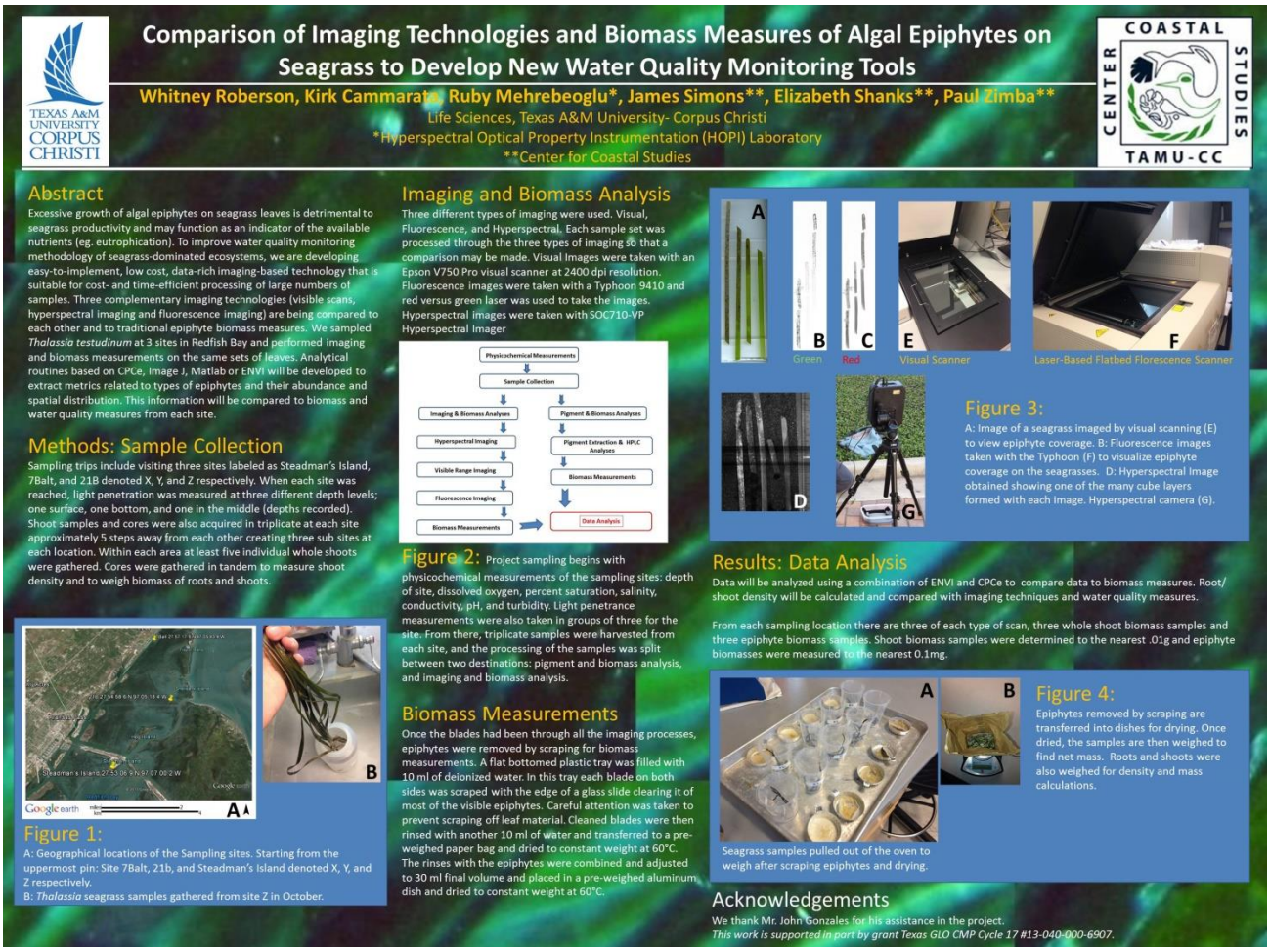

Investigation of Seagrasses under Hyperspectral Imaging System

Dustin K. Smith, Dr. Mehrube Mehrubeoglu , Dr. Kirk Cammarata, and Elizabeth Shanks
[1]The HOPI Lab, School of Engineering and Computing Sciences, Texas A&M University, Corpus Christi, TX

ABSTRACT

Seagrasses are an integral part of the ecosystem. They provide a habitat for sea life, and are important for healthy marine environments. Seagrasses have been investigated by scientists and engineers alike to determine their abundance and changes in satellite images to identify their chlorophyll content, their changes in mass in temporal studies, and to investigate their epiphyte and epifauna coverage for an indication of the health and well-being of not only of the seagrasses themselves but also their environment. Traditional methods of data acquisition and analysis present themselves as labor-intensive, expensive or highly dependent on environmental conditions. As a noninvasive approach, hyperspectral images of the seagrasses were acquired and analyzed spectrally as well as spatially. In this study we report the variation of percent coverage of seagrasses with total epiphytes and epifauna across three different sites in the Corpus Christi Bay based on hyperspectral image analysis. The results show variations among the three sites. The results suggest that hyperspectral imaging can be used as a potential method in the observation and study of sea grass communities.

INTRODUCTION

Seagrasses are flowering plants found in shallow marine habitats. They are vital to the ecosystem since they stabilize the sea bottom, provide food and habitat, help maintain water quality, serve as nursery areas, and support local economies. Seagrasses serve as bioindicators since they are sensitive to changes in water quality. Epiphytic coverage on the seagrasses correlate with their marine environmental conditions. On the one hand, epiphytes on seagrasses in low quantities are able to protect seagrasses from desiccation or UV radiation above low tide levels. On the other hand, too much epiphytic coverage may cause poor health and possibly death of the seagrasses, if dense coverage prevents efficient photosynthesis. Accurate and fast technologies are needed to assess seagrasses and their surface coverage.

Hyperspectral imaging (HSI) is a relatively new technology that provides both spectral and spatial information in hyperspectral data cubes. Hyperspectral imaging technology allows differentiation of a multitude of materials and objects in the processed data. In this experiment hyperspectral images of seagrasses are analyzed to investigate their epiphytic relationship. Using color maps obtained from the ratio of different spectral color frames, the relative abundance of epiphytes, tubeworms, and seagrasses is calculated and compared.

HYPERSPECTRAL IMAGING SYSTEM

Hyperspectral imaging system is set up in reflection mode to collect hyperspectral data cubes representing seagrasses with different surface coverage and states of health (Fig. 1).

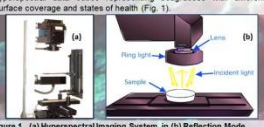

Figure 1. (a) Hyperspectral Imaging System, in (b) Reflection Mode

SEAGRASS SAMPLE

Figure 2. Tip of a seagrass blade (turtle grass, or *Thallassia testudinum*). This seagrass is abundant though the Texas coast and is easy to image due to its flat structure. Epiphytes (fuzzy structures) an tubeworms (white circular structures) can be seen on the surface.

SAMPLING LOCATIONS

Figure 3. Sampling Sites (7B, 21B, Steadman's Island) in Corpus Christi Bay indicated by stars
Orange: 7B Red: 21B Green: Stedman's Island

METHODS

Sampling and Data Collection:
- Seagrasses were collected from 3 different sites (Fig. 3)
- Seagrasses were labeled according to shoot, blade and slice (cut portion)
- Each slice was imaged with the hyperspectral imaging system

Data and Data Processing
- Data were analyzed using ENVI 4.8 software tool
- 3 blades from 3 different shoots from each site were analyzed
- Further analysis was completed using MATLAB and MS Excel

Hyperspectral Image Processing

Raw hyperspectral image cubes from the 3 sites were uploaded into ENVI 4.8 where each image slice (picture frame at a given spectral band) could be viewed and then processed.

Figure 4. Raw hyperspectral image of a seagrass blade in ENVI using RGB color mode (R:640nm, G:550nm, B:460nm)(from the same seagrass blade in Fig. 2). Each seagrass blade was imaged with a gray panel with 18% reflectance used for image calibration and normalization, seen above the seagrass blade in the figure. "Region of interest" tool in ENVI was used to select an image segment and save the grey panel spectral profile along the horizontal direction. Gray panel spectrum was then pixel-duplicated to match the size of the image. This scaling process was achieved by using "Resizing" in the basic tools tab. The seagrass image was normalized by using spectral math and dividing the seagrass spectral image by grey panel spectral image.
(Normalized Image = Original Image / Gray Panel)

Figure 5. Normalized image from Fig. 4. The normalization process results in improved color contrast. Note that the gray panel appears almost completely white since it is divided by itself.

Figure 6. Cropped seagrass blade image of Fig. 5, achieved through the region of interest tool in RGB color mode (R:860nm, G:650nm, B:550nm). Image was then saved, and the background pixels (seen as darkest pixels along the frame of the blade image) was replaced with black or a value of 0. Using the RGB ratio function in ENVI, 3 different wavelengths were chosen from the hyperspectral blade image to get the high-contrast image that showed fine details on the blade as seen above.

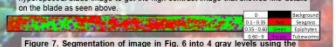

Figure 7. Segmentation of image in Fig. 6 into 4 gray levels using the density slice tool(RGB color mode R:860nm, G:650nm, B:550nm). Each gray level is represented by a false color for classification of seagrass (red), epiphyte (green), tubeworm (purple), and background (black).

RESULTS

Figure 8. (Left) Average length in cm for 10 seagrass blades from each site. (Right) Average length of seagrass blades (cm) used in this study at each site.

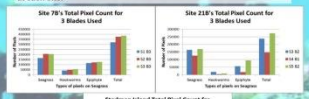

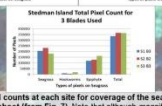

Figure 9. Pixel counts at each site for coverage of the seagrass blade used in each shoot (from Fig. 7). Note that although magnification is the same for each scanned image, blade length is different.

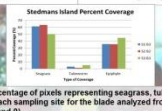

Figure 10. Percentage of pixels representing seagrass, tubeworms and epiphytes at each sampling site for the blade analyzed from each shoot (From Figs.7 and 9).

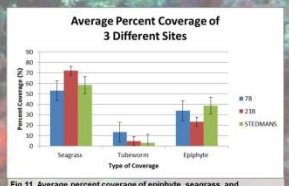

Fig 11. Average percent coverage of epiphyte, seagrass, and tubeworms at each site. (Averaging across 3 blades per site.)

RESULTS (cont.)

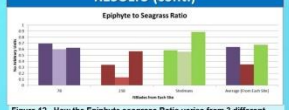

Figure 12. How the Epiphyte seagrass Ratio varies from 3 different site. Similar trends are observed. Both depend on seagrass coverage and blade length.

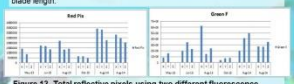

Figure 13. Total reflective pixels using two different fluorescence.

Discussion

Figures 4 though 7 clearly show the differentiation among epiphytes, tubeworms, and seagrass in hyperspectral images processed using ENVI. Although only single blades were used from 3 shoots per site, the data in Figures 8 through 12 show differences among seagrass coverage among the 3 sites. From Fig. 11, as expected, in each site, seagrass blades have the highest percentage followed by epiphytes followed by tubeworms. However, Fig. 11 also shows that Site 21B had lowest epiphyte coverage and highest exposed seagrass blade, whereas site 7B seagrasses displayed the highest tubeworm coverage. Figure 12 shows that there is a correlation between biomass and total pixels for seagrass from the three sites; however since, as Figure 8 shows, there is a difference in average length of seagrass blades that have been randomly selected for data analysis here, pixel count, which is directly related to blade length and blade coverage, is not the most reliable measure for interpretation of seagrass coverage.

The independent fluorescence spectroscopy study of Red F and Green F, where reflected light from a narrow waveband shown on the sea grasses were collected, shows variances across seasons (Fig. 13).

CONCLUSION AND FUTURE WORK

Hyperspectral imaging can be used to differentiate epiphyte coverage, efficiently and non-invasively; however, more seagrass samples must be analyzed for statistically more significant results. ENVI software tool proved to be an effective tool in image normalization and band ratio calculations, and in generating classification maps that can then be used to compute relative seagrass coverage. We also see changes in the seagrass over time in figure 13This could be due to the change in light availability, and causing a decline in seagrass this causes a decrease in epifauna.

References

M. Y. Teng, M. Mehrubeoglu, S. King, K. Cammarata, and J. Simons, "Investigation of Epifauna Coverage on Seagrass Blades Using Spatial and Spectral Analysis of Hyperspectral Images," *5th Workshop on Hyperspectral Image and Signal Processing: Evolution in Remote Sensing, Gainsville, Florida, June 25-28, 2013.*

D. Balata, U. Nesti, L. Piazzi, and F. Cinelli, "Patterns of Spacial Variability of Seagrass Epiphytes in the North-west Mediterranean Sea," *Marine Biology*, vol. 151, pp. 2025-2035, 2007. [1] J. S. Wood, *Hyperspectral Analysis of Seagrass in Redfish Bay, Texas*, Dissertation, Texas A&M University-Corpus Christi, December 2012.

Acknowledgement

This project is funded in part by the Texas General Land Office through a grant from National Oceanic and Atmospheric Administration (NOAA Award No: NA12NOS4190164. GLO Contract No.: 13-040-000-6907)

APPENDIX C

(Copyrighted Material) (Available with authorized access from http://ieeexplore.ieee.org/Xplore/home.jsp)

Empirical Mode Decomposition of Hyperspectral Images for Segmentation of Seagrass Coverage

Mehrube Mehrubeoglu, Chris Trombley, Susan E. Shanks, Kirk Cammarata, James Simons, Paul V. Zimba
College of Science and Engineering
Texas A&M University-Corpus Christi
Corpus Christi, Texas, USA
ruby.mehrubeoglu@tamucc.edu

Lifford McLauchlan
Dept. of Electrical Engineering and Computer Science
Texas A&M University-Kingsville
Kingsville, Texas, USA
lifford.mclauchlan@tamuk.edu

Abstract—Seagrasses are an integral part of the marine ecosystem, and can provide information about their environment based on their surface content. In particular, epiphytes and epifauna on seagrass blades are of interest to scientists. Empirical mode decomposition is applied to hyperspectral images obtained from seagrasses to separate hyperspectral data into component modes, and then to segment and classify the seagrass coverage. A sample spectrum is taken from the image for reference for each of the classes (seagrass leaf, tubeworm, epiphyte). Hypothesis testing on the higher modes for an entire image gives a semi-automated algorithm for classifying the contents of unknown spectra. A classifier is developed to segment the seagrass hyperspectral images and identify epiphytes on the seagrasses.

Keywords—seagrasses; empirical mode decomposition; hyperspectral imaging; hyperspectral image processing; classification; segmentation;

I. Introduction

Seagrasses are an integral part of the ecosystem. They provide a habitat for sea life, and are important for healthy marine environments. Seagrasses have been investigated by scientists and engineers alike to determine their abundance and changes in satellite images [1], to identify their chlorophyll content and their changes in mass in temporal studies [2]-[5], and to investigate their epiphyte and epifauna coverage that is an indication of the health and well-being of not only the seagrasses but also their environment [6]-[8]. Traditional methods of data acquisition and analysis present themselves as labor intensive, expensive or highly dependent on environmental conditions. Hyperspectral imaging involves a relatively fast and effective data collection and exploration methodology for the identification and mapping of seagrass composition.

Hyperspectral imaging refers to the process, technology and analysis of image frames collected at multiple wavelengths that create a 3D data cube which contains both 2D image details at specific wave bands, and 1D spectral information at each spatial pixel location. A hyperspectral image captures a wide range of spectral bands typically limited by the light source, the spectrometer and the image sensor. Spectral signatures help infer the distribution of light at each image pixel location, and allow the interpretation of the underlying physical content associated with that pixel location. Access to spectra at each image point thus enables a more detailed analysis of an image than is possible with a standard image, including the use of distributional methods; however, these distributions are often noisy, multimodal and otherwise ill-behaved. Since generally no *a priori* information is present to discern the particular shape the distribution should take, non-parametric and data-driven methods offer a viable tool for informed analyses of hyperspectral images.

Hyperspectral images from seagrasses have been previously analyzed for binary classification of seagrasses to separate tubeworms from the rest of the seagrass surface [6]. In this work we focus on using empirical mode decomposition (EMD) for three-class segmentation of the seagrass to represent the host (seagrass), epiphytes and tubeworms.

In the rest of this paper, the EMD is described in section II. Data acquisition and application of the EMD are explained in Section III. The preliminary results are presented in Section IV. Conclusions are summarized in Section V.

II. Background

Empirical mode decomposition is a data driven method [9] which adaptively decomposes data into oscillating components called intrinsic mode functions (IMFs). IMFs are based on oscillations around the mean found in the data, which makes IMFs more natural for a given problem than a prescribed basis for spectra such as is done in Fourier or Wavelet analysis. The IMFs are found in steps: first an envelope is formed around the data by cubic splines from maximum to maximum or minimum to minimum. Characteristic timescales between mean crossings are identified, and the mean value between the upper and lower envelope is given for this timescale. Thus the first IMF is extracted. This means that the EMD can be used to denoise data [10], since each step is a smoothing out of extrema. Higher level EMD will be smoother than lower level EMD. This process is repeated until a stopping criterion such as

978-1-4799-5220-5/14/$31.00 ©2014 IEEE

having too few maxima or minima to make a meaningful IMF is reached. Frequently, the IMF derived from this method will have physical meaning [9]–[12].

In their paper, Rilling *et al.* describe the empirical mode decomposition algorithm [13], and Nunes *et al.* describe bidimensional EMD applied for image analysis [14]. Demir *et al.* [15], Zhang *et al.* [16] and Erturk *et al.* [17] use EMD for hyperspectral image classification. In this research, the authors also use EMD to separate hyperspectral data into component modes. To accomplish identification and classification of spectral signals, a statistical decision must be made. The shape of the reference spectra (signals from host or green seagrass, epiphytes and tubeworms) can be extracted manually, which then provides *a priori* shapes for each. In this case, even after the EMD is applied, the data has been smoothed and the dominant IMF has been extracted, a nonparametric test is applied. The Kolmogorov-Smirnov Test [18] is the method chosen in this project. The Kolmogorov-Smirnov statistic is computed by determining at which waveband the test spectral density and the reference spectral density have the largest difference in their cumulative density function (CDF). First the smoothed spectral density function is obtained from the above-outlined EMD algorithm. This function is then cumulatively summed and normalized to obtain the cumulative density function. CDF allows the computation of the Kolmogorov-Smirnov statistic and makes a meaningful hypothesis test without making presumptions on the distribution of the spectral data.

III. Methods

A. Hyperspectral Data Acquisition

Hyperspectral data cubes were collected from seagrass samples outdoors under natural lighting conditions using a portable hyperspectral imager (Surface Optics Corp., USB Visible Hyperspectral Camera 0710-0001). A standard calibration panel with known reflectance (gray panel with 18% reflectance) was inserted in the imaged seagrass scene, and used as a reference to normalize the hyperspectral data after the images were acquired. Normalization is achieved by dividing the difference between each spectrum of interest (seagrass area) and dark current signal by the difference between the reference spectrum and dark current signal as in (1).

$$\mathbf{I_n} = (\mathbf{I_s} - \mathbf{I_d}) / (\mathbf{I_r} - \mathbf{I_d}), \quad \ldots\ldots\ldots\ldots\ldots\ldots (1)$$

where $\mathbf{I_n}$ is the normalized spectrum, $\mathbf{I_s}$ is the spectrum to be classified, $\mathbf{I_d}$ represents the dark current signal, and $\mathbf{I_r}$ is the reference spectrum. (If $\mathbf{I_r}$ is from white reference, then $\mathbf{I_n}$ is the calculated reflectance [19].) The normalized spectra associated with each 2D pixel location are then fed into the EMD algorithm for binary hypothesis testing, classification, and segmentation of the 2D seagrass images.

B. Application of EMD on Seagrass Hyperspectral Data

Most spectra of real biological interest have unknown and variable spectral distributions; therefore, it is one strength of this methodology that the class-specific (in this case, seagrass, epiphyte, tubeworm) reference spectra for computing the Kolmogorov-Smirnov Statistic are obtained. To choose spectra meaningful to the biologist, these reference spectra are identified manually from within the image. The spectra are then compared to one another's EMD smoothed spectral density by the Kolmogorov-Smirnov test outlined above.

This method, unlike the previously used methods, has the advantage of being extensible. The test can be computed for multiple reference spectra, limited only by the bandwidth of the original image. This means that this algorithm can be utilized for multiple-class identification. Here, a group of picture elements for both tubeworms and epiphytes are examined to demonstrate the differentiation and identification process.

IV. Preliminary Results

Figure 1 shows a sample hyperspectral image frame that contains the calibration panel (far left), a ruler, and two seagrass blades (middle, right). The white 'dots' on the seagrasses are tubeworms. The discoloration on the each blade represents epiphytes.

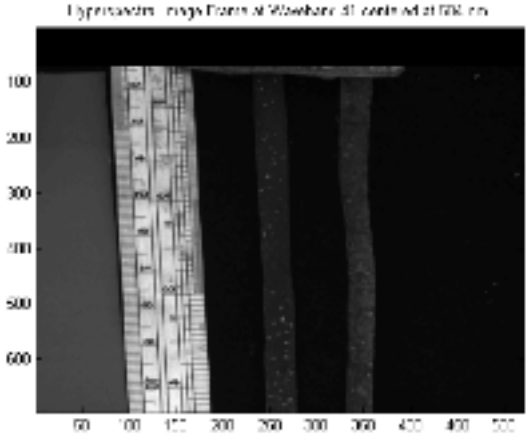

Fig. 1. Hyperspectral image frame showing the gray panel (far left) and two seagrass blades with tubeworms and epiphytes. (Image axes are represented in pixels).

Hyperspectral data is acquired for 128 bands from 400 nm to 1000 nm. Figure 2 shows a normalized sample noisy hyperspectral signature from an image pixel location that represents epiphytes.

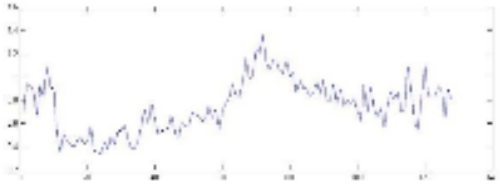

Fig. 2. Sample noisy normalized hyperspectral signal known to have epiphytes (Spectral signature associated with a single image pixel location). Horizontal axis represents the band number from 400 nm to 1000 nm (total 128 bands). Vertical axis represents normalized spectrum.

Figure 3 demonstrates the same spectral signature as in Figure 1 together with sample components extracted through the empirical mode decomposition method.

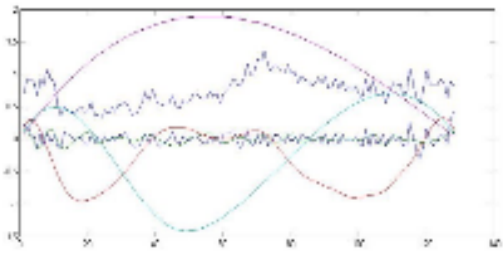

Fig. 3. Hyperspectral signal in Figure 1, and its sample components from EMD.

Figure 4 shows the cumulative density function associated with the signal in Figure 1.

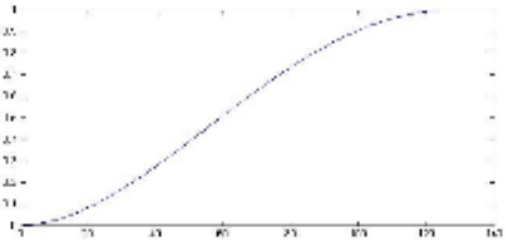

Fig. 4. Cumulative Density Function (CDF) of the Sample signal in Figure 1.

In Figure 5, the CDF for a spectrum associated with epiphytes and CDF for spectral signature for seagrass can clearly be differentiated. Correlation among these features can then be established for simple classification of unknown spectra within an entire hyperspectral image.

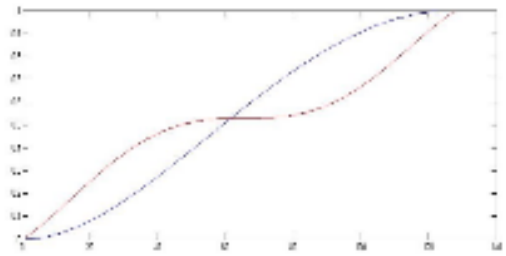

Fig. 5. Comparison of CDF in Figure 4 to CDF associated with a pixel location lacking epiphytes. (Red = seagrass; Blue = epiphyte)

Figure 6 depicts seagrass blades that have epiphytes and tubeworms on them. Unnormalized and normalized spectra for the tubeworms are shown in Figures 7 and 8, while the unnormalized and normalized spectra for epiphytes are depicted in Figures 9 and 10. In this case, normalization was achieved without a gray panel, but was still valuable to remove common system-specific response in the spectral signatures.

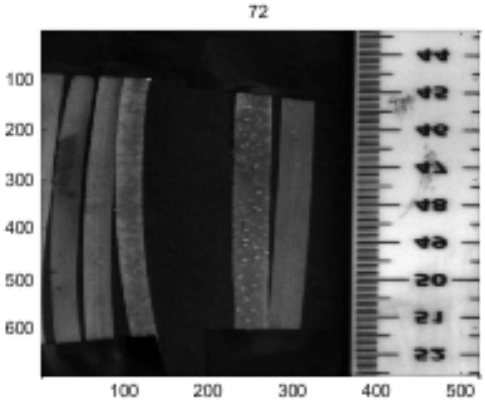

Fig. 6. Hyperspectral image frame showing seagrass blades with tubeworms and epiphytes (frame 72 out of 128). The horizontal and vertical axes represent pixel numbers. The ruler (right) demonstrates the millimetric scale on its left.

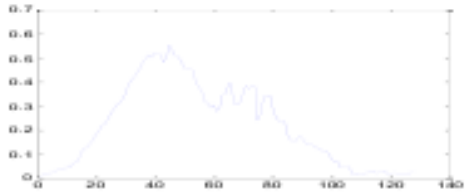

Fig. 7. Unnormalized tubeworm spectrum. Horizontal axis represents band number (total 128 bands) representing 400 nm to 1000 nm. Vertical axis represents relative spectral intensity of the raw signal (arbitrary units).

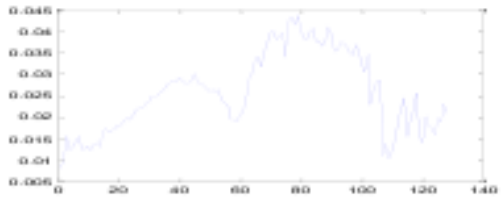

Fig. 8. Normalized noisy tubeworm spectrum of Fig. 7. Horizontal axis represents band number (total 128) from 400 nm to 1000 nm. Vertical axis represents normalized spectral intensity (no units).

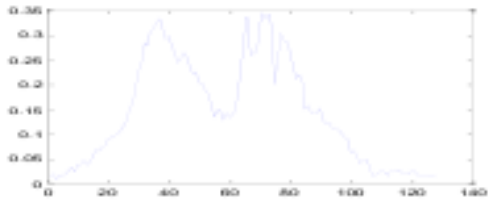

Fig. 9. Unnormalized epiphyte spectrum. Horizontal axis represents band number (total 128) from 400 nm to 1000 nm. Vertical axis represents relative spectral intensity of the raw signal (arbitrary units).

Fig. 10. Normalized epiphyte noisy spectrum. Horizontal axis represents band number (total 128) from 400 nm to 1000 nm. Vertical axis represents normalized spectral intensity (no units).

The Empirical mode decomposition results for epiphytes in Figure 6 are depicted in Figure 11 a)-e). Five components are displayed for the epiphytes in the image. Figure 12 shows the epiphyte classification results (identified epiphytes) for the seagrass image found in Figure 6 after pixel-by-pixel spectral analysis and binary classification. The dark areas in this figure represent epiphytes whereas the white areas represent non-epiphyte regions. Note in Figure 12 that the tubeworms are correctly identified as not being epiphytes (white circular regions).

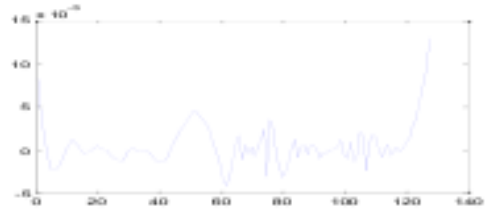

a) C_1 component

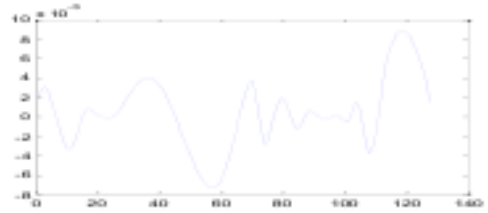

b) C_2 component

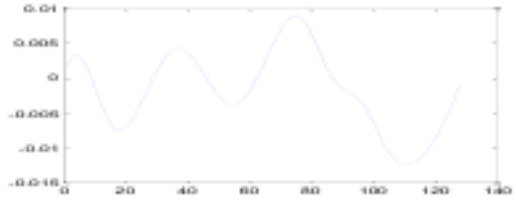

c) C_3 component

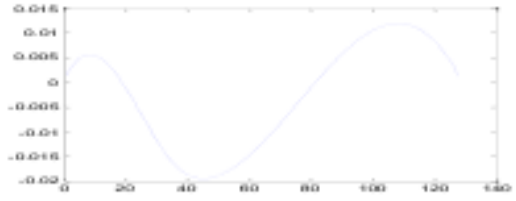

d) C_4 component

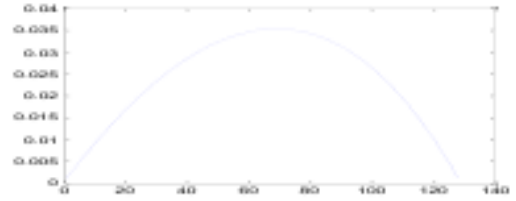

e) C_5 component

Fig. 11. a)-e) EMD components C_1-C_5 for the epiphytes from Figure 6.

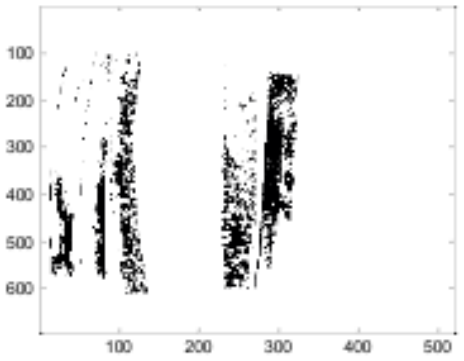

Fig. 12. Epiphyte classification for the image in Figure 6.

V. Conclusions

Preliminary results demonstrate the differentiation of spectral signatures from hyperspectral image locations containing epiphytes and tubeworms using empirical mode decomposition. Assuming unmixed spectra, classification can be achieved by simple correlation and thresholding. Classification would permit determination of epiphyte coverage of seagrass leaves, a metric of biological importance. Since some mixing of the spectra from the three classes (host seagrass leaf, tubeworms, epiphytes) are inevitable, signal distributions are expected to show some overlap, and will need to be analyzed further for proper segmentation of the seagrass images and calculation of percent coverage using the EMD methodology. Independent methods of validating the results are also necessary, and the subject of ongoing work.

Acknowledgment

This work has partially been funded by Coastal Management Program Grant #13-040 from Texas General Land Office.

References

[1] J. S. Wood, "Hyperspectral Analysis of Seagrass in Redfish Bay, Texas," Dissertation, Texas A&M University-Corpus Christi, December 2012.

[2] J. S. Krumholz, Spatial and Temporal Patterns in Nutrient Standing Stock and Mass-balance in Response to Load Reductions in a Temperate Estuary, Dissertation, University of Rhode Island, 2012.

[3] J. W. Fourqurean, A. Willsie, C. D. Rose, and L. M. Rutten, "Spatial and Temporal Pattern in Seagrass Community Composition and Productivity in South Florida," Marine Biology, vol. 138, pp. 341-354, 2001.

[4] R. Fisher, "Spatial and Temporal Variations in Nematode Assemblages in Tropical Seagrass Sediments," Hydrobiologia, Vol. 493, pp. 43-63, 2014.

[5] D. Yang, Y. Yang, C. Yang, J. Zhao, and Z. Sun, "Detection of seagrass in optical shallow water with quickbird in the Xincun Bay, Hainan province, China," Image Processing, IET, vol. 5, pp. 363-368, 2011.

[6] M. Y. Teng, M. Mehrubeoglu, S. A. King, K. Cammarata and J. Simons, "Investigation of epifauna coverage on seagrass blades using spatial and spectral analysis of hyperspectral images," 5th Workshop on Hyperspectral Image and Signal Processing: Evolution in Remote Sensing, Gainsville, Florida, 4 pages, 25-28 June 2013.

[7] D. Baluta, U. Nesti, L. Piazzi, and F. Cinelli, "Patterns of Spatial Variability of Seagrass Epiphytes in the North-west Mediterranean Sea," Marine Biology, vol. 151, pp. 2025-2035, 2007.

[8] G. Martin and A. Plaza, "Spatial-Spectral Preprocessing Prior to Endmember Identification and Unmixing of Remotely Sensed Hyperspectral Data," IEEE Journal of Selected Topics in Applied Earth Observations and Remote Sensing, vol. 5, pp. 380-395, 2012

[9] N. Huang, Z. Shen, S. Long, M. Wu, H. Shih, Q. Zheng, N. Yen, C. Tung, and H. Liu, "The empirical mode decomposition and the Hilbert spectrum for nonlinear and nonstationary time series analysis," Proc. R. Soc. Lond. A, vol. 454, no. 1971, pp. 903-995, 8 March 1998.

[10] A. Boudraa and J. Cexus, "Denoising via empirical mode decomposition," Proc. Second International Symposium on Communications, Control and Signal Processing, Morocco, 4 pages, 2006.

[11] K. Coughlin and K. Tung, "11-year solar cycle in the stratosphere extracted by the empirical mode decomposition method," Advances in Space Research, vol. 34, no. 2, pp. 323-329, 2004.

[12] J. Echeverria, J. Crowe, M. Woolfson, and B. Hayes-Gill, "Application of empirical mode decomposition to heart rate variability analysis," Medical and Biological Engineering and Computing, vol. 39, no. 4, pp 471-479, 2001.

[13] G. Rilling, P. Flandrin and P. Goncalves, "On empirical mode decomposition and its algorithm," Proc. of the 6th IEEE/EURASIP Workshop on Nonlinear Signal and Image Processing, Grado, Italy, pp. 8-11, 8-11 June 2003.

[14] J. Nunes, Y. Bouaoune, E. Delechele, O. Niang, and P. Bunel, "Image analysis by bidimensional empirical mode decomposition," Image and Vision Computing, vol. 21, pp. 1019-1026, 2003.

[15] B. Demir and S. Ertürk, "Empirical mode decomposition of hyperspectral images for support vector machine classification," IEEE Trans. Geoscience and Remote Sensing, vol. 48, pp. 4071–4084, 2010.

[16] M. Zhang and Y. Shen, "Ensemble empirical mode decomposition for hyperspectral image Classification," Proc. Advances in Adaptive Data Analysis, Theory and Application, no. 4, 2012.

[17] A. Erturk, M. Gullu and S. Erturk, "Hyperspectral image classification using empirical mode decomposition with spectral gradient enhancement," IEEE Trans. Geoscience and Remote Sensing, vol. 51, pp. 2787–2798, 2013.

[18] R. Wilcox, "Kolmogorov-Smirnov test," *Encyclopedia of Biostatistics*, John Wiley & Sons, 15 July 2005 (published online; DOI: 10.1002/0470011815.b2a15064).

[19] G. Lu and B. Fei, "Medical hyperspectral imaging: a review," J. Biomedical Optics, vol. 19, no. 1, pp. 010901-1 - 010901-23, January 2014.

AVAILABLE WITH AUTHORIZED ACCESS THROUGH
http://ieeexplore.ieee.org.manowar.tamucc.edu/stamp/stamp.jsp?tp=&arnumber=6958441&tag=1

APPENDIX D

Legend used for labeling random pixels in seagrass visible scans using CPCe 3.6 (Coral Point Count with Excel extensions)

Legend
4
C,“Coral”
L,“Leaf”
E,“Epiphyte”
TWS,“Tape, wand, shadow”
T,“Tubeworm”,“E”
LB,“Leaf blade”,“L”
AE,”Gray Algal Epiphyte”,“E”
OC,“Dead Leaf”,“C”
OT,“Background”,”TWS”
GE,“Green Algal Epiphyte”,“E”
NOTES,NOTES,NOTES

APPENDIX E

HYPERSPECTRAL IMAGING WITH THE PORTABLE HYPERSPECTRAL CAMERA

Powering up and Getting Started

1. Connect power source to camera.
2. Connect camera to computer.
3. Open acquisition software.

Acquisition Software

1. Make sure scanner settings match factory settings in file ”SOC710_scanner_settings”
2. Use com4
3. Note the following:
   Scan start position= scanner_home_position
   On-center position=scanner_center_position
   Focus position=focus_home_position
   Step-size=scanner_step_size

Focusing the Camera

1. Click purple button. New window opens. (This allows real-time a visible camera to view the sample so focusing can be accomplished faster without the hyperspectral camera scans)
2. Rotate the lens until the image in focus. Once focused, click button again to close the window, and switch to hyperspectral imaging mode. (Note: The focusing visible camera is not perfectly aligned with the hyperspectral camera. What is focused in the visible camera may not be focused in the hyperspectral camera. With experience, the user will learn to keep the visible image slightly off focus to ensure hyperspectral camera is in focus).

Acquiring Hyperspectral Images

1. Press the green button to start hyperspectral image acquisition

(Recommended pixel range values are 500-3000. Values over 4096 are saturated, since this is a 12-bit camera)

Calibration frames:

Typical normalization of a hyperspectral image involves the following formula:

$$I_N(i) = (I(i) - D_k(i)) / (C_L(i) - D_k(i)),$$

Where $I_N(i)$ is the i^{th} normalized image pixel in the I_N normalized image, $I(i)$ is the i^{th} acquired image pixel in the I hyperspectral image, $D_k(i)$ is the i^{th} dark frame pixel in the D_k dark image, and $C_L(i)$ is the i^{th} calibration pixel in the C_L calibration image. Normalization is applied to all pixels in the hyperspectral image.

If the noise levels are low, normalization can be simplified as $I_N = (I / C_L)$ applied to all pixels in the image.

D_k records dark frame. This corresponds to dark noise image, and captures camera noise when there is no light entering the viewing lens. To acquire a dark frame, leave the cap of the lens on. Capture the image, and save with an extension .drk
C_L records calibration frame. Use a grey reference panel (sheet) for this purpose. Save image as .cal

Calibration can be accomplished by inserting the gray reference panel in the field of view within the scanned seagrass images. This reduces the acquisition time, since less number of hyperspectral image frames need to be acquired, and allows better synchronization of lighting conditions between the seagrass samples and calibration panel, as the gray panel appears in the same image as the seagrasses. Note: Care must be taken to keep the gray calibration panel dry (which can be a challenge in the field on a boat), as the gray panel loses its integrity when wet. Similarly, care must be taken to ensure it does not fly off in the wind. The gray panel is held down with the same weights used to hold down the seagrass leaves flat.

Saving Hyperspectral Image Cubes

Once the image is acquired, it must be saved as a BIL file. Save image using "SOC710 standard (with BIL header)" option.
Note: Image does not save automatically. If the green button is pressed again for a new hyperspectral scan without saving the previous image, the previous image is overwritten and lost.

Camera Settings

If the weather is cloudy, or otherwise ambient light levels are low, increase camera integration time to compensate for low light. This must be done relatively frequently if there is cloud cover, moving clouds, or as the day progresses and the position of the sun changes.

Alternatively, to increase the amount of light entering the camera, the camera's gain can also be increased, but this will increase noise since the gain is amplified together with the useful signals.

Conversely, if the day gets brighter during acquisition time, integration times must be reduced to prevent saturation of the camera. Decrease integration time in bright light. Smaller integration times will also reduce time needed to acquire a hyperspectral cube. If possible, sunny and bright days are prepared for sample imaging.

Keep the camera lens 21.75" in from object. This will allow minimal fine adjustments for focusing. (This is specific to our system, and will vary depending on the lens used. However such distances can be determined off-line before field trips for each system to conserve time during image acquisition during sampling events.)

Spectral Radiance Analysis Software

Once the images are acquired the images can be calibrated and analyzed.
Open image cube in the Spectral Radiance Analysis Software associated with the portable camera.
Three levels of calibration options are:

- Spectral
- Dark level offset
- Spatial and spectral radiometric

Reflectance calibration:

Under image tab, check box by “select region”.
Select an area in image containing grey panel
Using “write” button save as .txt
Go to calibration tab and read in file using “set light” button

Setting Dark Calibration:

Click “set dark” under calibration tab. Select .drk file

Data Naming Convention

The portable camera software automatically appends the image acquisition date and time to the image file name. For the images, shoot number and blade (leaf) number was appended to the file name. Other acquisition parameters were added as part of the file name.

APPENDIX F

NORMALIZING A SEAGRASS IMAGE WITH GREY REFERENCE PANEL TO ACCOUNT FOR AMBIENT LIGHT AND OTHER SYSTEM VARIATIONS DURING DATA ACQUISITION

(Normalization: Seagrass Image (S1) / Calibration Strip (Gray Reference Panel) Image (S2))

1) Open ENVI Software tool
2) Open selected pic (hyperspectral image with grey reference panel)
    a. File → Open Image File → search image → okay

    (Available Bands List pops up)

3) Select Band and then load band (this will show only one of the image frames at the selected band)
4) Elongate #1 band
5) On "#1 Band" click tool → region of interest → ROI tool. (ROI: Region of Interest)

    (#1 ROI tool box should appear)

6) Select ROI type

    (Rectangle is preferred but any shape can be chosen)

7) Surround region of study with red box (This will be the gray reference panel region of interest). Move red box, as needed, to capture the ROI. When satisfied, right click inside red box, select whole region to be measured.

    (The identified ROI should become red)

8) Click on ROI toolbox, and, on File tab, click subset via ROI
9) Select sample
10) Click ok
11) Select again
12) Click 'choose and name file', click okay
13) On available bands list box, select ROI resize band needed
14) Click new display, then load band
15) Now, find the image size:

    (Includes lines and samples that can be scaled for both images)

    a. Go to tools, pixel locator
    b. Click right bottom and go down as far as possible
    c. Exit ROI box
    d. Record lines and samples for image

e. Record lines and samples for ROI (gray panel section)

16) Divide image sample and lines (entire seagrass image), by ROI sample and lines (gray panel ROI) to get scale factors

(May want to write down all information) (The purpose of this process is to expand the strip of grey reference panel to the size of the image for normalization, since the gray panel strip will be much narrower than the seagrass image, or entire image frame)

17) Click on ENVI 4.8 box, basic tools, resize data
    a. Click unscaled and okay
    b. Put scale factors (that were just calculated above) in samples and lines boxes for scale factors
    c. Choose file to save, and save

    (Will take a few minutes to process and loading bar will appear)

18) Open Scaled image in available list
19) Make a new display
20) Click ENVI 4..8 box, basic tools, spectral math

(In spectral math, click on help to learn expressions:
    a. Everything is in s1, s2, s3, …, format
    b. Seagrass image will be assigned s1; gray panel will be assigned as s2.
    c. This information will show in help)

21) After entering the formula (s1/s2), add to list and hit okay
22) Click s1 or (or whatever s# used) with “undefined variable with it”
    a. Click map variable to input file and select spectral profiles according to equation
    b. Choose file name, click okay
23) On available bands list click final results band for the normalized image.

(The above process normalizes seagrass image with gray reference panel by division. If dark image is to be subtracted, the appropriate formula needs to be written, for example (s1-s3)/(s2-s3), where s1 is the seagrass image, s3 is the dark image (same size as seagrass image), and s2 is the size-scaled gray panel image.)

APPENDIX G

HYPERSPECTRAL IMAGE PROCESSING USING MATLAB SOFTWARE AND EML METHOD (see conference paper, (Mehrubeoglu *et al.* 2014))

The following list of codes' parameters is optimized for the hyperspectral image file:
_I80_L0-511_6-8-2014_17.54.8_7b_s2b1_it250_46p5cm (BIL file and its associated HDR file)
Individual adjustments of parameters are necessary for each seagrass image.

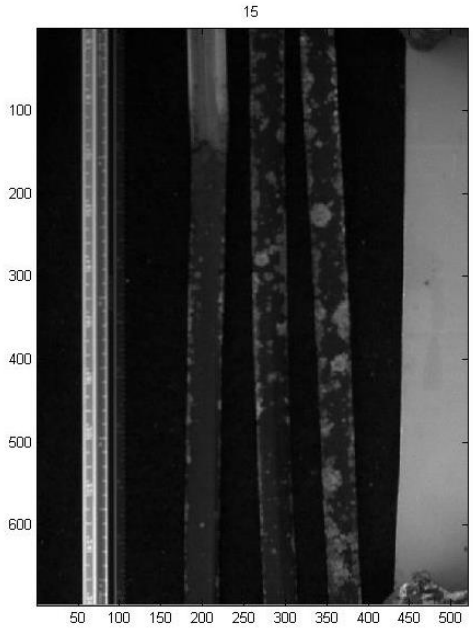

_I80_L0-511_6-8-2014_17.54.8_7b_s2b1_it250_46p5cm, hyperspectral image frame 15

MATLAB files necessary to perform the EMD:
a) openHeader.m, **b)** cubeOpener.m, **c)** imagePreparation.m, **d)** emd.m, **e)** findpeaks.m

The files in which binary classification is performed:
f) epiphyteFinderScript.m, **g)** seagrassFinderScript.m, **h)** tubewormFinderScript.m

The code for combining the above classifications: i) combinedClassifications.m

```
/*************************************************************************/

% a) openHeader.m

function [names, values] = openHeader(header);
```

```
%'header' is hyperspectral image file name;

%header = '_I10_L0-511_14-8-2013_15.55.47_seagrass4.hdr';

fid = fopen(header);

C = textscan(fid, '%s','Delimiter','\n');
[a,b] = size(C{1});

names{1} = C{1}{1};

for ii = 2:13
    assignmentLocation = strfind(C{1}{ii},' = ');
    names{ii} = C{1}{ii}(1:assignmentLocation);
    names{ii} = strtrim(names{ii});
end

for ii = 2:13
    stringSize = length(C{1}{ii});
    assignmentLocation = strfind(C{1}{ii},' = ');
    values{ii} = C{1}{ii}(assignmentLocation:stringSize);
    for jj = 1:length(values{ii})
        if values{ii}(jj) == '='
            values{ii}(jj) = ' ';
        end
    end
    values{ii} = strtrim(values{ii});
end

for ii = 3:6
    values{ii} = str2double(values{ii});
end

names{14} = C{1}{16};
for iii = 1:length(names{14})
    if names{14}(iii) == '=' || names{14}(iii) == '{'
        names{14}(iii) = ' ';
    end
end
names{14} = strtrim(names{14});

temp = C{1}{17};
for iii = 1:length(temp)
    if temp(iii) == '}'
        temp(iii) = '';
    end
end
seperationLocation = strfind(temp,', ');
values{14}(1) = str2double(temp(1:(seperationLocation(1)-1)));
for jjj = 2:length(seperationLocation)
    values{14}(jjj) = ...
        str2double(temp((seperationLocation(jjj-
1)+2):(seperationLocation(jjj)-1)));
end
```

```
values{14}(jjj+1) =
str2double(temp((seperationLocation(jjj)+2):length(temp)));
values{14} = values{14}';

temp2 = C{1}{18};
assignmentLocation = strfind(C{1}{18},' = ');
names{15} = C{1}{18}(1:assignmentLocation);
names{15} = strtrim(names{15});


/*************************************************************************/

% b) cubeOpener.m

function [im,lines,samples,bands] = cubeOpener(fileName)

headerFile = [fileName,'.hdr'];

[names, values] = openHeader(headerFile);
for ii = 1:length(names)
    if strcmp(names{ii},'lines')
        lines = values{ii};
    elseif strcmp(names{ii},'samples')
        samples = values{ii};
    elseif strcmp(names{ii},'bands')
        bands = values{ii};
    elseif strcmp(names{ii},'interleave')
        interleave = values{ii};
    elseif strcmp(names{ii},'header offset')
        headerOffset = values{ii};
    end
end

cubeName = [fileName,'.cube'];

im =
multibandread(cubeName,[lines,samples,bands],'uint16',headerOffset,interleave
,'ieee-le');

/*************************************************************************/

% c) imagePreparation.m

function [normIm,lines,samples,bands,im] = imagePreparation(fileName)

[im,lines,samples,bands] = cubeOpener(fileName);

for ii = 1:bands
    im = im - min(min(im(:,:,ii)));
    im = im./max(max(im(:,:,ii)));
end

[a,b,c] = size(im);
```

```
normIm = zeros(a,b,c);
for jj = 1:bands
    normal = mean(mean(im(100:600,460:485,jj)));
    shadow = 0*mean(mean(im(322:334,320:330,jj)));
    normIm(:,:,jj) = (im(:,:,jj)-shadow)/normal;
end

for kk = 1:bands
    normIm = normIm - min(min(normIm(:,:,kk)));
    normIm = normIm./max(max(normIm(:,:,kk)));
end
```

/*/**

% d) emd.m

```
function imf = emd(x)

% Empiricial Mode Decomposition (Hilbert-Huang Transform)
% imf = emd(x)
% Func : findpeaks

x   = transpose(x(:));
imf = [];
while ~ismonotonic(x)
   x1 = x;
   sd = Inf;
   while (sd > 0.1) | ~isimf(x1)
      s1 = getspline(x1);
      s2 = -getspline(-x1);
      x2 = x1-(s1+s2)/2;

      sd = sum((x1-x2).^2)/sum(x1.^2);
      x1 = x2;
   end

   imf{end+1} = x1;
   x          = x-x1;
end
imf{end+1} = x;

% FUNCTIONS

function u = ismonotonic(x)

u1 = length(findpeaks(x))*length(findpeaks(-x));
if u1 > 0, u = 0;
else,      u = 1; end

function u = isimf(x)

N  = length(x);
u1 = sum(x(1:N-1).*x(2:N) < 0);
```

```
u2 = length(findpeaks(x))+length(findpeaks(-x));
if abs(u1-u2) > 1, u = 0;
else,              u = 1; end

function s = getspline(x)

N = length(x);
p = findpeaks(x);
s = spline([0 p N+1],[0 x(p) 0],1:N);
```

/*/**

% e) findpeaks.m

```
function n = findpeaks(x)
% Find peaks.
% n = findpeaks(x)

n    = find(diff(diff(x) > 0) < 0);
u    = find(x(n+1) > x(n));
n(u) = n(u)+1;
```

/*/**

% f) epiphyteFinderScript.m

```
clear
clc

fileName = '_I80_L0-511_6-8-2014_17.54.8_7b_s2b1_it250_46p5cm';


[normIm,lines,samples,bands,im] = imagePreparation(fileName);
%for ii = 1:bands
%    normIm(:,:,ii) = histeq(normIm(:,:,ii));
%end

x = 271; %Sample site
y = 256; %Sample Site

x1 = 0; %Test Site Origin
y1 = 0; %Test Site Origin
nX = lines; %Test Site Size
nY = samples; %Test Site Size

aY = 338; % SPECIFIC TO IMAGE; REQUIRES USER INPUT
bY = 348; % SPECIFIC TO IMAGE; REQUIRES USER INPUT
ySize = bY-aY;
aX = 215; % SPECIFIC TO IMAGE; REQUIRES USER INPUT
bX = 235; % SPECIFIC TO IMAGE; REQUIRES USER INPUT
xSize = bX-aX;
```

```
for ii = 1:bands
    unnormSpectra(ii) = im(aX,aY,ii);
end
z = figure;
plot(unnormSpectra)
saveas(z,'unnormalizedEpiphyteSpectra.fig');
%pause
close(z)

for ii = 1:bands
    normSpectra(ii) = normIm(aX,aY,ii);
end
z = figure;
plot(normSpectra)
saveas(z,'normalizedEpiphyteSpectra.fig')
%pause
close(z)

sampleSpectra = zeros(xSize,ySize,bands); % create an image of size of
                                          % selected epiphyte region
for ii = 1:xSize
    for jj = 1:ySize
        for kk = 1:bands
            sampleSpectra(ii,jj,kk) = normIm(ii+(aY-1),jj+(aX-1),kk); %upload
                                    % the epiphyte pixels in sampleSpectra
        end
    end
end
sampleSpectra = sum(sum(sampleSpectra))/(xSize*ySize); %average sample
                                                       %epiphytes
finalTestSpectra = zeros(1,bands);
for iii = 1:bands
    finalTestSpectra(iii) = sampleSpectra(:,:,iii); %Transpose average
                                                    %epiphyte vector
end
z = figure;
plot(finalTestSpectra);
saveas(z,'preEMDAverageEpiphyteSpectra.fig')
close(z)

imf = emd(finalTestSpectra); %Find intrinsic mode functions (IMFs)
[alpha,beta] = size(imf);
for ii = 1:beta
    z = figure;
    title = ['EMD',num2str(ii),'.fig'];
    plot(imf{ii});
    saveas(z,title)
    close(z)
end

emdTestMatrix = zeros(bands,beta); %Remove the first IMF to take out noise
for kk = 1:beta
    emdTestMatrix(:,kk) = imf{kk};
end
emdSmoothedSpectra = zeros(bands,1); %The denoised spectra is the pdf
```

```
for kk = 2:beta
    emdSmoothedSpectra(:,1) = emdSmoothedSpectra+emdTestMatrix(:,kk); %Add
                        % the non-noise IMF to make the pdf (add all imf
                        % functions together, except the first imf function)
end
z = figure;
plot(emdSmoothedSpectra);
saveas(z,'testEpihpyteSpectra.fig')
close(z)

sampleCDF = cumsum(emdSmoothedSpectra); %Convert the above pdf to a cdf
sampleCDF = sampleCDF./max(sampleCDF);
z = figure;
plot(sampleCDF)
saveas(z,'testEpiphyteCDF.fig')
close(z)

outMatrix = zeros(nX,nY); %Compare the above CDF to the CDF for each pixel
for ii= 1:nX
    disp(ii);
    for jj = 1:nY
        vec = zeros(bands,1);
        for kk = 1:bands
            vec(kk) = normIm(ii+x1,jj+y1,kk);
        end
        testCDF = cumsum(vec);
        testCDF = testCDF./max(testCDF);
        [h,p] = kstest2(vec,emdSmoothedSpectra,.01); %KS Test at 95%
                                                     %confidence
        outMatrix1(ii,jj) = p;
        outMatrix2(ii,jj) = h;
        clear vec
    end
end

z = figure;
colormap gray
imagesc(outMatrix2);
saveas(z,'epiphyteClassifier.fig');
close(z)

z = figure;
colormap gray
imagesc(1-outMatrix1);
saveas(z,'epiphytePValues.fig');
close(z)

save('isEpiphyte.mat','outMatrix2');

testMatrix = outMatrix1;
for ii = aX:bX
    for jj = aY:bY
        testMatrix(ii,jj) = 1;
    end
end
z = figure;
```

```
imagesc(testMatrix);


epiphytePixels = sum(sum((1-outMatrix2)));


/*************************************************************************/
```

% g) seagrassFinderScript.m

```
clear
clc

fileName = '_I80_L0-511_6-8-2014_17.54.8_7b_s2b1_it250_46p5cm';


[normIm,lines,samples,bands,im] = imagePreparation(fileName);

x1 = 0; %Test Site Origin
y1 = 0; %Test Site Origin
nX = lines; %Test Site Size
nY = samples; %Test Site Size

aX = 195; % SPECIFIC TO IMAGE; REQUIRES USER INPUT
bX = 220; % SPECIFIC TO IMAGE; REQUIRES USER INPUT
xSize = bX-aX;
aY = 20;  % SPECIFIC TO IMAGE; REQUIRES USER INPUT
bY = 120; % SPECIFIC TO IMAGE; REQUIRES USER INPUT
ySize = bX-aX;

for ii = 1:bands
    unnormSpectra(ii) = im(aX,aY,ii);
end
z = figure;
plot(unnormSpectra)
saveas(z,'unnormalizedTubewormSpectra.fig');
%pause
close(z)

for ii = 1:bands
    normSpectra(ii) = normIm(aX,aY,ii);
end
z = figure;
plot(normSpectra)
saveas(z,'normalizedTubewormSpectra.fig')
%pause
close(z)

sampleSpectra = zeros(xSize,ySize,bands); % create an image of size of
                                          % selected epiphyte region
for ii = 1:xSize
    for jj = 1:ySize
        for kk = 1:bands
            sampleSpectra(ii,jj,kk) = normIm(ii+(aY-1),jj+(aX-1),kk); %upload
```

```
                                        %the epiphyte pixels in sampleSpectra
        end
    end
end
sampleSpectra = sum(sum(sampleSpectra))/(xSize*ySize); %average sample
                                                       %epiphytes
finalTestSpectra = zeros(1,bands);
for iii = 1:bands
    finalTestSpectra(iii) = sampleSpectra(:,:,iii); %Transpose average
                                                    %epiphyte vector
end
z = figure;
plot(finalTestSpectra);
saveas(z,'preEMDAverageTubewormSpectra.fig')
close(z)

imf = emd(finalTestSpectra); %Find intrinsic mode functions
[alpha,beta] = size(imf);
for ii = 1:beta
    z = figure;
    title = ['EMD',num2str(ii),'.fig'];
    plot(imf{ii});
    saveas(z,title)
    close(z)
end

emdTestMatrix = zeros(bands,beta); %Remove the first IMF to take out noise
for kk = 1:beta
    emdTestMatrix(:,kk) = imf{kk};
end
emdSmoothedSpectra = zeros(bands,1); %The denoised spectra is the pdf
for kk = 2:beta
    emdSmoothedSpectra(:,1) = emdSmoothedSpectra+emdTestMatrix(:,kk); %Add
                          %the non-noise IMF to make the pdf (add all imf
                          %functions together , except the first imf function)
end
z = figure;
plot(emdSmoothedSpectra);
saveas(z,'testSeagrassSpectra.fig')
close(z)

sampleCDF = cumsum(emdSmoothedSpectra); %Convert the above pdf to a cdf
sampleCDF = sampleCDF./max(sampleCDF);
z = figure;
plot(sampleCDF)
saveas(z,'testSeagrassCDF.fig')
close(z)

outMatrix = zeros(nX,nY); %Compare the above CDF to the CDF for each pixel
for ii= 1:nX
    disp(ii);
    for jj = 1:nY
        vec = zeros(bands,1);
        for kk = 1:bands
            vec(kk) = normIm(ii+x1,jj+y1,kk);
        end
```

```
        testCDF = cumsum(vec);
        testCDF = testCDF./max(testCDF);
        [h,p] = kstest2(vec,emdSmoothedSpectra,.2); %KS Test at 95%
                                                    %confidence
        outMatrix1(ii,jj) = p;
        outMatrix2(ii,jj) = h;
        clear vec
    end
end
z = figure;
colormap gray
imagesc(outMatrix2);
saveas(z,'seagrassClassifier.fig');
close(z)

z = figure;
colormap gray
imagesc(1-outMatrix1);
saveas(z,'seagrassPValues.fig');
close(z)

save('isSeaGrass.mat','outMatrix2');

testMatrix = outMatrix1;
for ii = aX:bX
    for jj = aY:bY
        testMatrix(jj,ii) = 1;
    end
end
z = figure;
colormap gray
imagesc(testMatrix);
%}

tubewormPixels = sum(sum((1-outMatrix2)));
```

/*/**

% h) tubewormFinderScript.m

```
clear
clc

fileName = '_I80_L0-511_6-8-2014_17.54.8_7b_s2b1_it250_46p5cm';


[normIm,lines,samples,bands,im] = imagePreparation(fileName);


x1 = 0; %Test Site Origin
y1 = 0; %Test Site Origin
nX = lines; %Test Site Size
```

```
nY = samples; %Test Site Size

aX = 335; % SPECIFIC TO IMAGE; REQUIRES USER INPUT
bX = 349; % SPECIFIC TO IMAGE; REQUIRES USER INPUT
xSize = bX-aX;
aY = 222; % SPECIFIC TO IMAGE; REQUIRES USER INPUT
bY = 234; % SPECIFIC TO IMAGE; REQUIRES USER INPUT
ySize = bX-aX;

for ii = 1:bands
    unnormSpectra(ii) = im(aX,aY,ii);
end
z = figure;
plot(unnormSpectra)
saveas(z,'unnormalizedTubewormSpectra.fig');
%pause
close(z)

for ii = 1:bands
    normSpectra(ii) = normIm(aX,aY,ii);
end
z = figure;
plot(normSpectra)
saveas(z,'normalizedTubewormSpectra.fig')
%pause
close(z)

sampleSpectra = zeros(xSize,ySize,bands); % create an image of size of
                                          % selected epiphyte region
for ii = 1:xSize
    for jj = 1:ySize
        for kk = 1:bands
            sampleSpectra(ii,jj,kk) = normIm(ii+(aY-1),jj+(aX-1),kk); %upload
                                      %the epiphyte pixels in sampleSpectra
        end
    end
end
sampleSpectra = sum(sum(sampleSpectra))/(xSize*ySize); %average sample
                                                       %epiphytes
finalTestSpectra = zeros(1,bands);
for iii = 1:bands
    finalTestSpectra(iii) = sampleSpectra(:,:,iii); %Transpose average
                                                    %epiphyte vector
end
z = figure;
plot(finalTestSpectra);
saveas(z,'preEMDAverageTubewormSpectra.fig')
close(z)

imf = emd(finalTestSpectra); %Find intrinsic mode functions
[alpha,beta] = size(imf);
for ii = 1:beta
    z = figure;
    title = ['EMD',num2str(ii),'.fig'];
    plot(imf{ii});
    saveas(z,title)
```

```
    close(z)
end

emdTestMatrix = zeros(bands,beta); %Remove the first IMF to take out noise
for kk = 1:beta
    emdTestMatrix(:,kk) = imf{kk};
end
emdSmoothedSpectra = zeros(bands,1); %The denoised spectra is the pdf
for kk = 2:beta
    emdSmoothedSpectra(:,1) = emdSmoothedSpectra+emdTestMatrix(:,kk); %Add
                          %the non-noise IMF to make the pdf (add all imf
                          %functions together , except the first imf function)
end
z = figure;
plot(emdSmoothedSpectra);
saveas(z,'testTubewormSpectra.fig')
close(z)

sampleCDF = cumsum(emdSmoothedSpectra); %Convert the above pdf to a cdf
sampleCDF = sampleCDF./max(sampleCDF);
z = figure;
plot(sampleCDF)
saveas(z,'testTubewormCDF.fig')
close(z)

outMatrix = zeros(nX,nY); %Compare the above CDF to the CDF for each pixel
for ii= 1:nX
    disp(ii);
    for jj = 1:nY
        vec = zeros(bands,1);
        for kk = 1:bands
            vec(kk) = normIm(ii+x1,jj+y1,kk);
        end
        testCDF = cumsum(vec);
        testCDF = testCDF./max(testCDF);
        [h,p] = kstest2(vec,emdSmoothedSpectra,.2); %KS Test at 95%
                                                    %confidence
        outMatrix1(ii,jj) = p;
        outMatrix2(ii,jj) = h;
        clear vec
    end
end
z = figure;
colormap gray
imagesc(outMatrix2);
saveas(z,'tubewormClassifier.fig');
close(z)

z = figure;
colormap gray
imagesc(1-outMatrix1);
saveas(z,'tubewormPValues.fig');
close(z)

save('isTubeworm.mat','outMatrix2');
```

```
testMatrix = outMatrix1;
for ii = aX:bX
    for jj = aY:bY
        testMatrix(jj,ii) = 1;
    end
end
z = figure;
colormap gray
imagesc(testMatrix);
%}

tubewormPixels = sum(sum((1-outMatrix2)));


/*************************************************************************/

% i) combinedClassifications

clear
clc

x = open('isTubeworm.mat');
tubeWorm = x.outMatrix2;

x = open('isEpiphyte.mat');
epiphyte = x.outMatrix2;

x = open('isSeaGrass.mat');
seaGrass = x.outMatrix2;


[a,b] = size(tubeWorm);
testMatrix = zeros(a,b);
for ii = 1:a
    for jj=1:b
        if tubeWorm(ii,jj) == 0 && seaGrass(ii,jj) == 0 && epiphyte(ii,jj) ==
0
            testMatrix(ii,jj) = 0;
        elseif tubeWorm(ii,jj) == 1 && seaGrass(ii,jj) == 0 &&
epiphyte(ii,jj) == 0
            testMatrix(ii,jj) = 1;
        elseif tubeWorm(ii,jj) == 0 && seaGrass(ii,jj) == 1 &&
epiphyte(ii,jj) == 0
            testMatrix(ii,jj) = 2;
        elseif tubeWorm(ii,jj) == 1 && seaGrass(ii,jj) == 1 &&
epiphyte(ii,jj) == 0
            testMatrix(ii,jj) = 3;
        elseif tubeWorm(ii,jj) == 0 && seaGrass(ii,jj) == 0 &&
epiphyte(ii,jj) == 1
            testMatrix(ii,jj) = 4;
        elseif tubeWorm(ii,jj) == 1 && seaGrass(ii,jj) == 0 &&
epiphyte(ii,jj) == 1
            testMatrix(ii,jj) = 5;
```

```
        elseif tubeWorm(ii,jj) == 0 && seaGrass(ii,jj) == 1 &&
epiphyte(ii,jj) == 1
            testMatrix(ii,jj) = 6;
        elseif tubeWorm(ii,jj) == 1 && seaGrass(ii,jj) == 1 &&
epiphyte(ii,jj) == 1
            testMatrix(ii,jj) = 7;
        end
    end
end

z = figure;
imagesc(testMatrix)
saveas(z,'combinedClassification.fig');


/*************************************************************************/
```

APPENDIX H

MATLAB routine to analyze fluorescence images (Red F and Green F), and compute percent coverage from spatial analysis

%%%%%%%%%%%%%%%%%%%%%

```
clear

imNameGreenF = '8-9-14FXG2Ag.tif'; % Green F fluorescence image name; user
entered
imNameRedF   = '8-9-14FXG2Ar.tif'; % Red F fluorescence image name; user
entered

imgfe = imread(imNameGreenF); % upload image of fluorescence image for
                              % epiphyte area (green F) into a matrix
imgfs = imread(imNameRedF); % upload image of fluorescent image for seagrass
                            %area (red F) into a matrix

figure(1)
imshow(imgfe);
axis equal

figure(2)
imshow(imgfs);
axis equal



% Use the area of seagrasses in imgfs to determine total area of seagrass
% leaf.
% Use the area of epiphytes to determine the total epiphytes (overlapping
% area)
% Use the ratio to compute percent epiphytes on the seagrasses.

weightfs = 0.95; % weighting factor;
                 % THIS IS IMAGE SPECIFIC AND REQUIRES USER INPUT

threshg = weightfs*max(max(imgfs)); % compute threshold value for the image
[rfs,cfs] = size(imgfs);        % find number of rows (rfs) and columns
                                %(cfs)in green F (seagrass indicator)
imgfs_bw = zeros(rfs,cfs);      % create a new binary matrix for thresholded
image

[rfsbw,cfsbw,val] = find(imgfs<threshg);  % find the location and values of
                                          % pixels below threshold

for i=1:length(cfsbw),
    imgfs_bw(rfsbw(i),cfsbw(i)) = 1;      % create binary image
end;
```

```
figure(3)
imagesc(imgfs_bw);
colormap gray
axis equal

%morphological image processing to remove noise
%structuring element

e = [0 1 0; 1 1 1; 0 1 0];

imc = imclose(imgfs_bw,e); % apply closing with the structuring element to
                           % remove noise
imc = imclose(imc,e);      % apply closing 2nd time with the structuring
                           % element to remove noise
imo = imopen(imc,e);       % apply closing 3rd time with the structuring
                           % element to remove noise
imo = imopen(imo,e);       % apply closing 4th time with the structuring
                           % element to remove noise



figure(4)
imagesc([imgfs_bw imc imo]); % plot the images side by side
colormap gray
axis equal
axis off

%%%%%%%%%%%%%%%%%%%%%%%%%%%%%%%%%%%%%%%%%%%%

save im8-9-14FXG2Agr  % save workspace; generic name

%%%%%%%%%%%%%%%%%%%

% Repeat thresholding for green F image for epiphytes.

weightfe = 0.95; % weighting factor; image dependent; REQUIRES USER INPUT

threshe = weightfe*max(max(imgfe));
[rfe,cfe] = size(imgfe);
imgfe_bw = zeros(rfe,cfe);
imgfe_bw2 = 256*ones(rfs,cfs);

[rfebw,cfebw,val] = find(imgfe<threshe);

for i=1:length(cfebw),
    imgfe_bw(rfebw(i),cfebw(i)) = 1; % binary image showing epiphytes
    imgfe_bw2(rfebw(i),cfebw(i)) = 0;% inverted binary images for the same
end;

figure(5)
imagesc(imgfe_bw);
colormap gray
axis equal
```

```
%%%%%%%%%%%%%%%%%%

% clean noise in the image (remove isolated pixels not part of the seagrass
% image as before)

%structuring element

e = [0 1 0; 1 1 1; 0 1 0]; % use the same structuring element for green F
                           % binary as red F binary image

figure(6)
imagesc([imgfe imgfe_bw*256 imgfe_bw2]); % plot 3 images together (original
              % green F, scaled binary green F, noise-removed binary green F)
colormap gray
axis equal
axis off

% User entered values specific to an image to to isolate seagrass leaves and
% their cut portions in a given shoot.
% THIS WILL BE DIFFERENT FOR IMAGE DEPENDING ON SEAGRASS ORIETNTATION IN
% THE IMAGE

x11 = 1;   x12 = 150;
x21 = 151; x22 = 290;
x31 = 291; x32 = 400;
x41 = 401; x42 = 550;


% Isolate the each seagrass leaf (s1, s2, s3, s4 in this case) from the
% image of the entire shoot with all leaves using the above boundaries

imgfe_bw_s1 = imgfe_bw(:,x11:x12);
imgfe_bw_s2 = imgfe_bw(:,x21:x22);
imgfe_bw_s3 = imgfe_bw(:,x31:x32);
imgfe_bw_s4 = imgfe_bw(:,x41:x42);

imgfe_s1 = imgfe(:,x11:x12);
imgfe_s2 = imgfe(:,x21:x22);
imgfe_s3 = imgfe(:,x31:x32);
imgfe_s4 = imgfe(:,x41:x42);

imgfs_bw_s1 = imgfs_bw(:,x11:x12);
imgfs_bw_s2 = imgfs_bw(:,x21:x22);
imgfs_bw_s3 = imgfs_bw(:,x31:x32);
imgfs_bw_s4 = imgfs_bw(:,x41:x42);

imgfs_s1 = imgfs(:,x11:x12);
imgfs_s2 = imgfs(:,x21:x22);
imgfs_s3 = imgfs(:,x31:x32);
imgfs_s4 = imgfs(:,x41:x42);


%Compute percent coverage of epiphytes on fluorescent images per segment,
```

```
%from left to right

perEpiCover_s1 = (sum(sum(imgfe_bw_s1)) / sum(sum(imgfs_bw_s1)))*100
perEpiCover_s2 = (sum(sum(imgfe_bw_s2)) / sum(sum(imgfs_bw_s2)))*100
perEpiCover_s3 = (sum(sum(imgfe_bw_s3)) / sum(sum(imgfs_bw_s3)))*100
perEpiCover_s4 = (sum(sum(imgfe_bw_s4)) / sum(sum(imgfs_bw_s4)))*100

% Alternatively, to get the same number

[s1e] = find(imgfe_bw_s1>0);
[s1s] = find(imgfs_bw_s1>0);
perEpiCover_s1 = size(s1e)/size(s1s)*100 % percent epiphyte coverage per leaf
                                         %or segment

[s2e] = find(imgfe_bw_s2>0);
[s2s] = find(imgfs_bw_s2>0);
perEpiCover_s2 = size(s2e)/size(s2s)*100 % percent epiphyte coverage per leaf
                                         %or segment

[s3e] = find(imgfe_bw_s3>0);
[s3s] = find(imgfs_bw_s3>0);
perEpiCover_s3 = size(s3e)/size(s3s)*100 % percent epiphyte coverage per leaf
                                         %or segment

[s4e] = find(imgfe_bw_s4>0);
[s4s] = find(imgfs_bw_s4>0);
perEpiCover_s4 = size(s4e)/size(s4s)*100 % percent epiphyte coverage per leaf
or segment


%%%%%%%%%%%%%%%%%%%%%%%%%%%%%
```

SOP

for

Seagrass and Epiphyte Hyperspectral Imaging for Efficient Integrated Measurement of Water Quality

GLO CMP Cycle 17 #13-040-000-6907

Introduction

The abundance of epiphytes is often considered to be an integrated measure of nutrient conditions in a seagrass bed, but is the result of complex interactions between a variety of factors (discussed in Borum 1985; Lin *et al.* 1986; Frankovich and Fourqurean 1997; Moore and Wetzel 2000; Hays 2005; Heck and Valentine 2007; Peterson *et al.* 2007; Burkholder *et al.* 2007). Eutrophication affects growth of epiphytes and seagrass leaves directly via nutrition and indirectly by stimulation of phytoplankton and changes in top-down control by grazers and predators.

Overview

The project will use monitoring of seagrass condition and water quality indicators, and various epiphyte analyses to compare epiphyte accumulation on seagrass from Redfish Bay. Site selection is based on the project goal of assessing epiphytes under differing water quality conditions (particularly nutrients).

Three complementary imaging technologies (visible scans, hyperspectral imaging and fluorescence imaging) will be compared. We will develop advanced image analysis routines, based on wavelength-, shape- and texture-based properties, to robustly extract the information encoded within the spatial distribution of different epiphytes, relative to the seagrass growth. Moreover, we will also obtain, compare and interpret hyperspectral imagery for complementary information. Imagery-based data will be compared to traditional epiphyte analyses obtained by traditional removal and biomass-based measures. Importantly, a more efficient epiphyte removal protocol (Zimba et al. 1999) will be used, in conjunction with HPLC pigment analysis, to characterize the epiphyte communities at the divisional level and thereby “groundtruth” the imagery-based determinations.

The project will use traditional measures of seagrass condition and water quality indicators, seagrass and seagrass epiphyte image analysis, biomass measures and HPLC pigment analyses to study epiphyte accumulation on *Thalassia testudinum* seagrass from three project sites. Dr. Mehrube Mehrubeoglu will be overall Project Director and will oversee hyperspectral imaging and image analysis efforts. The Project Director will assure that all project personnel are aware and committed to requirements and procedures specified in this SOP and any amendments or revisions of this plan. James Simons will manage field sampling and data management activities. Kirk Cammarata will manage laboratory imaging using visible and fluorescence scanners, as well as seagrass and epiphyte biomass measurements. Paul Zimba will oversee HPLC pigment analyses of algal epiphytes and associated biomass measurements. Graduate students Whitney Roberson and Elizabeth Shanks will assist Co-PIs with field work, imaging, image analysis, biomass measures and HPLC pigment analyses. All personnel will contribute to data compilation, data analysis and interpretation, report writing, and dissemination and outreach activities.

Amendments to the SOP

Revisions to the SOP may be necessary to reflect changes in project organization, tasks, schedules, objectives, and methods; to improve operational efficiency; and to accommodate unique or unanticipated circumstances. Amendments are effective immediately upon approval by the Project Director. They will be incorporated into the SOP by way of attachment and distributed to all personnel.

Site Selection

Primary consideration is given to accessibility and safety for all project sampling sites. Three sites will be chosen in coordination with agency staff and peer scientists based on previous sampling data and proximity to a TCEQ water quality monitoring site, as well as seagrass (*Thalassia testudinum*) condition and adjacent land use (wastewater discharge or reference condition), if applicable. Sediment characteristics may be used as an indicator of overall water quality.

Sampling Frequency

Sampling and all measurements will be obtained for at least three sampling events (Spring/Summer/Fall), scheduled to allow for seasonal variations to be observed. Additional sampling may take place on an as-needed basis to facilitate methods development.

Field Sampling Design

Seagrass condition indicators, water quality indicators, and seagrass samples will be taken at sites representative of differing water qualities, particularly with respect to nutrient levels, near established TCEQ quarterly monitoring stations at 7B (Station ID: 14817), 21B (Station ID: 17709) and Stedman Island (Station ID: 175694). Instantaneous physicochemical measurements, long-term physicochemical measurements, Secchi depth, and light measurements will be made. Seagrass cores, used to obtain seagrass condition measures, will be collected in an undisturbed area. Seagrass shoots, used for epiphyte measurements by both conventional (biomass) and imaging and HPLC techniques, will also be taken in an undisturbed area.

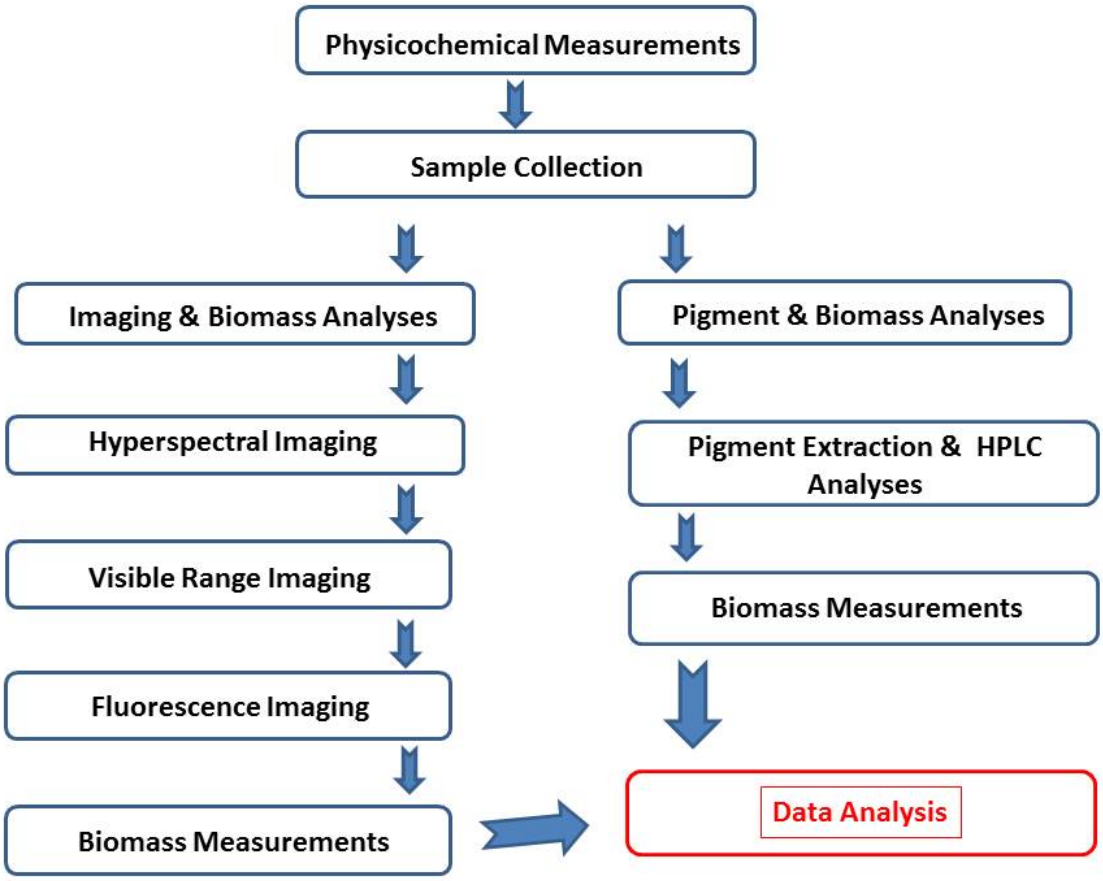

Sample Processing Workflow

Project staff will participate in field and laboratory work as described. Quarterly water quality monitoring data from TCEQ will be obtained for the nearest applicable monitoring station. Basic water quality analyses will also be conducted during sampling events using a Water Quality Sonde Model #: YSI 6920V2 (YSI Multiprobe). During sampling events, staff travel to each site and deploy the YSI Multiprobe for basic water quality data and then record site-specific characteristics including time, weather conditions, depth, Secchi depth, dissolved oxygen and temperature. Typically, measurements will be made first for water chemistry, instantaneous physicochemical measurements, light measurements and Secchi depth, as these can be made from a boat before any other field work. Next, seagrass cores and shoots will be collected. This collection will be done on the "up-current" side of the boat and any other activities to prevent sample contamination.

Seagrass cores (15 cm diameter) will be collected, field processed and stored in 1 gallon plastic bags in the dark and on ice for subsequent processing to assess the seagrass condition indicators shoot density, above-ground biomass and below-ground biomass. Processing of seagrass cores is

described later. Then 6 replicate samples, each comprising 5 whole *Thalassia* shoots, will be collected so as to minimally disturb the epiphytes and leaf morphology. Three replicate samples will be or placed in 1 L plastic bottles filled with ambient water and stored dark and on ice. These samples will be used for the pigment analyses by HPLC (described below).

The remaining 3 replicate shoot samples (for visible and fluorescence imaging) will be collected into 1 L plastic bottles (without filling with water) and stored dark and cool in a cooler, but without coming directly into contact with ice (because subzero temperatures induce leaf damage). Samples are returned to the laboratory as soon as possible and stored under dark and cool conditions (4 °C) until further processing. Storage time will be minimized and laboratory-based imaging will commence as soon as practicable after delivery to the laboratory. All imaging work (described below) will be complete within 48 hours of sample collection.

Leaf disks were sampled using blades collected at sites. Leaf disks will be collected using cork borers (size depedant on blade size). Leaf disks are immediately placed on ice, frozen at -80C, until processed using HPLC techniques (Zimba et al. 1999).

Epiphyte Pigment Analyses

Epiphytes will be removed from blades using a MES buffer approach and this method will be compared to the more commonly used scraping method. The scraping method involves rubbing the seagrass blade with a glass slide edge to scrape epiphytes. The MES buffer (0.1 M, pH 6.1) solution is often used in physiological studies of photosynthesis (Spencer et al. 1996). Leaves were placed in MES buffered seawater and shaken at 1 RPM for 30 seconds, leaves were then removed and epiphytes quantified using HPLC methods (Zimba et al. 1999). Authentic standards (VKI, Denmark) were used to develop standard curves for all chlorophyll, xanthophyll, and carotenoid standards.

Hyperspectral Imaging in the Field

The remaining 3 replicate shoot samples will be imaged in the field using the portable hyperspectral camera (SOC 710, Surface Optics Corp., San Diego, CA), following standardized procedures described below. For each shoot, individual leaves will be distinguished by their leaf length measurement, taken at the time of imaging. Ideally both sides of each leaf will be imaged. The shoots must be separated to keep track of leaf information from each shoot (number, length, etc.). Each leaf will be placed on an opaque non-reflective black material for hyperspectral imaging. The leaves will be held down flat using small weights. A reference panel image will

also be imaged to later normalize hyperspectral data. Camera parameters (integration/acquisition time) will be adjusted for optimal quality hyperspectral images to accommodate for changes in lighting conditions. Dark current images will also be acquired for normalizing the hyperspectral data during data processing. The blades will be imaged at a standard distance with the camera lens vertically above the imaged samples on the horizontal surface. To stabilize the camera with respect to the motion of the boat, the camera will be held stationary by placing it on a tripod. Proper care will be taken to cause minimal disturbance and drying of the epiphytes on the blades. After field-imaging, the leaves of the 3 shoot samples will undergo other imaging processes (visible scans and fluorescence scans) followed by biomass lab analysis.

Hyperspectral Imaging in the Laboratory

Parallel samples designated for **laboratory-based image analysis** will be processed as follows: Whole shoots are gently rinsed in 500 mL of artificial sea water (ASW) to remove loose mud and debris. All handling is performed so as to minimize disturbance of accumulated epiphytes. Individual leaves of each whole shoot are distinguished by leaf length. Leaves of one (each) shoot are imaged together, first one side (A), then the other (B). Sample and filename nomenclature will be established to identify sample information, and all samples and scans will be recorded in sample and scanning logs, respectively. Lab-based hyperspectral imaging will be performed with a benchtop hyperspectral imaging system (Headwall Photonics).

The individual blades are placed in a black non-reflective plastic tray and submerged in approximately 2 cm of ASW. Blades too long for the scanning range of the hyperspectral camera (>12.5 cm) are cut diagonally, kept side-by-side and arranged in a standard pattern that distinguishes the pieces of each blade. In many cases, natural twisting of the leaves necessitates the application of weight from about 1” x 1” x 1.5” piece of lead to keep the blade flat.

When imaging is complete, each blade is carefully placed into a non-reflective transfer tray. This tray contains a paper towel, and enough artificial saltwater to cover the towel. This set up holds the blades in place without allowing them to dry out during transfer to the next imaging station or other processing.

Sample and filename nomenclature will be established to identify sample information, including date of scanning, and all samples and scans will be recorded in sample and scanning logs, respectively.

Note: For hyperspectral imaging of seagrass leaves that will not be followed by other processing, the leaves are simply laid flat and held down by weights on a non-reflective black tray, and imaged using the Headwall Photonics hyperspectral imaging system.

Visible Wavelength Range and Fluorescence Scans (Laboratory)

Visible wavelength range (V) images are first obtained for both sides of the seagrass leaves with the Epson Perfection V750 Pro flatbed scanner (or equivalent), followed by fluorescence-based (F) imaging of both sides with the Typhoon 9410.

The individual blades are laid flat on the scanning platen, which is then flooded with ASW. In many cases, natural twisting of the leaves necessitates the application of weight (clear glass microscope slides) to keep the blade flat. Submersion is important as it minimizes the air bubbles trapped underneath the blade. Any air bubbles are removed by lightly tapping the leaf.

Visible wavelength range scans are obtained using 24-bit color scanning at 1200 dpi and saved as .tiff files. Standard file-naming conventions have been established (see below) to designate date, site, shoot, leaf, imaging technology, and leaf side.

Immediately following visible scanning, leaves are soaked for 3-5 min in 250 mL of DI water to remove salts that cause imaging artifacts upon drying.

DI water-soaked leaves are transferred to the fluorescence scanner platen maintaining the established leaf orientation, weighted with glass microscope slides if necessary, and imaged as described previously (Radloff *et al.*, 2010; Radloff *et al.*, 2011; Sweatman and Cammarata, in preparation) and below except that both sides of all leaves are imaged, first one side (A), then the other (B).

See below for details of the fluorescence scanning procedure.

Seagrass Biomass Measurements of Scanned Leaves and Fluorescence Plate Assays of Removed Epiphytes

For comparative purposes, the same leaves scanned for image analysis were also used for biomass analysis of both removed epiphytes and the underlying epiphyte-free seagrass leaf. Determinations of epiphyte and seagrass dry weights, as well as fluorescence plate assays are described below (Radloff *et al.*, 2011; Cammarata and Sweatman, in preparation). Following the sequential image analysis described above, leaves of each shoot will be transferred to a flat-bottomed plastic tray with a small volume (approximately 10 mL) of distilled water and scraped with glass microscope slides to remove epiphytes as completely as possible without excessive removal of the seagrass leaf cells. Removed epiphytes will be quantitatively transferred with DI water rinses into 50 mL graduated centrifuge tubes. Volume will be adjusted to a standard amount (approximately 25 mL) and recorded. Representative aliquots (0.5 mL) of the removed epiphytes will be transferred to 1.7 mL microcentrifuge tubes and stored dark at 4° C for subsequent fluorescence plate assay measurements. The remainder of the removed epiphytes

will be quantitatively transferred into pre-labeled, pre-weighed 7 cm diameter aluminum dishes and dried to constant weight at 60°C for determinations of epiphyte dry weight. Dry weights must be corrected for the removed aliquots. Seagrass leaves from which epiphytes were removed will be transferred into pre-labeled, pre-weighed paper bags or beakers and dried to constant weight at 60° C for determinations of seagrass leaf dry weight.

Plate Fluorescence Assay and Quantification

For measurements capturing the green algal seagrass epiphyte components, and to detect potential shifts in algal family composition, seagrass epiphyte samples removed from the seagrass blades will be transferred into optical 96-well microplates and measured for epiphyte fluorescence. Representative aliquots (0.5 mL) of the removed epiphytes will be transferred to 1.7 mL microcentrifuge tubes and stored dark at 4° C for subsequent fluorescence plate assay measurements. Fluorescence assays will be made after vigorously vortexing the samples and transferring 50 µL aliquots (using cut-off micropipettor tips with enlarged openings to facilitate transfer of particulate matter) into the wells of 96-well optical microplates. Fluorescence imaging for the Plate Assay will be performed with both green- and red-excited fluorescence imaging as described above, except that: 1) scanning will take place in the "+3 mm" focal plane instead of focusing at the platen-level; 2) PMT voltage will be set to 500 V; and 3) the pixel resolution will be set at 50 µm.

Documentation of Field Sampling Activities

Field sampling activities are documented in field notebooks. The following will be recorded:

1. Station ID or latitude and longitude information
2. Location
3. Sampling time
4. Sampling date
5. Sampling depth
6. Sample collector's name/signature
7. Values for measured field parameters
8. Detailed observational data, including:
   a) water appearance
   b) weather (Sunny/partly/cloudy; Estimate of wind speed & direction)
   c) water current flow severity
9. Other observational data (*as applicable*), including:
   a) biological activity
   b) pertinent observations related to water quality (*e.g.*, exceptionally poor water quality conditions or disturbances, etc.)
   c) unusual odors
   d) specific sample information
   e) missing parameters (*i.e.*, when a scheduled parameter or group of parameters is not collected)

f) algal blooms, fish kills, or pollution complaints

Seagrass Condition Indicators

Seagrass core samples (n = 3) will be collected at 3 sampling sites as described later. Samples will be analyzed for the following parameters using standard protocols (e.g., Radloff *et al.* 2010):

Biomass (above- and below-ground)

Root-to-shoot biomass ratio

Shoot density

Laboratory Data Reports

Data reports from laboratories will report the test results clearly and accurately. The test report will include the information necessary for the interpretation and validation of data and will include the following:

- a clear identification of the sample(s) analyzed
- identification of samples that did not meet any SOP requirements and why (*e.g.*, holding times exceeded)
- date of sample analysis
- sample results

Recording Data

For the purposes of this section and subsequent sections, all field and laboratory personnel follow the basic rules for recording information as documented below:

1. Legible writing;
2. Correction of errors with a single line followed by an initial and date;

Electronic Data

Numerical data will be submitted electronically to Project Manager as Microsoft Excel files. Imagery will be archived in the format(s) required for subsequent analyses.

Deviations from Sampling Method Requirements or Sample Design, and Corrective Action

Examples of deviations from sampling method requirements or sample design include but are not limited to such things as inadequate sample volume due to spillage or container leaks, failure to preserve samples appropriately, contamination of a sample bottle during collection, storage temperature and holding time exceedance, sampling at the wrong site, samples drying out before completing imaging, etc. Any deviations will invalidate resulting data. Corrective action may include samples being discarded and if possible, re-collected. Imaging may also need to be conducted on parallel samples instead of the same samples if the leaves change their physical properties in between scans.

Detailed Protocols

Sampling Sites

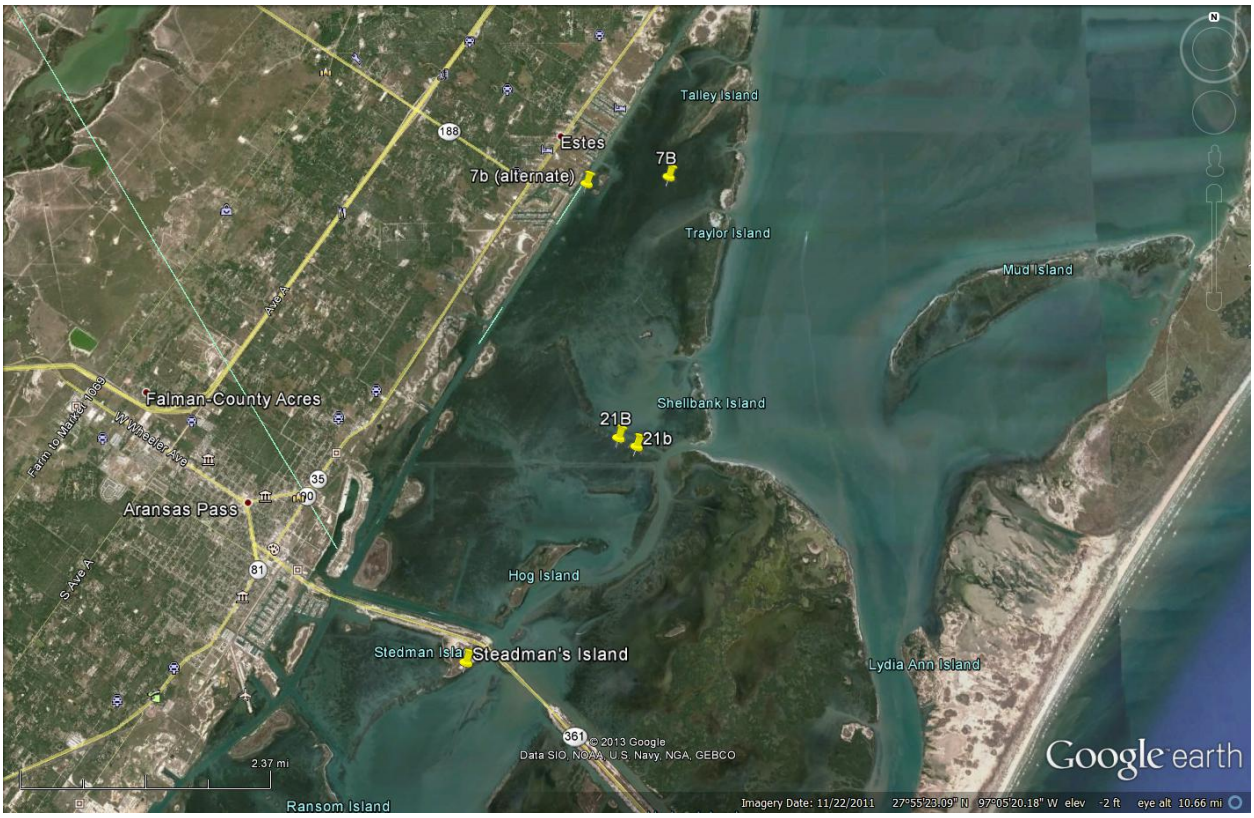

Sampling trips include visiting three sites labeled as Steadman's Island, 7Balt, and 21B also denoted as X, Y, and Z, respectively.

Physicochemical Parameters

Dissolved oxygen, conductivity, salinity, pH and temperature will be measured in the field using pre- and post-calibrated datasondes. Secchi depth and water depth will be measured at each sampling.

Measurements of percent surface irradiance (% SI) and the diffuse light attenuation coefficient (*k*) will be made from measurements of surface and underwater irradiance.

Percent Surface Irradiance and Light Attenuation

(Adapted from Ken Dunton and Kim Jackson (Radloff *et.al.* 2010))

Field Measurements

Measurements of percent surface irradiance (% SI) and the diffuse light attenuation coefficient (*k*) are made from simultaneous measurements of surface (ambient) and underwater irradiance. Measurements of photosynthetically active radiation (PAR = ca. 400 to 700 nm wavelength) are collected on the surface using an LI-190SA quantum-sensor that provides input to a Licor datalogger (LI-COR Inc., Lincoln, Nebraska, USA). Underwater measurements are made using a LI-193SA sensor. Care is taken to reduce extraneous sources of reflected light (from boats or clothing).

Light attenuation will be calculated using the transformed Beer Lambert equation:

$$K_d = -[\ln(I_z/I_0)]/z$$

where *k* is the attenuation coefficient (m^{-1}) and I_z and I_0 are irradiance (µmol photons m^{-2} sec^{-1}) at depth z (m) and at the surface, respectively. Percent surface irradiance available at the seagrass canopy will be calculated as follows:

$$\% \text{ SI} = (I_z/I0) \text{ x } 100,$$

where I_z and I_0 are irradiance (µmol photons m^{-2} sec^{-1}) at depth z (m) and at the surface, respectively.

For each type of measurement, field staff will ensure that the site is not disturbed prior to sample collection. Typically, measurements will be made first for water chemistry samples, instantaneous physicochemical measurements, light measurements and Secchi depth, as these can be made from a boat before any other field work.

Seagrass Condition Indicators

Sampling will take place in monotypic or nearly-monotypic stands of *Thalassia testudinum.*
Three replicate cores will be used for estimates of seagrass condition indicators (above- and below-ground biomass, root-to-shoot ratio, and shoot density) as described in Detailed Procedures below.

Seagrass Biomass

Three replicate cores are used for estimates of above- and below-ground biomass. A 15 cm (ID) diameter corer is used to sample *Thalassia* from monotypic stands. Species present (i.e. seagrass species composition) will be determined by visual in situ analysis of plants observed within a 25 m radius of each site. Samples are placed in pre-labeled Ziploc bags and immediately placed on ice. Following placement of the large 15-cm core on the seabed and before pressing the corer into the sediment, the diver runs their fingers carefully around the bottom of the core. If grass has been pulled under the core, it is removed. The diver then presses and twists the core down

into the sediment 10-15 cm. The core is rocked back and forth with the suction hole covered by thumb or rubber stopper. The diver then works their hand under the core and removes it from the grass bed, making sure to keep their hand under the bottom of the core (to prevent loss of sample). After emptying the core into a 1 mm mesh bag or sieve, broken shoots are removed since these are likely exterior shoots that were cut by the core tube. The sample is washed free of sediment by agitation in the water. Remaining seagrass samples are placed in pre-labeled Ziploc bags and immediately placed on ice.

In the laboratory, collected samples are further washed free of sediment and debris. The number of short vertical shoots is counted, and shoots are separated from the root + rhizome fraction. Biomass is determined for each fraction as described above.

Hyperspectral (HS) Imaging

HS Imaging In the Field

The following procedure will be followed when collecting images in the field, or outdoors after returning from field trips using the portable Hyperspectral Imaging System, SOC710, Surface Optics Corp.:

Powering up and Getting Started

1. Connect camera to laptop and power
2. Open acquisition software.

Acquisition Software

1. Make sure scanner settings match factory settings in file ”SOC710_scanner_settings”
2. Use- com4
3. Note the following:
   Scan start position= scanner_home_position
   On-center position=scanner_center_position
   Focus position=focus_home_position
   Step-size=scanner_step_size

Focusing the Camera

1. Click purple ‘play’ button for gray-scale real-time viewing of the scene. Use real-time viewing for coarse focusing of seagrass samples.
2. Rotate the lens until the image in focus. Once focused, click the purple button again to close the real-time viewing window, and switch to hyperspectral imaging mode. (Note: The focusing visible camera is not perfectly aligned with the hyperspectral camera. What is focused in the visible camera may not be focused in the hyperspectral camera. The real-time

gray-scale image must actually remain slightly off focus to ensure hyperspectral camera is in focus).

Acquiring Hyperspectral Images

1. Press the green 'play' button to start hyperspectral image acquisition

(Recommended pixel range values are 500-3000. Values over 4096 are saturated, since this is a 12-bit camera)

Calibration frames:

Typical normalization of a hyperspectral image involves the following formula:

$$I_N(i) = (I(i) - D_k(i)) / (C_L(i) - D_k(i)),$$

Where $I_N(i)$ is the i^{th} normalized image pixel in the I_N normalized image, $I(i)$ is the i^{th} acquired image pixel in the I hyperspectral image, $D_k(i)$ is the i^{th} dark frame pixel in the D_k dark image, and $C_L(i)$ is the i^{th} calibration pixel in the C_L calibration image. Normalization is applied to all pixels in the hyperspectral image.

If the noise levels are low, normalization can be simplified as $I_N = (I / C_L)$ applied to all pixels in the image.

D_k records dark frame. This corresponds to dark noise image, and captures camera noise when there is no light entering the viewing lens. To acquire a dark frame, leave the cap of the lens on so no light enters through the lens. Capture the image, and save with an extension .drk. Alternatively, save it with any other extension or name that clearly identifies the dark image. C_L records calibration frame. Use a grey reference panel (sheet) for this purpose. Save image as .cal. Alternatively, C_L can also be saved under a different extension that clearly identifies the calibration image.

Calibration can be accomplished by inserting the gray reference panel in the field of view within the scanned seagrass images as well. This is preferred, since it reduces the acquisition time (less number of hyperspectral images must be collected), and allows better synchronization of lighting conditions between the seagrass samples and calibration panel, as the gray panel appears in the same image as the seagrasses. Note: Care must be taken to keep the gray calibration panel dry (which can be a challenge in the field on a boat), as the gray panel loses its integrity when wet. Similarly, care must be taken to ensure it does not fly off in the wind. The gray panel is held down with the same weights used to hold down the seagrass leaves flat.

Saving Hyperspectral Image Cubes

Once the image is acquired, it must be saved as a BIL file. Save image using "SOC710 standard (with BIL header)" option.

Note: Image does not save automatically. If the green button is pressed again for a new hyperspectral scan without saving the previous image, the previous image is overwritten and lost.

Camera Settings

If the weather is cloudy, or otherwise ambient light levels are low, increase camera integration time to compensate for low light. Increasing integration time allows longer exposure to light. This must be done relatively frequently if there is cloud cover, moving clouds, or as the day progresses and the position of the sun changes.

Alternatively, to increase the amount of light entering the camera, the camera's gain can also be increased, but this will increase noise since the gain is amplified together with the useful signals. The result will be reduced signal-to-noise ratio (SNR).

Conversely, if the day gets brighter during acquisition time, integration times must be reduced to prevent saturation of the camera. Decrease integration time in bright light. Smaller integration times will also reduce time needed to acquire a hyperspectral cube. If possible, sunny and bright days are prepared for sample imaging.

Keep the camera lens 21.75" in from object is based on the lens of the camera system, and may be different for different lenses used). This will allow minimal fine adjustments for focusing. (This is specific to our system, and will vary depending on the lens used. However such distances can be determined off-line before field trips for each system to conserve time during image acquisition during sampling events.)

Lab Hyperspectral (HS) Imaging

Hyperspectral data cubes will be acquired with a benchtop Hyperspectral Imaging System (Headwall Photonics Hyperspec™ VNIR P-Series, S/N 64-195). This is a push-broom system that uses a line scan camera to build a 3D image one line at a time. The lines are merged together through the motion of a horizontal stage. The horizontal stage control setting will be adjusted to the starting position of 100 units with a scan length of 17 mm, scanning increments of 100 μm, camera integration time of 500 ms. These optimum values have been identified experimentally. The images will be brought to focus through a semi-automated focus-control capability developed in house through a vertical stage and controlled by LabVIEW software. A broadband light and power source will be used as the illuminator in reflection mode, illuminating the sample from the top, or same side as the imaging system's light collecting lens. A separate ring light of LEDs will also be tested for reflection mode measurements. The sample holders have been painted with matt black paint used for the weights that held down seagrasses flat during imaging to minimize unwanted reflection from the surroundings. At the beginning of the measurements, a gray reference panel with 18% reflectance will be used within the same image as the grass blade as a calibration panel. The gray panel will be needed during post processing of images for calibration and normalization purposes of the seagrass hyperspectral data. Hyperspectral images from seagrasses produce both spatial and spectral data. Seagrass blades will be cut at lengths to fit within the view of the camera, and imaged in multiple independent scans resulting in more images than one for most seagrass leaves. For long leaves, multiple scans of leaf portions will be necessary to limit the size of the image and allow more manageable data processing afterwards.

For example, for a 1.7 cm scan length, hyperspectral data cubes occupy computer memory space of 866 MB each, with the above image acquisition parameters resulting in hyperspectral images

with dimensions of 1600x170x811 (in pixels) or 220,592,000 (over two hundred and twenty million) data points per image. After the acquisition of hyperspectral scans, the data will be processed through the software tools ENVI 4.8 and MATLAB.

Visible Range Imaging (V):

Visible wavelength range (V) images will be obtained for both sides of the same seagrass leaves that were imaged with the HS platform, using the Epson Perfection V750 Pro flatbed scanner (or equivalent). Blades will be carefully removed from the transfer tray and arranged side-by-side on the scanner platen, maintaining a standard pattern that distinguishes the pieces of each blade.

Care is taken to make sure segmented leaf pieces and sides are aligned parallel to one another and the image frame, and amenable to subsequent image analysis. In many cases, natural twisting of the leaves necessitates the application of weight (clear glass microscope slides) to keep the blade flat. The individual blades are laid flat on the scanning platen, which is then flooded with ASW. Submersion is important as it minimizes the air bubbles trapped underneath the blade. Any air bubbles are removed by lightly tapping the leaf. Visible wavelength range scans are obtained using 24-bit color scanning at 1200 dpi and saved as .tiff files. Standard file-naming conventions have been established (see below) to designate date, site, shoot, leaf, imaging technology, and leaf side. Standard sample and filename nomenclature are followed to readily identify sample information, and all samples and scans will be recorded in sample and scanning logs, respectively.

Immediately following visible scanning, leaves are soaked for 3-5 min in 250 mL of DI water in preparation for fluorescence imaging. This step is to remove salts that cause fluorescence imaging artifacts upon drying.

Seagrass Epiphyte and Leaf Fluorescence Imaging Measurements (F)

A novel fluorescence technique will be used to measure the abundance and accumulation profiles of epiphytes on seagrasses. The abundance of epiphytes is believed to be an integrated measure of nutrient conditions in a seagrass bed. This method measures fluorescence of specific photosynthetic accessory pigments as a proxy for epiphyte abundance. The scanning method achieves significantly greater spatiotemporal resolution compared to traditional measures of epiphyte biomass. It enables plotting of incremental epiphyte abundance along the age gradient of the seagrass leaf, providing a record of epiphyte recruitment and growth *relative to* the growth of the seagrass leaf. The cross-sectional leaf area for a seagrass sample can also be estimated.

This method digitally images epiphytes which absorb light in the green range of the visible spectrum (532 nm) and emit fluorescence at wavelengths between 550 nm and 610 nm. These organisms comprise primarily red algae, but other classes of algae also exhibit some (albeit much less) absorption of green light (some cyanobacteria, diatoms, cryptomonads, brown algae and dinoflagellates) (Raven *et al.* 2005; Frouin 2006; Robertson 2009). The pigment primarily responsible for this absorption is phycoerythrin, but the carotenoids fucoxanthin and peridinin can also contribute (French and Young 1952; Dawson *et al.* 1986). The method is based on the preferential excitation and fluorescence emission signatures of the accessory pigments in epiphytes relative to those of the underlying seagrass leaf which contains only chlorophylls and lutein-based carotenoids. The latter pigments absorb green wavelengths of light only very weakly, so their contribution to fluorescence is minimal in relative terms.

Scanning seagrass leaves by this method does not quantify green algal components of seagrass epiphytes, because the red light needed to excite the chlorophylls of the green algae also excites the seagrass leaf pigments. If epiphytes are removed from the seagrass blade by scraping, then

removed epiphytes can be fluoresced and quantified using *both* red and green excitation wavelengths. This provides a measure that includes all of the different types of epiphytic algae, including green. Changes in the relative contributions of green and red algae to total epiphyte abundance can be captured by comparing the ratio of red-excited fluorescence to green-excited fluorescence. Previous work has documented changes in primary producer composition by nutrient addition (see for example Armitage *et al.* 2005), so it will be useful to monitor for such changes.

Within the laboratory, all properly stored samples will be carefully tracked by standardized sample nomenclature using sample and scanning logs. . Samples designated for laboratory-based image analysis will be sequentially processed as follows: 1) Lab-based hyperspectral imaging (HS); 2) Visible range imaging (V); 3) Fluorescence imaging (F); and 4) Traditional epiphyte and seagrass leaf dry weight biomass measurements. All efforts will be made to perform laboratory-based imaging work immediately upon receipt of samples and within 48 h of collection. DI water-soaked leaves are transferred to the fluorescence scanner platen maintaining the established leaf orientation, weighted with glass microscope slides if necessary, and imaged as described previously (Radloff *et al.,* 2010; Radloff *et al.,* 2011; Sweatman and Cammarata, in preparation) and below except that both sides of all leaves are imaged, first one side (A), then the other (B).

Fluorescence Scanning and Quantification

Fluorescence imaging of seagrasses and algal epiphytes is performed with a 2-D scanning imager (Typhoon 9410 Multi-Mode Imager; GE Healthcare; Piscataway, NJ) using green (532 nm) or red (633 nm) laser excitation (EX) and filter-selected fluorescence emission (EM) detection. Resolution to 10 µm pixels can be obtained and the imaging mechanism can be focused either at the platen surface, or 3 mm above the surface for samples in 96-well optical plates. The platen surface measures 35 cm x 43 cm and can accommodate leaves of 5 or more whole shoots of *T. testudinum*.

Seagrass leaves transferred from visible wavelength range imaging, (or removed directly from storage bottles), will be gently handled and carefully transferred into a shallow tray of distilled water to briefly (3 - 5 minutes) and gently wash off salt, sediments or other unattached debris. Seagrass leaves are to be handled gently and at the base only, to avoid disturbing attached epiphytes. Individual blades will be severed from the shoot at the ligule and transferred to the platen of the scanning fluorescence imager. The blades of each *Thalassia* shoot will be imaged, first one side, then the other. Only living (green) blades will be imaged. Blades will be positioned lying flat, vertically-aligned and in a parallel, non-overlapping orientation. Sample washing, transfer to the scanning platen and initiation of scanning will occur within ten minutes to prevent excessive drying. Any blades exhibiting curling will be re-wetted with a few drops of distilled water (but care will be taken to avoid pools of water on the platen). The scanning compartment lid will be closed immediately upon loading. After the initial green- and red-

fluorescence scans, the scanned seagrass blades will be flipped to facilitate scanning the other side. Fluorescence scanning parameters are described below.

Instrument Settings and Adjustments

For each sample, two types of scans will be obtained. "Green Scans" will utilize green 532 nm laser excitation to excite fluorescence from accessory photosynthetic pigments (primarily phycoerythrin) and "Red Scans" will utilize green 633 nm laser excitation to excite fluorescence from chlorophyll photosynthetic pigments. Standard default instrument settings will be as follows, with any deviation so noted in the laboratory log.

Green Scans

The X:Y coordinates of the platen area to be scanned will be selected.
Acquisition Mode: Fluorescence
Setup Parameters:
- Laser: 532 nm (green) excitation
- Emission Filter: 580 bp 30 nm emission filter
- PMT: 360 V (500 V for samples in 96-well plates)
- Sensitivity: Normal

Orientation: "R"
Pixel Size: 200 µm for typical quantification/10 µm for high resolution archival images
Press: Yes
Focal Plane: Platen (use +3 mm for samples in 96-well plates)

Red Scans

The X:Y coordinates of the platen area to be scanned will be selected.
Acquisition Mode: Fluorescence
Setup Parameters:
- Laser: 633 nm (red) excitation
- Emission Filter: 670 bp 30 nm emission filter
- PMT: 360 V (500 V for samples in 96-well plates)
- Sensitivity: Normal

Orientation: "R"
Pixel Size: 200 µm for typical quantification/10 µm for high resolution archival images
Press: Yes
Focal Plane: Platen (use +3 mm for samples in 96-well plates)

Upon sample scan completion, the platen will be rigorously cleaned as follows: All samples are removed and debris is gently blotted away with lint-free laboratory wipers. The platen is washed and wiped clean using, in all cases, non-scratching optical wipers with a defined sequence of solutions: distilled water, 70% ethanol, 10% H_2O_2 and distilled water. (Appropriate safety equipment for use of 10% H_2O_2 includes gloves, eye protection and lab coat).

Plate Fluorescence Assay and Quantification

For measurements capturing the green algal seagrass epiphyte components, and to detect potential shifts in algal family composition, seagrass epiphyte samples removed from the seagrass blades will be transferred into optical 96-well microplates and measured for epiphyte fluorescence. Representative aliquots (0.5 mL) of the removed epiphytes will be transferred to 1.7 mL microcentrifuge tubes and stored dark at 4° C for subsequent fluorescence plate assay measurements. Fluorescence assays will be made after vigorously vortexing the samples and transferring 50 µL aliquots (using cut-off micropipettor tips with enlarged openings to facilitate transfer of particulate matter) into the wells of 96-well optical microplates. Fluorescence imaging for the Plate Assay will be performed with both green- and red-excited fluorescence imaging as described above, except that: 1) scanning will take place in the "+3 mm" focal plane instead of focusing at the platen-level; 2) PMT voltage will be set to 500 V; and 3) the pixel resolution will be set at 50 µm. Both red- and green-excited fluorescence intensity values for samples are corrected by subtracting control fluorescence values (water). These results are used to calculate R/G Ratios (red-escited fluorescence intensity divided by the green-excited fluorescence intensity) are an indicator of the algal community composition.

File Naming, Data Storage and Data Backup

Epiphyte image data obtained at 200 µm resolution will be labeled by the unique sample identification number with "r" or "g" ("red" or "green") appended as a suffix. Raw image data is obtained in a ".gel" file format. Scan data will be saved in this format, and additionally in ".tif" file format. All scan data will be backed up onto a portable hard drive device following scanning of all samples for an individual sampling trip. Sample data will additionally be backed up onto DVD media as well.

Data Processing

Epiphyte image data obtained at 200 µm resolution will initially be quantified from a ".gel" file format using "ImageQuant" software. The image area(s) to be analyzed is (are) delineated with an object box. Then, for each object on a scan, the following parameters will be determined:

- Total signal above background from green-excited fluorescence (epiphyte fluorescence intensity)
- Total signal above background from red-excited fluorescence (leaf + epiphyte fluorescence intensity)
- Total number of pixels above background from green-excited fluorescence (area with epiphytes)
- Total number of pixels above background from red-excited fluorescence (area with leaf or epiphytes)

Numerical values will be recorded into a spreadsheet for calculations and analysis. Subsequent analyses for quantification will be performed on both individual blades and on all of the blades collectively for each whole shoot.

Data Analysis

Data for the following parameters will be compiled into a spreadsheet which will serve as the data quantification log and compared for each site, sampling event, and seagrass shoot.

- Total number pixels red-excited fluorescence above background (an estimate of scanned leaf area for normalizing epiphyte signal measurements; also a proxy for leaf biomass)
- Total green-excited fluorescence signal above background (a measure of total epiphyte load in leaf samples)
- Total green-excited fluorescence signal above background divided by total number pixels red-excited fluorescence above background (a *normalized* measure of epiphyte accumulation based on scanned leaf area)

Processed data will be transmitted to the Project Manager in electronic format for collective analysis of total project data as described elsewhere. All processed data will additionally be compiled in the Final Report.

Epiphyte Biomass Measurements for Imaged Samples

Epiphyte biomass measurements will follow the procedure described in the section titled "**Seagrass Biomass Measurements and Fluorescence Plate Assays"**

Sample Preparation for HPLC Analysis

Samples will be maintained in the dark until lab processing. Seagrass shoots will be placed on a flat surface and 2 ml of filtered seawater added. Shoots will be scraped on both sides using a glass slide, and algal biomass collected. Subsamples of this material will be dried (60C), and analyzed using HPLC pigment methods (Zimba et al. 1999).

HPLC and Associated Seagrass and Epiphyte Biomass Measurements

HPLC pigment analyses have been used to separate algal divisions for many years-a specific method for this has been used by the co-PI since 1996 (Zimba et al. 1999). Epiphyte removal methods developed by Zimba (Zimba and Hopson 1997) include mechanical agitation methods- these have been modified by the acidition of MES buffer (pH 6.5).

Dr. Paul Zimba of Texas A&M University – Corpus Christi has developed a novel technique to quantify epiphyte load on seagrass blades using a combined chemical mechanical separation technique. Seagrass blades from collected shoots will be separated from rhizomes and scraped using the traditional removal method, then shaken for 60 seconds in MES buffer. Epiphyte biomass will be quantified using dry weight and HPLC pigment analyses for the scraped portion, and using light microscopy for the MES removed portion.

HPLC Pigment Analyses

HPLC analytical methods include use of a reference standards library, and repeated injections of every one sample per analysis run-10% difference in standard deviation will require second sample analysis.

Epiphyte Chlorophyll *a* Extraction

Updated November 2009 , Ken Dunton/Kim Jackson

(Adapted from: ESS Method 150.1: Chlorophyll – Spectrophotometric, Environmental Sciences Section, Inorganic Chemistry Unit, Wisconsin State Lab of Hygiene, 465 Henry Mall, Madison, WI 53706. Equation for pigments from SCOR 1999.)

1.0 Introduction

Chlorophyll *a*, a characteristic algal pigment, constitutes approximately 1% to 2% (dry weight) of algal biomass; carotenoids can account for nearly the same percentage. Specific carotenoids are found in different algal species, genera, and algal divisions making these useful biomarkers.

2.0 Summary of Method

Algal cells are concentrated by filtering a known volume of water containing epiphytes removed from seagrass through a GFF filter (25 mm, 0.7 µm pore size glass fiber filter). The pigments are extracted from the concentrated algal sample in 100% acetone. The pigment concentration is determined by measuring the absorbance or optical density (OD) of the extract at various wavelengths after passage through HPLC columns. The resulting absorbance measurements are then applied to a standard equation.

3.0 Sample Preservation and Preparation

1) Pigment samples are placed in a dark cooler and packed on ice at the time of collection.
2) All chlorophyll work is carried out in low light conditions (all overhead lights must be off) since light degrades chlorophyll pigments. Arrange the filtering manifold, seawater trap, and vacuum pump (or aspirator) on the lab bench.
3) Using forceps, place a 075 µm pore size glass fiber filter on each filtering funnel, and filter a known volume (measure with a graduated cylinder) of sample (in the dark), applying vacuum until the sample is dry. The amount of sample required depends on the epiphyte density in the water sample. Record the volume filtered for each sample.
4) Fold the filter in half and wrap in pre-labeled aluminum foil or opaque tubes (or wrap test tube wrap with black plastic bag) and freeze. If samples are run immediately, proceed to step 4.0.

4.0 Procedure

1) Place the filter containing the concentrated algal sample in a pre-labeled test tube.
2) Add 2 mL of 100% acetone solution.
3) Cap tightly, vortex or shake until filter breaks apart.
4) Repeat until the all samples are processed.
5) Wrap test tube rack in a black plastic and place samples in a freezer. Allow extraction to occur overnight (up to 24 hours).
6) Remove samples from freezer. Keep samples covered in low light conditions at all times.
7) Clarify extract by centrifuging samples for 15 minutes at approximately 5000 g. Remember to balance the centrifuge (i.e., put equal number of samples on each side).
8) Turn on HPLC and allow it to stabilize while samples are centrifuging.
9) Remove samples from centrifuge. DO NOT SHAKE. Carefully transfer the samples to 1.5 mL HPLC vials. Pour using a continuous motion.
10) Load HPLC autosampler, initiate pigment programs.
11) When finished examine HPLC data and transfer to spreadsheet and save output file on computer hard drive and on a floppy disk.

5.0 Calculation

Pigment concentrations are calculated using the following equation:

Absorbance/slope from standard regression * (Volume filtered/volume shot on HPLC) *1/seagrass weight

Epiphyte Dry Weight Quantification Associated with HPLC Analyses

Estimates of algal epiphytic biomass will be made from separate leaf samples of entire shoots taken directly adjacent to the biomass cores. Leaf samples for epiphytic biomass must be processed within one day of collection. Using traditional methods, in the laboratory epiphytes are separated from the leaf surface by scraping with a glass slide. Scraped material is then collected and retained on pre-weighed glass fiber filters. The collected epiphytic biomass and scraped seagrass leaves are then dried to a constant weight at 60 °C for determination of dry weight biomass. Algal epiphytic dry weight biomass will be expressed as a percent of total dry weight biomass of seagrass tissue scraped.

Data Management

Data collected by field staff will be recorded in a field notebook, or may be recorded electronically. In either case, when an electronic file is the primary data source, either a hardcopy printout or a back-up electronic file will be created as soon as possible after sampling. Electronic data will be stored on the TAMUCC network Science DMZ and backed up on a second drive or on a compact disk. Copies of data sheets will be delivered, or electronic files will be emailed, to the Project Manager. Any data deemed unacceptable will not be used.

References

Cammarata, K. 2008. Texas Bays and Estuaries Final Program.

See http://www.utmsi.utexas.edu/its/tbem2008/tbem2008.htm. Accessed November 24, 2009.

Cammarata, K., J. Sweatman, E. Helander, V. Chilton, S. Dovalina and V. Graham. 2009. Seagrasses Under Stress: Linkages With Epiphytic Biofilms and Eutrophication. Abstract in: Plant Biology 2009, Honolulu, HI, July 18-23, 2009. See http://abstracts.aspb.org/pb2009/public/P22/P22003.html. Accessed December 22, 2009.

Congalton, R.G. 1991. A review of assessing the accuracy of classifications of remotely sensed data. Remote Sens. Environ. 37: 35-46.

Contreras, C., Whisenant, A., Bronson, J.M. and Radloff, P.L. 2011. **Final Report for: Seagrass Response to Wastewater Inputs: Implementation of a Seagrass Monitoring Program in Two Texas Estuaries.** GLO contract number: 10-049-000-3745/TPWD contract number: 211946. April, 2011. 260 pp. (Epiphyte fluorescence portion submitted as Final Report by Cammarata, K.V. February 25, 2011, 59 pp.) Available at: http://www.tpwd.state.tx.us/publications/pwdpubs/media/pwd_rp_v3400_1690.pdf

Dunton, K.H. and W. M. Pulich, Jr. 2007. Landscape Monitoring and Biological Indicators for Seagrass Conservation in Texas Coastal Waters. Draft final report for contract no. 0627, Coastal Bend Bays and Estuaries Program, Corpus Christi, Texas.

Folk, R.L. 1964. Petrology of Sedimentary Rocks. Hemphills's Press. Austin, Texas.

Fourqurean, J.W., J.C. Zieman, G.V.N. Powell. 1992. Phosphorus limitation of primary production in Florida Bay: evidence from the C:N:P ratios of the dominant seagrass *Thalassia testudinum.* Limnology and Oceanography 37:162-171.

Parsons, T.R., Y. Maita and C.M. Lalli. 1984. A manual of chemical and biological methods for seawater analysis. Pergamon Press, New York. 173 pp.

Pulich, W. M., Jr. 2006. Landscape Monitoring for Seagrass Conservation in Texas Coastal Waters. Quality Assurance Project Plan. Coastal Bend Bays and Estuary Program contract no. 0627. Texas State University-San Marcos, River Systems Institute, San Marcos, Texas.

Pulich, W.M., Jr., R.W. Virnstein, S. Wyllie-Echeverria, R. Fletcher, and H.D. Berry. 2003. Deriving landscape indicators of stress for the seagrass biome. Abstract for 17th International Conference of the Estuarine Research Federation, Seattle, WA. Sept. 2003.

Radloff, P.L. 2010. **Quality Assurance Project Plan (QAPP) for Seagrass Response to Wastewater Inputs: Implementation of a Seagrass Monitoring Program in Two Texas Estuaries.** Revision 2. GLO contract number: 10-049-000-3745/TPWD contract number: 211946. January 13, 2010. 105 pp. (Epiphyte fluorescence portion submitted by Cammarata, K.V.) Available at:

http://www.tpwd.state.tx.us/landwater/water/environconcerns/water_quality/QualityAssurance/QAPP%20rev%202%202010.pdf

Seagrass Conservation Plan for Texas (SCPT). 1999. W. Pulich, ed. Resource Protection Division, Texas Parks and Wildlife Department, Austin, Texas.

Solorzano, L. and J.H. Sharp. 1980. Determination of total dissolved phosphorus and particulate phosphorus in natural waters. Limnol. Oceanogr. 25: 754-758.

Spencer, W.E., Wetzel, R.G., Teeri, J. 1996. Photosynthetic phenotype plasticity and the role of phosphoenolpyruvate carboxylase in *Hydrilla verticillata*. Plant Sci 118:1-9.

Sweatman, J. Cammarata, K.V. (*In Preparation)* "Digital Fluorescence Imaging To Characterize Seagrass Epiphyte Accumulation"

Sweatman,J. & Cammarata, K.V. *(In Preparation)* "Accumulation of epiphytes on *Halodule wrightii* in response to nutrient enrichment in East Flats Corpus Christi Bay and Nighthawk Bay, Upper Laguna Madre, Texas"

TCEQ Sampling Stations
http://www.tceq.state.tx.us/cgi-bin/compliance/monops/crp/stationquery2.pl?basinid=24

Texas Commission on Environmental Quality. 2007. Surface Water Quality Monitoring Procedures, Volume 2: Methods of Collecting and Analyzing Biological Community and Habitat Data. Surface Water Quality Monitoring Program, Monitoring and Operations Division, Austin, Texas. Report #RG-416.

Texas Commission on Environmental Quality. 2008. Surface Water Quality Monitoring Procedures, Volume 1: Physical and Chemical Monitoring Methods for Water, Sediment, and Tissue. Surface Water Quality Monitoring Program, Monitoring and Operations Division, Austin, Texas. Report #RG-415.

TNRIS. 2009. 2008 – 2009 Texas Orthoimagery Program / National Agricultural Imagery Program. Texas Natural Resource Information Service, Austin, Texas.

Zimba, P.V., Dionigi, C.P., & Millie, D.F. 1999. Evaluating the relationship between photopigment synthesis and 2-methylisoborneol accumulation in cyanobacteria. *J. Phycol*.35:1422-1429.

Zimba, P.V. and Hopson, M.S. 1997. Quantification of epiphyte removal efficiency from submersed aquatic plants. *Aquatic Botany* 58:173-179.